Technische Universität Berlin
Institut für Energietechnik

John Pius John

An Investigation for Energy Sustainability in Cement Industries in Tanzania: The Case of Mbeya Cement

Berlin 2016

Dissertation

An Investigation for Energy Sustainability in Cement Industries in Tanzania: The Case of Mbeya Cement

John Pius John

Berlin 2016

Technische Universität Berlin

Institut für Energietechnik

An Investigation for Energy Sustainability in Cement Industries in Tanzania: The Case of Mbeya Cement

Vorgelegt von

Master of Science in Renewable Energy

John Pius John

aus Tansania

von der Fakultät III – Prozesswissenschaften

der Technischen Universität Berlin

zur Erlangung des akademischen Grades

Doktor der Ingenieurwissenschaften

– Dr.-Ing. –

genehmigte Dissertation

Promotionsausschuss:

Vorsitzender: Prof. Dr.Aleksander Gurlo

Berichter: Prof. Dr. Tetyana Morozyuk

Berichter: Prof. Dr. Predrag Raskovic

Berichter: Prof. Dr.-Ing. George Tsatsaronis

Tag der wissenschaftlichen Aussprache: 21st November 2016

Berlin, 2017

Acknowledgements

The research would have not been successfully completed without strong support from individuals and institutions of which I register my acknowledgements. Although I would like to mention everyone here, it would not be possible to do that.

I sincerely appreciate great knowledge and skills, invaluable guidance and support that I gained from my supervisors, Prof. Dr.-Ing.George Tsatsaronis and Prof. Dr. Tetyana Morozyuk. They were always available and willing to help me with great love, tolerance and encouragement during the whole process of carrying out and writing this Thesis. I thank them very much for great supervision and for giving me an opportunity to work with them.

I would like to thank the chairperson Prof. Dr. Alexander Gurlo and all the committee members for accepting to be part of my thesis examination and for giving their valuable advice.

I would like to extend my sincere gratitude to my external examiner Prof. Dr. Predrag Raskovic for intensive reviewing of my thesis and for his expert advice. Furthermore, he is thanked for his faithful support and help, tireless perseverance, love and commitment. His remarkable encouragements will never be forgotten.

I sincerely appreciate support and contributions from all my department colleagues especially Stefanie Tesch and Mathias Penkuhn.

I also express my deep gratitude to Prof. Dr. Martina Schäfer, the MES Postgraduate speaker at TU Berlin, and Mr. Jonas van der Straeten, the former Project Coordinator and all group mates for accepting me as an associate PhD student. Their good cooperation and efforts enabled me not only to successfully search for this Thesis supervisors, but also to have strong support to overcome ups and downs of PhD studies.

Special thanks are extended to the government of United Republic of Tanzania and to DAAD for granting me a scholarship for this Thesis. Also, much appreciation is extended to management of Mbeya University of Science and Technology (MUST) for financial support during field research and for granting me a study leave to do this Thesis. I grateful acknowledge financial support from Solar project Freilassing towards completion of my thesis. Special thanks are directed to Mr. Siegfried Popp and all board members for soliciting fund from various sources to support completion of my thesis.

Moreover, I extend my thanks to management of Mbeya Cement Company Limited for providing me with valuable and relevant information for the research.

Last but not the least, my sincere gratitude is due to my wife, Magreth John and our children, Anna John and Pius John for great support, love and caring, tolerance and understanding for the whole duration of my studies

To my family, wife and children
who stood strongly and
endured my long time absence

Abstract

Cement production processes are facing crucial sustainability issues such as inefficient energy and raw material use, product supply, production cost and environmental pollution. High energy and material use dominated by inefficient characteristics of cement production processes, in turn, lead into depletion of non-renewable resources, increased production costs as well as environmental degradation due to emissions.

The main objective of the study was to investigate performance of cement industry in Tanzania relative to sustainable energy utilization. Most of past researches have evaluated the performance of cement production processes using first law of thermodynamics alone (mass and energy balances) with the objective of improving energy efficiency. Although this approach sheds light on the question of improvement of energy use in the processes, it has some limitations. The limitations are imposed by the internal irreversibility due to combustion and other physico-chemical nature of reactions dominating the whole processes. The current emerging approach, which overcomes limitations imposed to the first law approach is exergy-based method, relatively new in evaluation of performance of cement production processes. However, owing to complexity of cement production processes, applying an exergy-based method manually is very difficult and complex.

The current study proposes combined approach of exergy based method and modeling as well as simulation. The model was successfully developed, validated using real plant data and was used to predict the performance of the cement dry rotary kiln system of Mbeya Cement production processes. Data obtained from modeling and simulation were further used to evaluate the performance of processes, individual components, sub-systems and overall kiln system at large using exergy based method. The approach not only simplifies the analyses but also gives detailed insight of real processes, source and type of real imperfections, its magnitudes and how imperfections can be minimized.

Major findings indicated that the rotary kiln sub-systems and the overall kiln system have poor exergetic performance, suggesting that potential for improvement exists. The overall exergy efficiency of the kiln system is around 33 %. Also results indicated that the rotary kilns have the lowest exergetic efficiency of about 14 % followed by the clinker cooler with exergetic efficiency of about 41.11 %. The highest source of irreversibility encompassed chemical reactions, especially calcination and clinker burning processes with exergy destruction of 2,813.75 $kJ \cdot kg_{cl}^{-1}$ and 1,148.17 $kJ \cdot kg_{cl}^{-1}$. Results from parametric analysis suggested that if measures for improvements of processes, components and sub-systems are taken, a significant amount of fuel and specific energy could be saved. Furthermore, it was confirmed that if the avoidable exergy destruction is minimized, processes, system components and sub-systems performance could be improved from exergetic point of view.

Zusammenfassung

Für Zement-Produktionsprozesse stellen sich einige entscheidende Nachhaltigkeitsfragen, zum Beispiel in Zusammenhang mit ineffizientem Energie- und Rohmaterialeinsatz, Produktversorgung, Produktionskosten sowie sozialen und ökologischen Auswirkungen. Der hohe Energie- und Materialeinsatz bedingt durch Ineffizienzen in Produktionsprozessen von Zement führt wiederum zur Erschöpfung nicht-erneuerbarer Ressourcen, erhöhten Produktionskosten sowie Umweltschäden durch erhöhten Emissionsausstoß.

Hauptziel dieser Studie ist es, die Leistungsfähigkeit der Zementindustrie in Tansania in Relation zur nachhaltigen Energienutzung zu untersuchen. Die meisten bisherigen Analysen, bewerteten die Leistung von Zement-Produktionsprozessen in Tansania ausschließlich anhand des ersten Hauptsatzes der Thermodynamik (Massen- und Energiebilanzen) mit dem Ziel, die Energieeffizienz zu steigern. Dieser Ansatz kann zwar Fragen der verbesserten Energienutzung in diesen Prozessen näher beleuchten, ist aber mit einigen Einschränkungen verbunden. Diese Einschränkungen ergeben sich aus der internen Irreversibilität aufgrund der Verbrennung und anderer physikalisch-chemischer Charakteristika von Reaktionen, die den gesamten Prozess dominieren. Mit dem Ansatz der Exergieanalyse lassen sich diese Einschränkungen, die dem ersten Hauptsatz inhärent sind, überwinden. Die Anwendung der Exergieanalyse auf Zement-Produktionsprozesse ist relativ neu. Aufgrund der Komplexität der Zementproduktion ist die manuelle Anwendung der Exergieanalyse sehr schwierig und komplex.

Diese Arbeit schlägt einen kombinierten Ansatz von Exergieanalyse und Modelierung und Simulation vor. Das Model wurde erfolgreich entwickelt und mit realen Anlagedaten validiert und im Anschluss dazu verwendet, um die Leistung der Produktionsprozesse von Mbeya Cement vorherzusagen.

Die durch Modellierung und Simulation gewonnenen Daten wurden weiterhin verwendet, um mit Hilfe der Exergieanalyse die Leistung von Prozessen, einzelnen Komponenten, Teilsystemen und des Drehofens als Ganzem zu bewerten. Dieser Ansatz vereinfacht nicht nur die Analyse, sondern gibt auch einen detaillierten Einblick in die realen Prozesse, die Quellen und Typen der realen Unvollkommenheiten, ihr Ausmaß und die Frage, wie diese Unvollkommenheiten minimiert werden können. Darüber hinaus können die vorgeschlagenen Maßnahmen für Verbesserungen leicht geprüft werden, um zu sehen, ob sie die Effizienz der Anlage wirklich zunimmt.

Die zentralen Ergebnisse der Arbeite weisen auf eine schwache exergetische Leistung der Teilsysteme des Drehofens und auch des gesamten Drehofen-Systems hin und zeigen dass Verbesserungspotential besteht. Die Gesamt-Exergieeffizienz des Ofensystems beträgt etwa 33 %. Die Ergebnisse zeigen weiterhin, dass die Drehöfen mit 14 % den niedrigsten exergetischen Wirkungsgrad haben, gefolgt von den Klinkerkühler mit einem exergetischen Wirkungsgrad von etwa 41 %. Die höchste Quelle von Irreversibilität waren chemische Reaktionen, vor allem Klinkerbrennverfahren mit einer Exergievernichtung von etwa 1,148.17 $kJ \cdot kg_{cl}^{-1}$. Die Ergebnisse einer Sensitivitätsanalyse legten nah, dass durch Maßnahmen zur Verbesserung der Prozesse, Komponenten und Teilsysteme erhebliche Mengen an Kraftstoff und spezifischer Energie eingespart werden können. Weiterhin wurde bestätigt, dass durch die Minimierung vermeidbarer Exergievernichtung die Leistung der Prozesse, Systemkomponenten und Subsystemen aus exergetischer Sicht verbessert werden können.

Contents

Nomenclature

e	– Specific exergy on mass basis, [kJ·kg^{-1}]
$\bar{e}$	– Specific exergy on molar basis, [kJ·kmol^{-1}]
$\dot{e}$	– Exergy flow rate per kg clinker flow, [kJ·kg$_{cl}^{-1}$]
$\dot{E}$	– Exergy flow rate, [kW]
ΔG	– Change of Gibbs free energy, [kJ]
h	– Specific enthalpy, [kJ·kg^{-1}]
HHV	– Higher heating value, [kJ·kg^{-1}]
S	– Specific entropy, [kJ·kg^{-1}·K^{-1}]
$\dot{m}$	– Mass flow rate, [kg·s^{-1}]
n	– Molar flow rate, [kmol·s^{-1}]
p	– Pressure, [Pa],[bar]
P	– Power, [kW]
q	– Specific heat energy consumption, [kJ·kg^{-1}]
$\bar{R}$	– Ideal gas constant, [kJ·kmol^{-1}·K^{-1}]
Q	– Rate of heat transfer, [kW]
T	– Temperature, [K], [°C]
$\dot{W}$	– Work rate, [kW]
x	– Mole fraction,[–]
X	– Fraction of a substance, [% wt]
y	– Mole fractions of the i-th component of specified stream, [–]

Greek letters

ε	– Exergetic efficiency, [%]
η	– Energy efficiency, [%]

Subscripts

0	– Exergy-reference environment
brn	– Burning
BS	– Booster
cl	– Clinker
CLINKER1	– Stream hot clinker exiting the rotary kiln
comb	– Combustion
cry	– Crystal
D	– Destruction
e	– Outlet (e = 1,2,….)
evln	– Evolution temperature of combined water and sulfur in raw feed
evp	– Evaporation temperature
EXGAS	– Exit gases stream from the preheater tower
exh	– Exhaust
F	– Fuel of a component
flame	– Combustion gases temperature
GASCLEAN	– Exhaust gas cleaner
HOTAIR	– Secondary combustion air stream
i	– Inlet (i = 1,2,….)
ID	– Induced draft
k	– Component (k =1,2,….)
KLN	– Kiln
L	– Loss
liq	– Liquid
P	– Product of a component
PH2GAS	– Exhaust gases stream at the 2nd stage preheater cyclone
PH3FEED	– Preheated raw feed and gases stream at the 3rd stage preheater cyclone
PH3GAS	– Exhaust gases stream at the 3rd stage preheater cyclone
PH4FEED	– Preheated raw feed and gases stream at the 4th stage preheater cyclone
PH4GAS	– Exhaust gases stream at the 4th stage preheater cyclone
PH4SOLID	– Preheated raw feed stream at the 4th stage preheater cyclone
PH5GAS	– Hot exhaust gases stream exiting the rotary kiln
PHT	– Preheater Tower
precalcin	– Precalcination
r	– Reactant
RC	– Rotary cooler
rm	– Raw Mill
SYS	– System
thr	– Threshold
tot	– Total
w	– Wall

Superscripts

CH	– Chemical
KN	– Kinetic
ov	– Vapor
ol	– Liquid
PH	– Physical
PT	– Potential
TOT	– Total

Abbreviations

ARM	– Arth River Mining
BAT	– Best available technology
BF-Fan	– Bag filter fan
cl	– Clinker
CV	– Control volume
DRC	– Democratic republic of Congo
ESP	– Electrostatic Precipitator
FabFl	– Fabric filter
FC	– Fixed carbon
GCT	– Gas conditioning tower
GDP	– Gross Domestic Product
GHS	– Green House Gases
ID-Fan	– Induced draft fan
LOI	– Loss of ignition
m	– Mixture
MCC	– Mbeya Cement Company Ltd.

MEM	– Ministry of Energy and Mineral resources
Mta	– Millions tons annually
N	– Normal hardening cement
p	– Product, -
PFD	– Process Flow Diagram
PHT	– Preheater tower
PLC	– Planetary clinker cooler
PSD	– Particle Size Distribution
r	– Reactant,
R	– Rapid hardening cement
rm	– Raw material
rpm	– Revolutions per minute
RTK	– Rotary kiln
Sfrac	– Solid fraction
SPD	– Simulation Process Diagram
TOE	– Tons equivalent
tpd	– Tons per day
tph	– Tons per hour
Vfrac	– Vapor fraction
Vm	– Volatile matter

List of Figures and Tables

Chapter One – General Context of Research

Tanzania is among developing countries in East Africa with a population of about 46 millions of which 70 % live in rural areas and 30% in urban areas. Tanzania has a total area of about 954,000 km^2. The national energy demand (consumption) is estimated at 22 million tons of oil equivalent (TOE) per annum or per capita useful energy consumption of 0.7 tons of oil equivalent (MEM 2003), 90% from biomass mainly used in the household sector; 8 % from petroleum as well as gas and 1.5 % from electricity. Contribution of coal and other renewable sources is 0.5% (Mwihava and Mbise, 2005).

According to PHDR (2009), electricity consumption per capita is estimated at 85kWh per year compared with 432 kWh and 2,176 kWh for Sub-Saharan Africa and world averages, respectively. Tanzania experiences a very serious electric energy supply imbalance. The total installed capacity is 1129 MW out of which 50 % is thermal, 49 % is hydro and 1 % is co-generation (Hurl et al. 2012). Current national maximum load demand is at 1031 MW, very close to the installed generation capacity. However, the average available capacity has been dropped to 650MW, a pattern, which makes industries face serious electricity power problems. The estimated grid connection in mainland Tanzania is about 12% in urban areas and only 2.5 % in rural areas (HBS 2007). The study by Confederation of Tanzania Industries (CTI 2011) points out that manufacturing industry in the country is still experiencing obstacles of intermittent power supply, frequent rationing and outages.

Nevertheless, the following scenarios are observed about cement industry in the country: There are four cement industries, namely, Mbeya Cement Company Limited, Tanzania Portland Cement Company Limited, Tanga Cement Company Limited and Lake Cement Company Limited. Currently, there are three international companies with significant ownership stakes in local cement-producing companies. The German based Heidelberg Cement owns 69 % of Tanzania Portland Cement Company Limited, the Swiss Holcim Cement owns 63 % of Tanga Cement Company Limited and the French Lafarge owns 14 % of Mbeya Cement Company Limited (Maasa and Marwa 2012). Additionally, there are three new international companies that have just entered the market. The companies are Arthi River Mining (ARM) from Kenya, based in Tanga and Dar es Salaam; Dangote cement from Nigeria and Banco. While ARM has already started production, Dangote expected to start at the end of 2015. Both Dangote and ARM are expected to produce up to 1.5mtpa. Based on the growing cement demand, other three old cement companies decided to implement expansion programs.

The current cement and clinker production capacity is 3.7 Mta and 2.8 Mta, respectively (IFC 2014). Also IFC points out that average cement price in the country is $ 120/ton and per capita cement use is 46 kg against global average of 2000 kg per capita. Maasa and Marwa (2012) as well as Zunga and Lopes-Pinto (2011) presented out the main driving force for cement industry's growth in the country to be opportunities for growth of the cement industry in the country.

Some discussed driving forces included the following: (Growth Domestic Product) GDP growth outpacing population growth; double digit growth in cement consumption outpacing GDP growth; massive infrastructure and housing demand, strong demand from neighbouring countries of Burundi, Rwanda as well as East Democratic Republic of Congo (DRC) an abundant source of high quality limestone deposits in Tanzania; and favourable retail price in the country.

On the other hand, there are factors that threaten growth of cement industry in the country. The most dominant factor includes energy constraints whereby prices for imported oil fuel and coal are hiking. Another energy constraint is electricity deficit, which necessitates companies to generate their own power using diesel generators thereby leading to higher operating costs and emissions to the environment. Other factors that affect growth of cement industries in the country are stiff competition from subsidized imports and inefficient transportation infrastructure in the country.

The imbalance of electric energy and ever increasing cost of imported fossil fuel in Tanzania adversely affects energy sustainability of cement production processes. Globally, there is evidence that energy cost in most energy intensive industries contributes from 30% to 60% of production costs (Brunke and Blesl 2014; Wang et al. 2009). Thus, high energy use dominated by inefficient characteristics of cement plant, in turn, leads into depletion of non-renewable energy resources as well as causes environmental pollutions due to emissions. Furthermore, inefficient energy use contributes to increased production costs. Despite an urgent need for overcoming energy constraints facing most industries in Tanzania, there is no evidence that measures towards energy efficient are given priority. To the contrary, Mohamed and Khan (2008) argue that energy efficiency and conservations are not realized in most Tanzania's industries, commercial consumers and residential consumers. While cement industries in the country are constrained with the issue of energy, they are additionally subjected to respond to global needs to face the challenge of global warming and climate change, all aspects believed to originate from greenhouse gases (GHG) emissions.

Globally, cement industries are believed to contribute from 5 % to 8 % anthropogenic CO_2 emissions (ECRA 2012; CSI/ECRA 2009; Napp et al. 2014; CEMBUREAU 1999; Worrell et al. 2013). In fact, CO_2 emissions from cement industries originate both from calcination of $CaCO_3$ and $MgCO_3$ from high volume of raw materials fed to cement kilns and combustion of fossil fuels. In order to reduce the effect of emitted CO_2 and other flue gases from the cement industry, then measures should be taken to reduce their emissions. In general, there are several methods proposed by scientists to reduce CO_2 and other flue gase emissions in cement industry (ECRA 2012, CSI/ECRA 2009, Napp et al. 2014; CEMBUREAU 1999; Worrell et al. 2013; Worrell et al. 2009). Although most results from researches suggest a wide range of technologies, which are potential for reducing industrial GHG emissions, they stress that energy efficiency is one of the most important solutions especially in short- to mid-term solutions.

Worldwide, many researches have been conducted in cement industries to evaluate losses and their causes; emissions; energy efficiency; and conservation opportunities (Saidur et al. 2009, Ates and Durakbasa 2012, Abdelaziz et al. 2011; Madlool et al. 2011). Nevertheless, most reported research works considered only energy analyses (mass and energy balances). However, performance evaluation of cement industries using the first law of thermodynamics alone is insufficient to reveal the real thermodynamic imperfection. This is due to the fact that cement production processes involve complex chemical and physical reactions during conversion of raw materials to final product. Moreover, it involves combustion reaction of fossil fuel and complex heat exchange between solids (from 50 °C inlet Raw-feed to 1450 °C in burning zone, then up to 100^0C in the cooler outlet) from raw materials and hot combustion gases up to 2000 °C. Also it involves mixing as well as separation of solid and fluids at various compositions, temperatures and pressures. All the aforementioned reactions and processes taking place in the cement production processes are major sources of internal irreversibility, which cannot be identified using mass and energy balance alone (Tsatsaronis 1993; Bejan et al. 1996). Figure 1.1 summarizes the gap between what has been done so far in the past studies. Also Fig. 1.1 indicates briefly what was proposed by the current study.

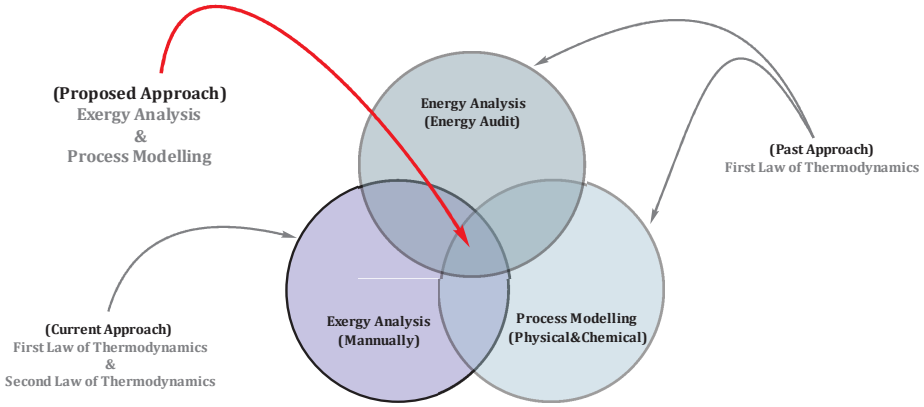

Figure 1.1. Gap between current and past studies

In addition, cement plant efficiency mainly depends on the type of cement kiln. Several researches discuss kiln efficiency based on technology used. Habert et al. (2010) point out that the less energy efficient kiln is the long rotary kiln, burning wet raw materials, then the semi-dry process, the dry process with preheater or precalciner kilns, while the most efficient is rotary kiln with preheaters, precalciner and heat recovery system that burn dry materials. Moreover, although Portland cement plants generate the same final product using similar processes, plant layouts vary according to fuels and raw materials used together with location, climate, site topography and equipment manufacturer. It should be pointed out that quality of fuel and used raw materials may significantly affect useful energy consumption of production process of a given factory.

Generally, it can be concluded that reasons furthering research in the area of efficient energy utilization in cement industries include, but not limited to, challenges facing cement industries

such as cost increases in energy supply with diminishing resources both of energy generation and raw materials and hence, limited supply of energy demand. Also there are requirements to reduce CO_2 emissions. Energy demand in clinker production has been significantly reduced over the last few decades. The best available techniques for new plants and major upgrades are reported in various researches (Schneider et al. 2011; Worrell et al. 2013; CEMBUREAU 1999; CSI/ECRA 2009). However, factors involved to further reduce this demand are plant-specific. It should be emphasized that in order to implement any of the technological and economically viable available energy efficient measures, plant performance evaluation is inevitable.

Building on the preceding discussion, the purpose of the current research was to improve energy efficiency of the cement industry in Tanzania. Thus, the central research question was, "What is the potential for energy savings in cement industries in Tanzania?"

To answer this question, the following additional research questions guided the study:

(i) Which factors affect the useful energy consumptions of various equipment used in cement production processes?
(ii) How verification, monitoring and analysis of energy use in cement industry can be conducted?
(iii) How inefficiencies and energy losses in cement industry can be identified?
(iv) How can energy be efficiently managed in cement industry in Tanzania?

Therefore, the current study investigated sustainable energy use in cement industries by using both the first and second laws of thermodynamics. The research considered exergy analyses complemented by computer simulation using Aspen Plus simulation software (AspenTech®, 2014) so as to quantify losses in each major component in cement industry. The study resulted into development of a steady state simulation model.

The model results were validated against real plant data and used to evaluate the plant's performance. The model was used to conduct "virtual" experiments to predict how variations of different input variables may affect performance of the plant and its environment. The model describes sufficiently all major processes and major known physio-chemical reactions taking place in the cement dry rotary kiln system. The informative data generated from the model simplified the work of further analyses of the kiln system using exergy based method and enhanced achievement of detailed useful results.

The combined approach of modeling and exergy-based evaluation method are able to indicate sufficiently contribution of each major process and physico-chemical reactions in imperfections of the kiln sub-systems including the overall systems at large. The approach of combined modeling and exergy based method not only simplify evaluation of cement production processes but also give more reliable solutions to problems relating sustainable energy and other resources use. With this approach, it is possible to determine the type of imperfection (exergy destructions and exergy losses), its location as well as magnitudes and demonstrate quantitatively how imperfections can be minimized.

The thesis is divided into seven chapters. Chapter One is an introductory chapter laying down the general background of the study. The chapter highlights the problem, motivation to tackle it and methods used. Furthermore, the chapter presents the research questions, list of contributions made so far and then it ends with the thesis structure. Chapter Two presents critical analyses of past related works, brief description of cement production processes and development in terms of technology as well as energy use. Moreover, the chapter introduces the aspect of sustainability as well as methods used to evaluate performance of cement industries. Chapter Three presents detailed methods and approach used to tackle the problem. Chapter Four starts with brief description of case study industry followed by detailed procedures used to develop, validate and analyses of the model. The chapter presents data, assumptions and choices of thermodynamic models used to develop the model. Chapter Five presents exergy analysis. The chapter presents results and discussion of results regarding performance of rotary kiln system from exergetic point of view. Chapter Six starts with a discussion about proposed measures to improve performance of the kiln system, presents discussion about obtained results after implementation of some proposed measures to test if they could really improve performance of the kiln system using both modeling and exergy analysis. Chapter Seven presents general concluding remarks to the study as well as future prospects.

Chapter Two – State of the Art

2.1. Introduction

This chapter contains sections that present a critical review of past related works. It also provides a general brief description of cement production processes and development made so far in terms of technology and energy use. Furthermore, the chapter discuses methods and approaches used in evaluation of cement production processes.

2.2. Description of Cement Production Processes

The whole process of cement production is presented in Fig. 2.1, while the major compound constituting clinker and clinker main phases are listed in Table 2.1. The raw materials required for clinker production are limestone, clay and sandstone. The main elements contained in the raw materials are calcium; silicon aluminum and iron oxides. There are four main process routes in the manufacturing of cement, namely, dry, semi-dry, semi-wet and wet process (CEMBUREAU 1999). Quarrying, raw material preparation, fuel preparation, clinker burning, mineral additions preparation, cement grinding and cement dispatch sub-processes are similar for all main processes.

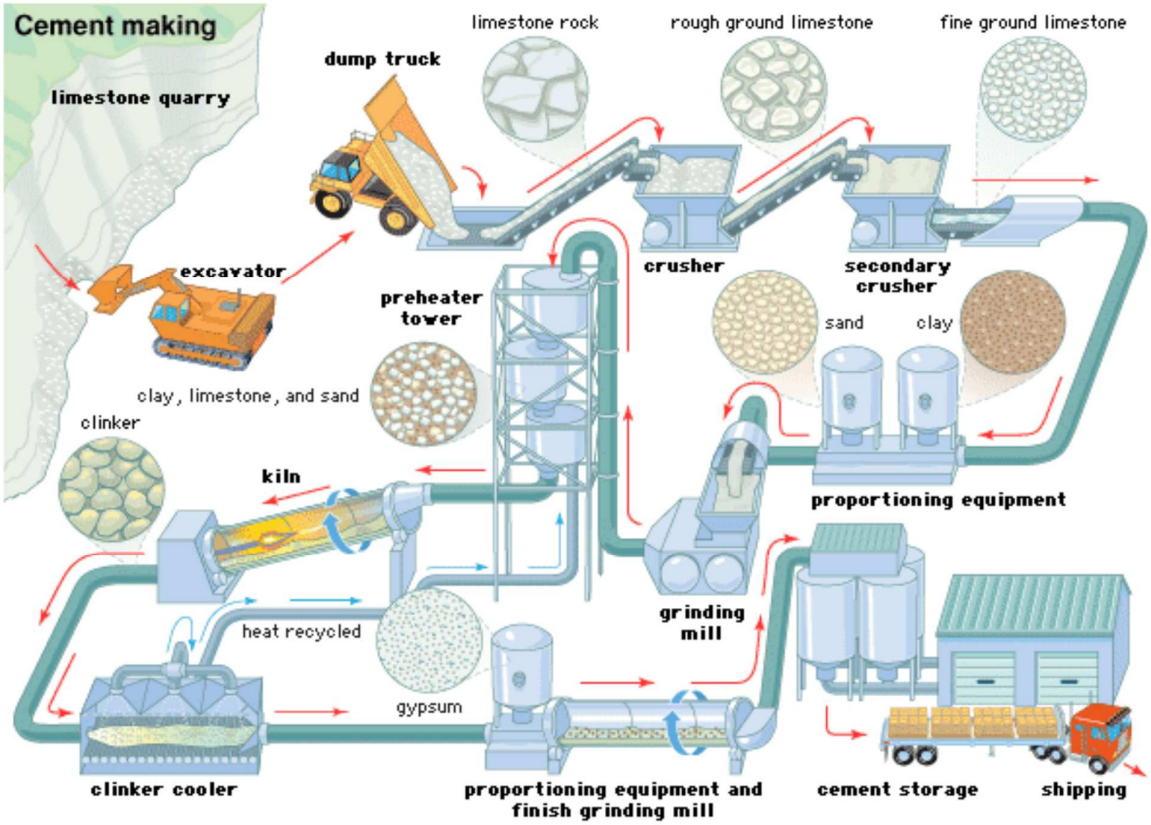

Figure 2.1. Cement production processes (Zunga and Lopes-Pinto, 2011)

Table 2.1. Major clinker compound, phases and its abbreviation

Compound	Abbreviation	Clinker Name	Clinker phase	Abbreviation
CaO	C	Tri-calcium silicate	Ca_3SiO_5	C_3S
SiO_2	S	Di-calcium silicate	Ca_2SiO_4	C_2S
Al_2O_3	A	Tri-calcium aluminate	$Ca_3Al_2O_6$	C_3A
Fe_2O_3	F		$Ca_4Al_2Fe_2O_{10}$	C_4AF
			$Ca_{12}Al_7O_{33}$	$C_{12}A_7$

Crushing and milling of raw materials are done using crushers as well as mills of different types followed by proportioning and then mixing in a homogenizer. Then the raw materials are fed to the kiln system at the upper preheater cyclones. The pre-heater cyclones dry and heat the raw materials to the required temperature of around 900^0C to 1000^0C. The number of pre-heater cyclone stages depends on moisture content of the raw materials. The latter has a direct impact on energy requirements of the process and the type of kiln used. The preheated raw-feed is then fed to the rotary kiln where it is fired with fuel burnt directly in the kiln thereby achieving gase flame temperature as high as 2000 °C and material temperature of 1450 °C at the kiln burning zone (CEMBUREAU 1999). At such high temperatures, calcination (decomposition of $CaCO_3$) takes place followed by formation of intermediate compounds and then finally, clinker formation. The clinker is then cooled in clinker coolers of different types (rotary, grate and planetary coolers). The cooled clinker is ground and blended with additives like gypsum and pozzolana to form cement.

2.3. Brief Description of Employed Technologies

Major equipment used for cement production processes include kilns, coolers, crushers, mills, preheater cyclones and auxiliary equipment like fans, compressors, conveyors as well as drivers. The kiln is one of the major and most important equipment in cement production processes. The most common kiln type today is the dry rotary kiln.

The rotary kiln is a rotating inclined cylinder used to heat solids to the point where a required chemical reaction takes place. It is used mainly for clinker burning. The rotary kiln is also used for a wide range of operations like reduction of oxide ore, reclamation of hydrated lime and calcination of petroleum coke. The dry rotary kiln systems with 5 to 6 staged pre-heater cyclones and a pre-calciner are considered to be the modern kiln system. On the other hand, the wet rotary kiln used for processing raw materials with high moisture content (15% ÷ 25%) is regarded an out-dated technology (Worrell et al. 2013, CEMBUREAU 1999). The wet process is very energy intensive due to evaporation of high moisture contained in raw feed. However, wet and semi-wet processes have the advantage of improved product handling, greatly efficient raw material grinding and reduced dust (Worrell et al. 2013).

There are several types of grinding mills in cement production processes. Ball mills use traditional method of grinding, accounting for around 60% of cement mills (Worrell et al. 2013). The

remaining mills are made up of highly modern mills, namely, vertical roller mills, roller press and horizontal mills. The said mills are highly efficient and use between 30 % and 40 % less energy than the ball mill (Worrell et al. 2013). The choice of mill depends on required grain size, clinker properties and final product quality. Current grinding technologies are still highly inefficient with over 95 % of energy input being lost as waste heat (Worrell et al. 2013). Advanced comminution technologies include non-mechanical milling technologies based on ultrasound, laser, thermal shock, electric shock or cryogenics. However, they are still in research phase and are still far from commercialization.

2.4. Sustainable Energy in Cement Industries

Sustainable industrial production processes can be considered to be non-polluting, conserve energy as well as natural resources, economically sound and safe for communities. Sustainability drivers include need to reduce energy use, raw material consumption including waste, growing recognition of climate change, limited resources and increasing regulatory requirements. Thus, energy efficiency is one of the major key components of sustainable production processes. Furthermore, climate change due to use of fossil fuels is posing a threat to the environment. Industrial energy efficiency is one of the most central ways for reducing this threat because there is a large untapped potential for energy efficiency in the cement industry (IPCC 2007).

Chemical and processing industries, specifically cement industries are facing challenges of sustainability issues that include sustainable energy supply, raw material use, product supply, production cost, environment conservation and so forth. The process consumes a significant amount of natural resources like raw materials and fossil fuels. The process is energy intensive, requiring high fuel consumption for the kiln operation, which, in turn, influences not only production costs, but also it generates CO_2. Energy costs represent 30 % to 40 % of production costs (Brunke and Blesl 2014). However, a large share of CO_2 emissions originates from chemical conversion of limestone to clinker. It is estimated that between 50 % and 60 % of CO_2 of cement production emissions are from calcination of $CaCO_3$, while between 30 % and 40 % of CO_2 emissions are produced by burning fossil fuels. The main factors determining thermal energy needs are nature and composition of raw materials including the employed process.

Globally, there are significant efforts made to promote sustainability in industries. Many literatures list organizations that mostly devoted their efforts to promote sustainability in industries. Ali Hassanbieg et al. (2012) listed most of such organizations. On the other hand, significant efforts have been done by researchers to find out solution for sustainable industrial processes. Napp et al. (2014) presented a comprehensive overview of technologies for energy efficiency and reducing emissions from industrial processes by collecting information from a wide range of sources. The study reports that although there have been significant improvements in energy efficiency in recent years, cost-effective energy efficient options still remain.

In regard to sustainability in cement industry in particular, a substantial amount of literature exists especially on energy efficiency topic (for example, ECRA 2012, CSI/ECRA 2009, Napp et al. 2014, CEMBUREAU 1999, Worrell et al. 2013). It was pointed out that the main ways in which energy usage and CO_2 emissions can be reduced in cement manufacturing processes include the following: phase out inefficient kilns and add pre-heaters as well as a pre-calciner to the efficient modern rotary kiln; increase the ratio of clinker substitutes in order to decrease process emission arising from calcination; and introduce efficient milling as well as grinding equipment. The International Energy Agency (IEA) estimates that the total specific energy savings available in cement industry are around 1GJ·per ton of cement. Fuel savings due to adoption of the most efficient kiln technology constitutes the largest share of these savings. Nevertheless, it should be noted that the theoretical minimum energy requirement for processes and physio-chemical reactions occurring in the rotary kiln system cannot be achieved in practice owing to unavoidable inefficiencies such as exergy destructions within the kiln system and exergy losses to the environment.

The energy efficiency of dry rotary kiln can be further increased by various heat integration and waste heat recovery options. For example, waste heat from the kiln exit gases, clinker cooler system and kiln pre-heater can be recovered as well as used to generate power. The most widely applied and economic option is installation of a waste heat recovery boiler and running a steam turbine. About $36 \div 83$ MJe·t_{cl}^{-1} ($10 \div 23$ kWh·t_{cl}^{-1}) can be generated with an estimated installation cost of $3 \div 4.5$ \$·t_{cl}^{-1} (Worrell et al., 2013).

However, in order to implement these heat recovery technologies, it is required to properly evaluate performance of the existing facility and pinpoint all possible measures that can be implemented. An energy audit employing the first law of thermodynamics (mass and energy balances) has been commonly used for the past few decades in evaluating cement production processes. However, with developments made in computer technology, modeling and simulation have also been employed in evaluation of cement production processes. The most current approach of evaluating cement production processes is the exergy based method. Nonetheless, application of exergy based methods in evaluating cement production processes is still very challenging due to the fact that cement production processes are very large and complex. Detailed discussions of these methods used to evaluate cement production processes are presented in the next sections of this thesis.

2.5. Conclusions on Sustainable Energy in Cement Industries

It can be concluded that in general, there is a problem of sustainable energy use in cement industries globally, owing to limitations imposed to technologies, inefficient characteristics of equipment and processes together with much reliance on fossil fuels. Other factors include, but are not limited to, type of technology and raw materials used. Furthermore, literatures indicate that energy contributes to substantial amount of production cost processes. However, there

have been several efforts towards sustainable energy use in energy intensive industries. Besides existence of BAT for cement production processes, there is still room for further improvements based on an individual cement plant assessment. There is still a pressing need for more improvements of energy intensive industries especially cement industries based on the following arguments: It has been indicated in literature that fossil fuels like coal will still dominate cement production processes at least for the next few decades. This implies that there is crucial need to improve the performance of cement plants so as to avoid losses, which result into demand for more fuel burning leading to higher production costs and more CO_2 emissions. Furthermore, demand for cement production is substantially increasing as the rate of development and need for more infrastructure increases. Comprehensive energy assessments should be the basis for energy efficiency initiative. There are several methods and techniques available for energy assessments like energy audit, optimization, process integration, pinch analysis, energy analysis, exergy analysis and modeling. Energy efficiency initiatives are the most attractive solutions because they can lower maintenance costs, reduce waste, increase production yield and provide safer working conditions in a wide range of operations.

2.6. Energy Use in Cement Industries

Literature searches reveal that the energy supply in the industrial sector is about 30 % of total energy used (Al-Ghandoor et al. 2008; Onut and Soner 2007; Saidur 2010; Saidur et al. 2010; Steenhof 2006; Subhes and Ussanarassamee 2005). Specific useful energy consumption in cement production varies from technology to technology. The dry process uses more electrical but much less thermal energy than the wet process. Pyro-processing requires the major share of the total thermal energy use. It accounts for about 93 % ÷ 99% of total fuel consumption (Junior 2003, Khurana et al. 2002). The typical electrical energy consumption of a modern cement plant is about 110 ÷ 120 kWh per ton of cement (Mejeoumov 2007). The main thermal energy is used during the burning process, while electrical energy is used for crushing and grinding.

Energy use distributions in all major sub-systems for dry rotary kiln with pre-calciner cement production are presented briefly in Fig. 2.2. It can be observed from Fig. 2.2 that only energy flows for intrinsic production system are presented, while energy used for quarrying and transportation is not included because it is not part of cement production processes. It can be concluded from Fig. 2.2 that for crushing operations, only electrical energy is used. After crushing, the obtained solid particles from raw materials, additives and coal fuel are further reduced using milling machines of various types, depending on employed technology at a given plant. Mainly, electrical energy is used for milling reduction processes except for raw materials and coal where thermal energy is needed for drying. Calcination, that is, decomposition of $CaCO_3$ is an endothermic reaction and therefore, in pre-calciner, only thermal energy is needed. Pyro-processing is accomplished in a rotary kiln whereby further calcination takes place followed by clinker phase formation in the burning zone. Thus, combustion of fuel provides heat

required for reactions taking place in the rotary kiln. Additionally, electrical energy is used for kiln drives. Energy used for clinker cooling and grinding is mostly electrical energy.

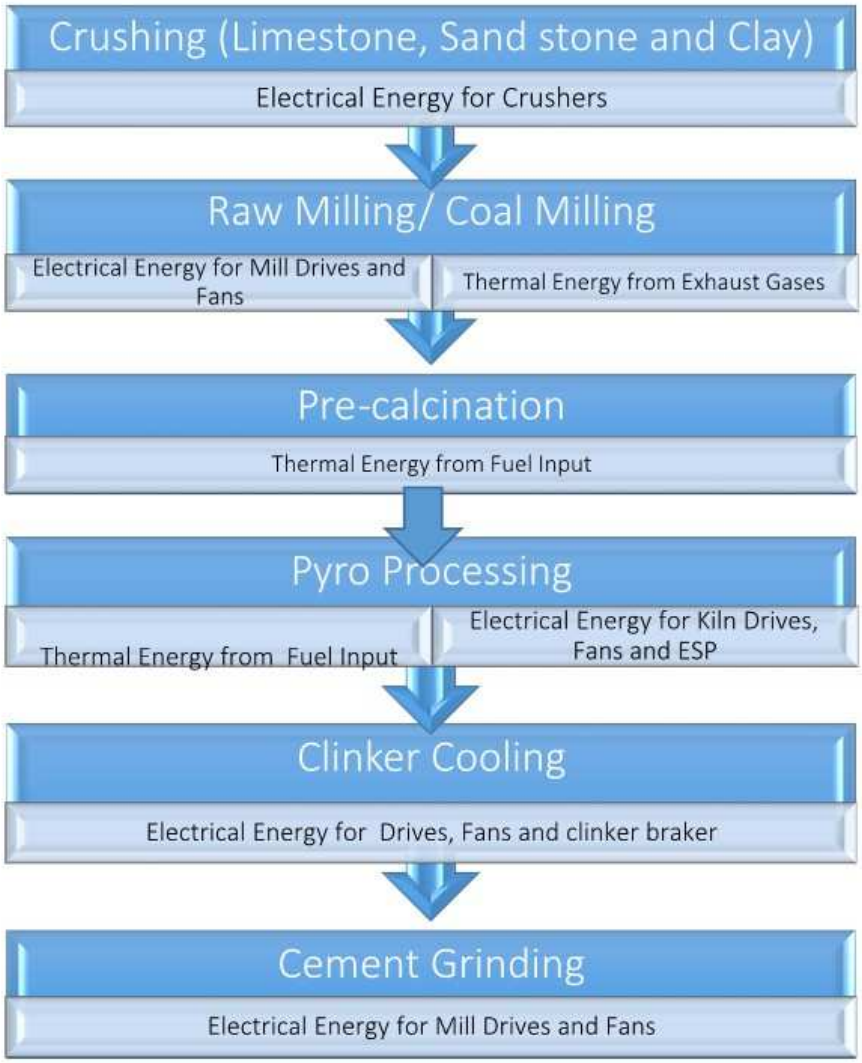

Figure 2.2. Energy flow in a cement production process

2.7. Modeling and Optimization of Cement Production Processes

This section presents briefly modeling works found in literature for cement production processes. The section starts with a brief presentation of definitions of modeling and simulation. Furthermore, objectives of modeling and simulation are briefly presented.

2.7.1. Overview of Process Simulation

A model is a mapping of the system of interest onto a simple representation, which approximates the behavior of the system under development, the environment in which the system operates or interactions with an enabling system and interfacing systems (Haskins 2006). Models can be categorized into two general categories, namely, representation and simulation models, respectively. Representation models employ some logical or mathematical rule to convert

a set of inputs to corresponding outputs with the same form of dependence like in the represented system but do not mimic the structure of the system (Haskins 2006). On the other hand, simulation model mimic the detailed structure of the simulated system, representing system's elements, connected in the same manner like in an actual system.

Furthermore, simulation models can be classified as predictive models and empirical models. Predictive models have full capability of predicting changes of the process parameters within a system, while empirical models can only describe a single specified process. Models can further be distinguished as steady state models also known as static and dynamic models. Dynamic models are types of models, which are time dependent describing the start-up or shut-down of a process or changes that occur when there is some type of disturbances in the process (Hökfors 2014). On the other side, the steady state models are models that can show how the process responds to process changes based on change in operating parameters like flow rates or conditions. Additionally, in modeling, there are so called chemical models and physical models. Physical models describe physical phenomenon or physical properties of the simulated system, for example, bed height of the solid material, flame characteristics, kiln speed and the like.

Process simulation is used for design, development, analysis, and optimization of processes. It is mainly applied to chemical plants and chemical processes. A process simulation software is used for description of different processes in flow diagrams. Process simulation serves the following purposes:

(i) Used to understand real processes in a plant;
(ii) Used during synthesis and design stage of plant processes;
(iii) Used when experimental tests are difficult to conduct;
(iv) Used when there are environmental risks, and
(v) Used in handling large process in a chemical industry.

The main simulation activity in process engineering is flow sheeting. Flow sheeting is a systemic description of material and energy streams in a process plant by means of computer simulation with the scope of designing a new plant or improving performance of an existing plant (Dimian 2003). The simulation model should mirror the behavior of the plant, such as the network of material and energy streams subjected to variations in raw materials, energetic utilities and product specifications. The following objectives of simulation models are listed:

(i) Deliver a comprehensive report of material and energy streams;
(ii) Determine the correlation between the reaction and separation systems;
(iii) Investigate the formation and separation of by-products and impurities;
(iv) Study how to eliminate wastes and prevent environment pollutions;
(v) Evaluate plant flexibility to changes in feedstock or products policy;
(vi) Validate the process instrumentation, and enhance process safety and control;
(vii) Update the process documentation and prepare future investments, and
(viii) Optimize the economic performance of the plant.

2.7.2. Models of Cement Production Processes

In the literatures, there are several models for cement production processes. Atul et al. (2012) presented a cement plant model designed on LabVIEW platform. The model generates process data and electrical parameters for all lines of workshops in the cement industry. The model is universal to all types of cement plants. However, the model is not predictive in a sense that it does not explain much about what happens to other parameters of the process in case of any system disturbance. Also it does not indicate clearly how optimization of the overall process of the plant can be performed.

In cement production processes, there are several studies presenting models for the purpose of studying use of alternative fuels in cement production processes (Benhelal and Rafiel 2012; Kääntee et al. 2004). Ibrahim et al. (2012) presented a simulation model for emission and particulate matter (PMs) from a cement plant. Yokota (2005) proposed a detailed model of cement clinker burning process using three different simulation software interfaces, namely, Aspen Plus. Thermodynamic data and solution models of FactSage were accessed in the Aspen Plus flow sheeting simulation via ChemApp interface.

A more recent rigorous model for cement production process is presented by Hökfors (2014). The model is a continuation of author's research (Kääntee et al. 2004) and it presented a detailed phase chemistry for cement clinker and lime production. The objective of the study was to evaluate if developed phase chemical process model for cement clinker and lime production processes is reliable to use as a predictive tool in understanding changes when introducing sustainability measures. The study described development of the process simulation model in application of sustainability measures as well as evaluation of the model.

The model used three computer simulation software, namely, Aspen Plus. Sustainability measures like use of new combustion technologies, which increase the ability to capture carbon dioxide were modeled. The model was used to evaluate oxy-fuel combustion. The developed model was validated against industrial data from one lime production plant and two cement industries. Simulated scenarios of co-combustion involving different fuels and different oxy-fuel combustion cases in both cement clinker and lime rotary kiln production are described as well as the influence of greater amount of sulfur on the cement clinker quality.

On the other hand, in literature, there are many physical models with limited chemistry. Examples of models using Computational Fluid Dynamics (CFD) were developed by some proponents (Mastorakos et al. 1996; Mujumda and Ranade 2006; Fidaros et al. 2007).

2.8. Conclusions on Models of Cement Production Processes

In concluding, it can be commented that Kääntee and colleagues (2004), Hökfors (2014) and Yokota's (2005) models are much focused on chemistry of clinker formation, and shed more light about chemical processes taking place during clinker formation including the final product.

However, all these models do not address issues of real inefficiency taking place in cement production processes, equipment and the overall system. They do not address, for example, issues of irreversibility associated with chemical reactions and therefore, did not discuss about energy use improvements in this aspect. Nonetheless, most models found in literature are based on the first law of thermodynamics alone. These models cannot give insight to improvement of energy systems in the perspective of minimization of irreversibility.

The purpose of the current study is to fill in the gap by providing a model that deals specifically with optimization of energy use in cement production processes using both first and second laws of thermodynamics. In due regard, the developed model was advanced by making use of exergy analysis so as to identify inefficient processes and components within the system. The study developed a model of a 4-stage preheater cyclone, dry process rotary kiln cement production process of Mbeya Cement (MCC) with production capacity of about 770 ton per day. In addition, the developed model was validated against actual plant data and utilized to examine influence of the main operating parameters on plant performance.

2.9. Application of Exergy Analysis in Cement Production Processes

2.9.1. Introduction

Exergy analysis is one of emerging powerful and effective analytic tools for designing as well as analysis of energy systems. Exergy analysis is also very useful for furthering the goal of highly efficient energy resources use by assessing meaningful efficiencies and enabling locations, types and true magnitudes of inefficiencies caused by waste including losses to be determined. Furthermore, exergy analysis reveals not only whether or not it is possible to design a greatly energy efficient energy systems, but also quantifies by how much designing of a more energy efficient systems is possible by reducing inefficiencies in the existing system processes and components.

2.9.2. Exergetic Analysis Studies in Cement Production Processes

In this subsection, review of developments made in using exergy analysis as a tool for evaluating cement production processes and major results obtained are briefly presented. Generally, exergy analysis has recently gained acceptance in evaluating cement production processes. The number of studies on this area is not so large and most of them aimed at particular equipment or unit of production processes like coal preparation unit (Sogut et al. 2009), raw mill (Utlu et al. 2006) and grate cooler (Madlool et al. 2012). There is a relatively substantial number of studies that evaluated the performance of the cement rotary kiln system using exergy based methods (Kolip and Savas 2010; Farag 2012; Farag and Taghian 2015; Gürtürk and Oztop, 2014; Parmar et al. 2016; Kolip 2010; Koroneos et al. 2005; Camdal et al. 2004; Kol and Chaube 2013, Boyaghchi 2014; Jijesh et al. 2015; Ajith et al. 2014; Rasul et al. 2005). Madlool et al. (2012) presented an overview of exergy analysis for cement production processes from various sources and concluded that the exergy destruction of different sub-systems vary from 18 % to 49 %. Exergy analyses have also

been used with a combination of other techniques, for example, exergoenvironmental evaluation for studying the environmental performance of cement production processes (Diji et al. 2013), exergoeconomic analysis (Atmaca and Yumrutas 2014) and thermoeconomic analysis (Valero and Abadias 2016).

Major results obtained from these studies, especially exergetic performance variables, are presented in Appendix 9. In general, results obtained from these studies are comparable and agree well in most cases, but also there are relative variations from one study to another. The source of variability could be due to differences in technology employed, namely, wet processes versus dry process, kiln system configuration, for example, kiln system with preheater cyclone and pre-calciner versus preheater cyclone without pre-calciner, variation of number of staged cyclones, different types of clinker coolers, different production capacities, variation in raw material composition and different types of fuel used.

Also another source of deviation from one study to another could be the choice of system boundary. Nevertheless, a few of such studies came up with contradicting results. For example, values of exergetic efficiencies for overall system and units were found to be larger than energetic efficiency (Madlool et al. 2012; Kol and Chaube 2013, Rasul et al. 2005). Such results are very surprising because usually exergy efficiency of systems and components are always less in magnitude than energy efficiency. Also Madlool et al. (2012) concluded that the raw feed pre-heating causes the lowest irreversibility within the cement plant, which contradicts with many studies found in literature as summarized in Appendix 9.

Most exergetic analyses studies found in literature correctly concluded that the main source of irreversibility encompasses chemical reactions and heat transfers taking place in the rotary kiln (Atmaca and Yumrutas 2014, Madlool et al. 2012, Camdali et al. 2004, Gutiérrez et al. 2013, Kolip 2010, Diji et al. 2013, Boyaghchi 2014, Rasul et al. 2005, Farag and Taghian 2015,). Results obtained from exergetic analysis refute conclusions from most studies done using the first law of thermodynamics alone. The studies found in literature using first law of thermodynamics to evaluate performance of cement production process have incorrectly concluded that the major source of inefficiency is heat loss due to exhaust gases and dust from preheater cyclone (Engin and Ari 2005; Khurana et al. 2002; Kabir et al. 2010; Farag et al. 2013). However, other exergetic analyses studies concluded that the major source of irreversibility is the preheater pre-calciner cyclone (Koroneos et al. 2005; Kolip and Savas 2010; Farag 2012; Farag and Tughian, 2015; Kol and Chaube 2013). The latter are not contradicting with the previous ones in any way but they are in good agreement. The truth is that in the rotary kiln with preheater pre-calciner calcination of up to 90 % and substantial amount of combustion of fuel up to 60% of fuel takes place in the preheater pre-calciner instead of the rotary kiln (CEMBUREAU 1999; ICR 2005; Farag and Taghian 2015). Thus, it is expected that there should be more irreversibility at the preheater pre-calciner than in the rotary kiln, since most of the chemical reactions that are major sources of irreversibilities are shifted from the rotary kiln to the pre-calciner.

Also most of the said studies have correctly indicated that exergetic efficiency to evaluate overall performance of systems and components is lower than the first law efficiency. The calculated exergetic efficiencies indicated that there is still a potential for further performance improvement. Some studies suggested various methods of lowering irriversibilities in each major component based on their types and causes (for example, Kolip 2010; Farag 2012; Farag et al. 2013; Farag and Taghian 2015, Parmar et al. 2016).

2.9.3. Exergy Analysis with Flowsheeting Simulators

Although exergy based method gained an acceptance as a powerful tool for optimization of energy systems, the method is rather complex. Hence, it is time consuming to carry it manually especially when analysis of large and complex energy systems is required. To simplify carrying out exergy analyses especially for large complex systems, researchers have made several attempts to develop exergy-based methods using computer software simulators. However, exergy analyses with flow sheeting simulators have been very challenging and not common due to limitation for most existing computer aided simulation software.

Furthermore, it has been even more difficult to simulate processes, which include themodynamic properties of fluids and solids in the same simulating environment software. It could be due to the aforementioned constraints that to the best of the author's knowledge, there are almost no exergetic studies using simulators carried out in the area of cement production processes. Due to lack of past works that specifically dealt with exergy analysis in cement production process using simulators, it is preferred to present few studies found in other areas to demonstrate achievement made so far. Nevertheless, even in such other areas of industrial processes and plants, only few studies exist.

Studies that made attempts to use a combination of more than one simulator or provision of sub-routine or other programming skills to enhance exergy analysis using simulators started around 1990s. Hinderink et al. (1996) presented a method for calculating absolute exergy of multicomponent liquids vapor of two phase flows in a synthesis gas plant. Aspen Plus and Exercom software were used in the study. The study successfully evaluated exergy analysis of a synthesis gas production plant. Within the study, the exergy destruction for each process was evaluated. Also the study evaluated the exergy destruction based on the final product yield and exergetic efficiency, and at the end, the study suggested improvement measures. Abdollahi-Demneh et al. (2011) proposed what is so called straightforward method for calculating physical and chemical exergies of material streams.

The study proposed a procedure for exergy calculation and implemented it in HYSYS flow sheeting simulator by utilizing fifteen main user variables for material streams. The study developed Visual Basic Codes for each of the mentioned user variables in order to enable exergy analysis in HYSYS process simulator. Ghannadzadeh et al. (2012), presented a general methodology for exergy balance in chemical and thermal process in ProSimPlus simulator. The study

presented a calculator that became part of ProSimplus process simulator without further need to any other external programs for performing exergy balance.

In general, the presented research works in regard to exergy analysis using flow sheeting simulator found in literature are few and are based on establishing a subroutine, which is coupled to Aspen Plus simulator or any other simulator for the purpose of enhancing the simulators to be able to carry exergy analysis. However, all trials found in literature did not include simulation of processes including both fluids and solid processing. Nevertheless, the past studies have contributed significantly on use of simulators in carrying out exergy analysis.

The development made pave a way on use of simulators to simplify exergy analysis especially for large and complex systems. On the other hand, efforts of scientists and researchers to carry exergy analysis using simulators resulted into a need for developing a highly powerful simulator that can handle exergy analysis. Apparently, it is good such efforts that resulted into development of Aspen One Plus V8 with features for exergy analysis and can work with both solids and fluids processing. However, there is still work to be done to further development of the simulator especially its data base so that it can include more compounds especially for cement production processes (Höfkors 2014; Kääntee 2004; Yokota 2005).

Chapter Three – Research Methodology

3.1. Introduction

In this chapter, the research methodology employed to achieve the objectives of the research is presented. Fig. 3.1 presents a summary of major steps followed in carrying out the study.

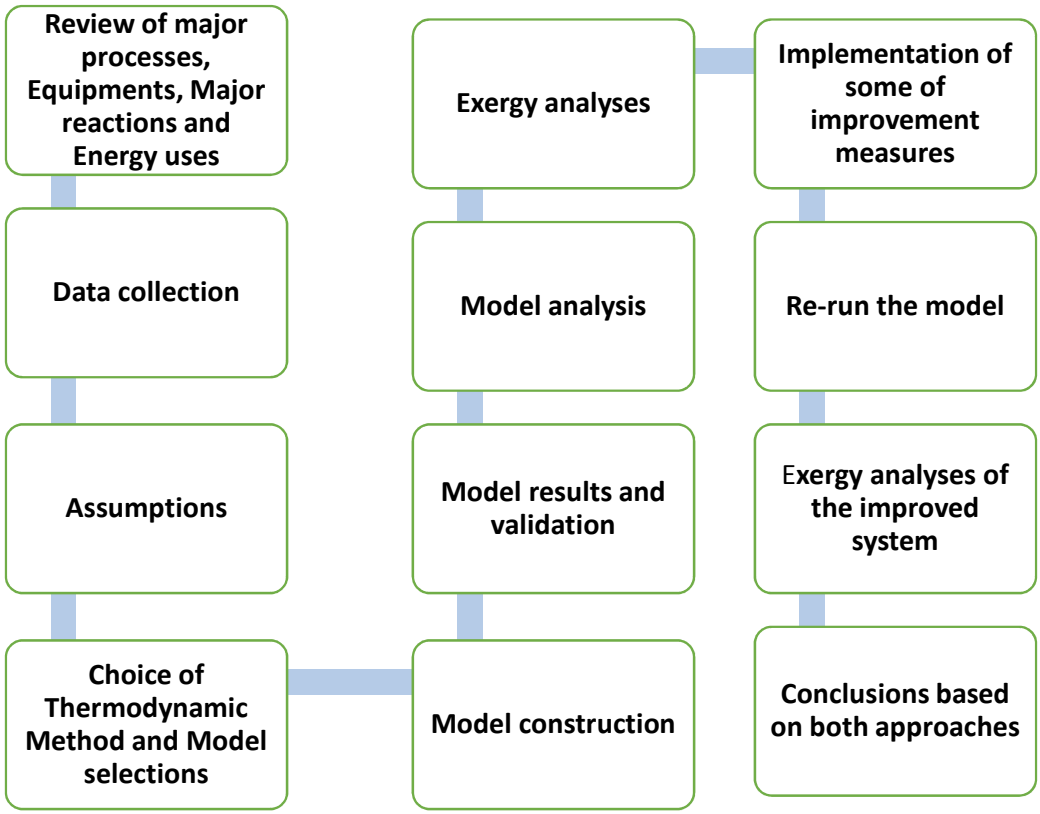

Figure 3.1. Summary of major steps in carrying out the study

Recall, the main objective of the study was to investigate performance of cement industry in Tanzania relative to sustainable energy utilization. The study focused on improving energy efficiency of the dry rotary kiln system at Mbeya cement industry, and sought to identify opportunities for energy conservation. In due regard, the study examined performance of the kiln system in the light of the first and second law of thermodynamics. The data for the existing system about current useful energy consumption were obtained and analyzed to identify inefficiencies and then improvement measures were proposed.

The main objective was achieved through two complementary approaches: The first approach involved modeling and simulation of cement production processes at Mbeya cement factory. The purpose of modeling was to develop a model of cement production process, validate the model by using actual plant data and utilize the model to predict performance of the cement dry rotary kiln system. The model was developed, validated and finally, it was used to

model cement production processes by identifying inefficient process in the system and major components. The following are sub-tasks involved for this approach:

(i) To develop a model for simulation of cement production processes at Mbeya cement factory;
(ii) To evaluate/validate relevance of the model against available plant operating data for simulating cement production processes;
(iii) To identify components including parameters having a large influence on useful energy consumption in the cement production processes together with potential inefficiency improvements, and
(iv) To evaluate alternative process improvement measures.

The outcomes from modeling are preliminary prediction of system characteristics and data were retrieved from the model for further analysis of the process by using exergy-based method.

The second approach involved use of exergy based method as a tool to identify causes, magnitude and specific location where thermodynamic inefficiencies occur. Bejan et al. (1996) suggested that the exergy method can be suitable for furthering the goal of more efficient energy-resource use, for it enables the locations, types and true magnitudes of wastes including losses to be determined. Therefore, exergy analysis can reveal whether or not and by how much it is possible to design highly efficient energy systems by reducing sources of inefficiency in existing systems. Furthermore, Tsatsaronis and Park (2002) pointed out that to evaluate the thermodynamic performance as well as the cost effectiveness of thermal systems, and to estimate the potential for improvements, it is always useful to know an avoidable part of exergy destruction and an avoidable investment cost associated with a system component. Improvement efforts should then focus only on these avoidable parts. To achieve the main objective, through the second approach, the following sub-tasks were involved:

(i) To apply mass and exergy balances to each individual component of Mbeya cement production process, sub- system and the whole system at large;
(ii) To evaluate exergetic efficiency of *k*-th component and of the overall system;
(iii) To identify major factors that affect the useful energy consumption of different cement production sub-processes, and
(iv) To suggest methods for efficiency improvements and conservation measures.

Exergy based method has been successfully applied in evaluating other energy systems like power generation and refrigeration systems (Kotas 1995; Bejan et al. 1996; Morosuk and Tsatsaronis 2008; Morosuk and Tsatsaronis 2009; Tsatsaronis and Park 2002; Cziesla et al. 2006; Yang et al. 2013; Petrakopoulou et al. 2012; Morosuk and Tsatsaronis 2011; Tsatsaronis and Morosuk 2010; Boyano et al. 2012; Sorgenfrei and Tsatsaronis 2016; Penkuhn et al. 2015; Tesch et al. 2016). Nevertheless, the method is not widely used in the field of chemical and processing industries like cement

production, paper manufacture, iron and steel, methanol, sulfuric acid and the like hence, it was lowly applied in these areas (Hinderink et al. 1999; Luis and Van der Bruggen 2014). It has been pointed out that low application of exergy based method in the field of chemical and processing industries could be due to complexity of processes taking place in the industries or may be influenced by most pioneer of exergy based method coming from mechanical engineering field and hence, applied the method mostly in energy and power generation as well as refrigeration systems (Hinderink et al., 1999; Luis and Van der Bruggen, 2014). However, Luis and Van der Bruggen (2014) argue that exergy-based methods should be more applied in the field of chemical and processing industries, since the industries are potential main target in which exergy destruction can be significantly reduced.

On the other hand, modeling and simulation have been applied successfully to the evaluation of a wide range of energy systems including cement production processes as discussed in Chapter Two of this thesis. Extensive reviews of different models of cement production processes are presented in Chapter Two of this thesis. Therefore, it is expected that this study will throw light on power of exergy-based methods with simulators in evaluating performance of cement production process.

The evaluation of complex processes like cement production processes needs adequate conceptual methods and powerful computer based tools. A systematic evaluation approach is needed for successful modeling of the process. Knowledge about cement production processes, major equipment principal of operation and physio-chemical reactions involved is very important. Therefore, study of type of energy being used, study of machines or technology employed and process study were necessary before starting of modeling work. In due regard, Chapter Two of this thesis presents extensive review of state of the art in cement production processes.

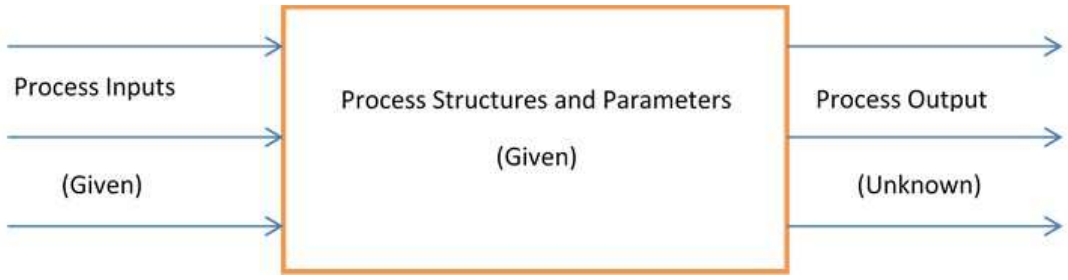

Figure 3.2. A typical process simulation problem (El-Halwagi 2012)

The purpose of simulation is to model and predict performance of a process. It involves decomposition of the process into its constituent elements (e.g. units) for an individual study of performance. The process characteristics (e.g. flow rates, compositions, temperatures, pressures, equipment sizes, etc.) are predicted using analysis techniques. In addition, process analysis may involve use of experimental means to predict and validate performance. In this case, real operating plant data were collected for model validation. Therefore, in process simulation, the process inputs as well as flow sheets are given and it is required to predict process outputs.

In order to reveal locations of major losses and irreversibility, the major process in the kiln system was split into three major sub-systems containing specific process steps, namely, preheater tower, rotary kiln and the cooler. Furthermore, the rotary kiln was divided into burning and calcination zones. However, the stage specifies where the following takes place: combustion, burning, belite formation, pre-heating, calcination and cooling of clinker. The detailed description of model development can be found in Section 4.2. of this thesis.

Exergy analyses for individual components, kiln sub-systems and overall kiln system are presented in Chapter Five. Exergy flow rates of all material streams were calculated with the flow sheeting simulator simultaneously with energy and mass balance calculations. Useful and waste streams leaving the system boundaries were defined. Overall performance was determined based on per unit clinker produced (per kg clinker output). Performance of sub-systems was determined by accounting and determining the nature of revealed imperfection (exergy destruction and loses due to irreversibility within sub-system's boundaries). Furthermore, exergetic variables for individual system components, kiln sub-systems and overall system were determined. Proposed improvement measures are presented in Chapter Six. Some of the improvement measures were tested to demonstrate if they can really improve performance of individual components, kiln sub-systems and the overall system.

3.2. System Boundary Definition and Scope of the Thesis

This section describes briefly the scope of the system considered for study. The study investigated useful energy consumption directly related to production processes in the kiln system. Other facilities like storing, packaging, logistics, offices, laboratory and transport are not part of this research work. The study identified efficiency improvement opportunities on the basis of performance of equipment relative to various materials and energy stream flows and interactions.

Thus, the discussion under this study focuses on the main unit operations constituting cement production processes referred to in this thesis as rotary kiln system. The cement kiln system consumes more than 90 % of energy input to the process and thus, it is worth to pay more attention on it (Junior 2003; Khurana et al. 2002; Worrell et al. 2009). Raw material preparation, cement grinding and fuel preparation were not considered in this study. The sub-process of quarrying, and cement dispatch are beyond the system boundaries selected for this study due to the fact that they are not intrinsic or specific for cement manufacturing processes (CEMBUREAU 1999). The overall generic cement production processes are presented in a simplified process flow sheet (Fig. 3.2). The system boundary considered for this study is presented in Fig. 3.3. Streams for material flows and exhaust gas flows through various sub-sections are shown using arrows with different types and colours. Also major equipment and sub-systems considered for study are shown in the same figure. In general, major sub-systems indicated in the figure and their boundaries are preheater tower, rotary kiln and clinker cooler. Therefore,

these three major sub-systems together form the rotary kiln system. The boundary for the rotary kiln system is indicated using dotted lines.

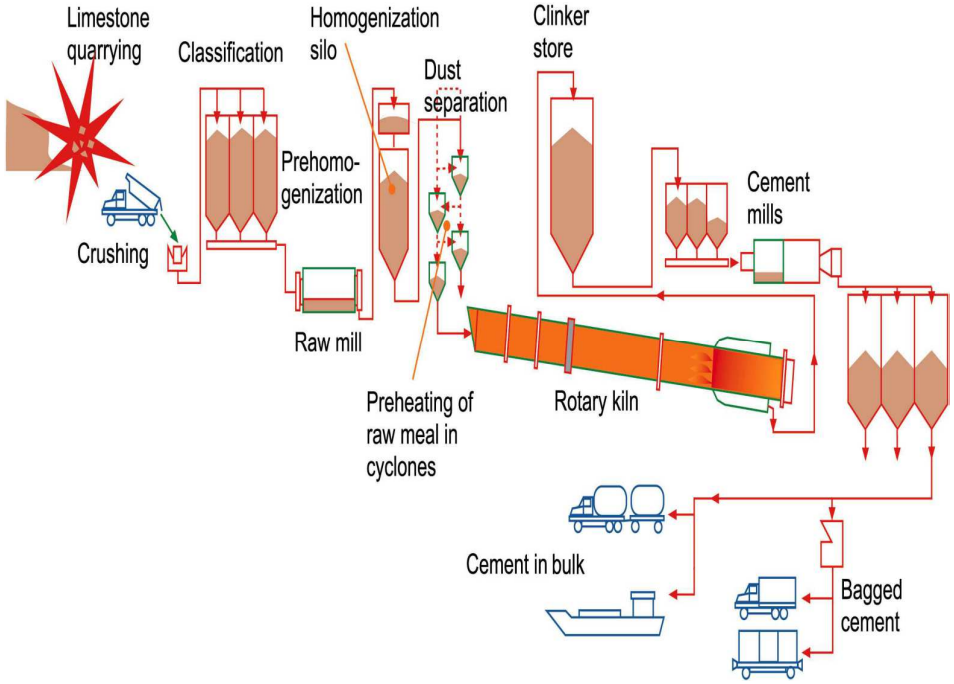

Figure 3.3. Flowsheet of cement production process (Kääntee et al. 2003)

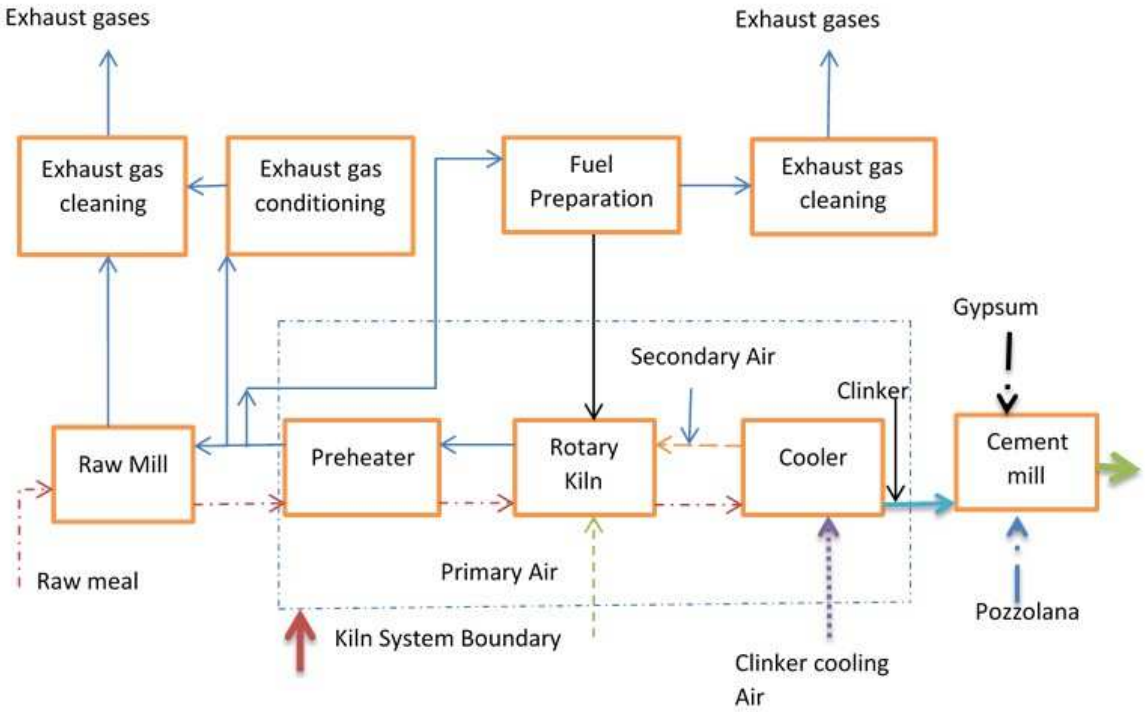

Figure 3.4. MCC plant system boundary for evaluation

3.3. Data Collection Methods

Data used for this research work were obtained from Mbeya Cement Company LTD (MCC). These data were retrieved from recorded plant data from daily measurements done manually or from plant automatic control system data base, from plant laboratory analyses and the like. The main collected data from the plant were categorized into two: System data that included process, type of kiln, nominal capacity, type of preheater, type of cooler, supplier, year of commissioning, fuel and firing system, type of burner, dimensions of main equipment (size, inclinations etc.) and data on fans, drivers and so forth. Operation data included various operating data (rotation in rpm, rated power in kW, temperature and pressure profiles along kiln system etc.), electrical power readings, chemical analysis of raw meals, coal analysis, ash analysis, dust analysis, clinker analysis and the like. The mentioned data are presented in Chapter Four of this thesis (Tables 4.1 ÷ 4.4) and Appendix 8.

3.4. Model Construction

The model developed in this study is a steady state model. The model was constructed based on analysis of simulation problem made based on the collected plant process flow sheets, and in-depth study of major process equipment constituting the defined system boundary. Also problem analysis involved in-depth understanding of all major processes in the cement production system as well as physio-chemical reactions taking place in the system. Cement production processes involve very complex physio-chemical reactions of which some are well known while others are not and hence, there are several attempts made by researchers to develop models for studying these phenomena (Kääntee et al. 2003; Kääntee et al. 2004; Hökfors 2014; Mastorakos et al. 1999; Teleschow 2012; Fidaros et al. 2007; Küssel et al. 2009; Miculcic et al. 2012; Yokota, 2005).

Real Process Flow Diagram (PFD) was translated into a scheme compatible with simulator by selecting simulator blocks interconnected with materials and heat streams. The global Aspen Plus model for a rotary kiln system is presented in Fig. 4.5. Thermodynamic conditions were specified accordingly, for example, operating pressure and temperature of the blocks and streams based on real operating pressure and temperature profile of the 4-stage preheater cyclone rotary kiln. Furthermore, the collected plant PFD was translated into Process Simulation Diagram (PSD) based on simulation goals of each major sub-process. For example, in real life, rotary kiln can be considered as a single reactor, while in Aspen Plus, the rotary kiln can be split into different sub-sections to simplify simulation work and clearly identify each process occurring in the kiln, depending on objectives of the study.

The procedures for problem analysis are summarized in Fig. 3.5. Detailed procedures for simulation problem analysis are found in Dimian (2003). However, some aspects worth to be considered include converting PFD into PSD, which involves splitting of the flow sheet into several

sub-flow sheets if necessary. Others include analyzing the simulation model for each flow sheet unit, defining chemical conversion components and choice of thermodynamic model.

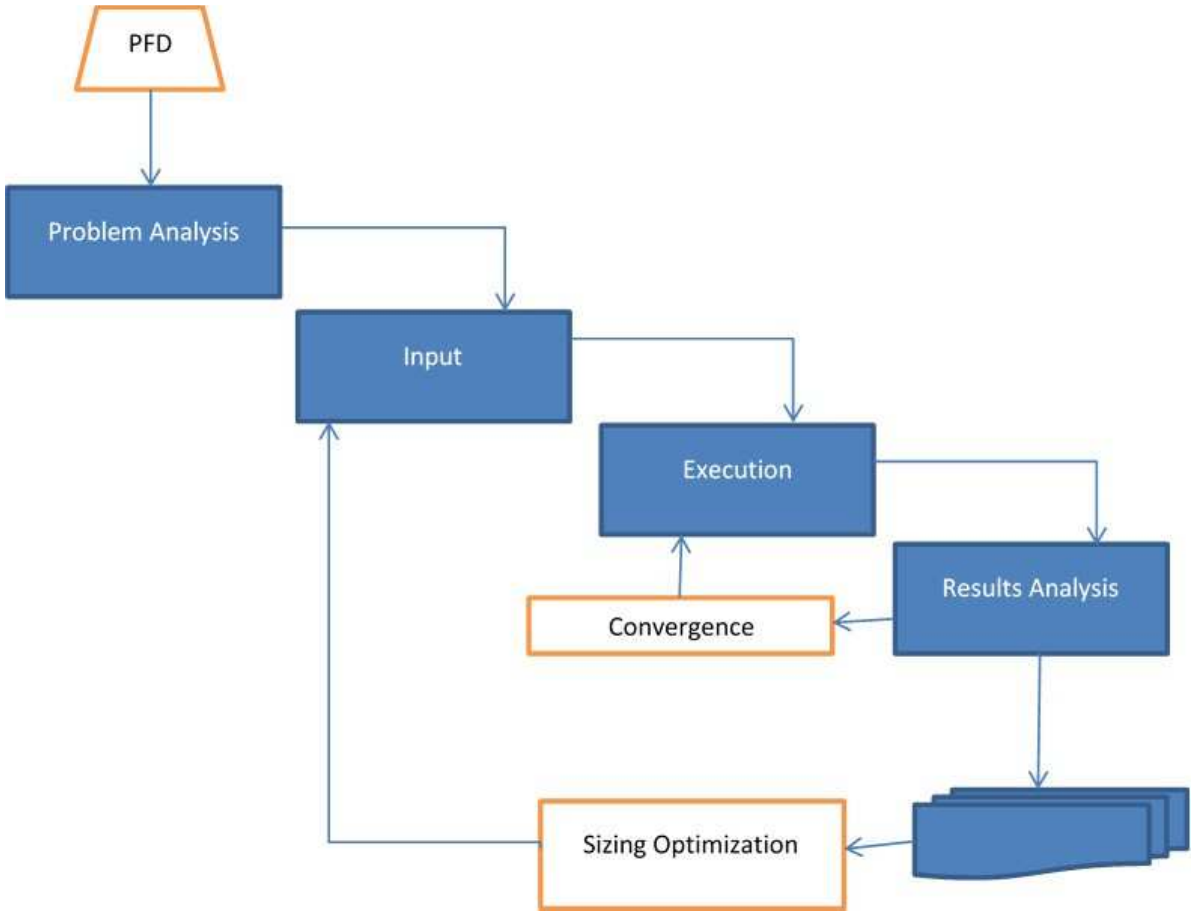

Figure 3.5. Methodological levels in a steady state simulation (Dimian 2003)

3.5. Model Validation

Results obtained from the model are compared and evaluated according to real plant performance data. Some parameter data from the model used to validate it against real plant data were production capacity, the amount of energy used in the process, clinker composition, kiln temperature profile, ID-FAN power, backend % O_2, downcomer % O_2 and combustion flame temperature. Comprehensive validation work is presented in Section 4.2.5. Simulation was done according to assumptions described in Chapter Four (Section 4.2.2.). The model's performance was checked based on postulated assumptions and real plant data collected. The model was verified to check if it behaved in the right way and accurate representation of the MCC production system simulated.

3.6. Model Analysis

The developed model was adjusted using model parameter sensitivity analysis to study the impact of change on input parameters of interest to the system like fuel flow rates to combustion product temperature intensity in burning zone, which, in turn, indicates clearly if it is

within the acceptable value for cement clinker burning. The combustion gases must reach a temperature of up to 2000 °C in real processes. Combustion efficiency in the kiln burner is equally important for kiln performance. Therefore, by varying fuel flow rate and combustion air, it was possible to investigate completion of combustion processes and composition of exhaust gases at the kiln back end, which is used to study optimal excess air required for clinker burning. Usually cement clinker burning must be done at 10 % – 15 % excess air for maintaining quality of clinker chemistry and also for maintaining stable operation condition of the kiln system (ICR 2005). Also gas composition analysis will indicate the amount of thermal energy waste in the kiln system. This is done by checking the temperature profile at the preheater cyclone stages and exit exhaust gases from the preheater tower.

3.7. Theories and Laws Underlying the Research

In this section, theories and laws underlying this study are presented. In general, the study was guided by the first and second laws of thermodynamics. The first law of thermodynamics points out that energy is always conserved and cannot be destroyed. The second law of thermodynamics is the law of entropy generation, which is the measure of all irreversibilities occurring within the control surface due to chemical reactions, heat exchange, mixing, friction, etc. (Tsatsaronis 1993).

The first law of thermodynamics has been widely applied for evaluation of energy efficiency in cement production processes. There exist several publications discussing performance of cement production process in this aspect (Engin and Ari 2005; Khurana et al. 2002; Kabir et al. 2010; Madlool et al. 2011; Farag et al. 2013). Although studies applying the first law of thermodynamics alone (analyses based on mass and energy balances) for evaluation of energy efficiency in cement production process shed light on performance improvement, however, these studies have some limitations. It has been proved that the first law of thermodynamics by itself fails at some points to reveal the real thermodynamic imperfection of energy systems (Tsatsaronis 1993; Bejan et al. 1996; Kotas 1995; Bejan 2002).

Some of the limitations of the first law as listed by Tsatsaronis (1993) are very applicable in disqualifying use of first law of thermodynamics alone for evaluation of cement production processes especially for the cement rotary kiln system. The processes taking place in the kiln system involves combustion reactions as well as other complex physical and chemical reactions, which are the major source of irreversibility. Also the processes involve complex heat exchange between solids from a large volume of raw materials fed in the kiln system and hot gases from both combustion of fuels (coal, pet coke, natural gas etc.) and decomposition reaction of $CaCO3$, calcium carbonate (limestone). Furthermore, the process involves mixing and separation of fluids and solids at various compositions and temperature as well as pressure profiles. Energy degradations taking place in all the aforementioned processes cannot be revealed by using mass and energy balances of the energy system (first law analyses) alone. For example, major

results from studies for cement production processes performance using the first law of thermodynamics alone suggest that the major cause of inefficiency is heat loss from flue gases and dust from the preheater cyclones (Engin and Ari 2005; Khurana et al. 2002; Kabir et al. 2010; Farag et al. 2013). Contrary, studies conducted using both first and second laws indicate correctly that the major source of real inefficiency in cement production processes is due to fuel combustion, chemical reactions and heat transfers taking place in the rotary kiln (Madlool et al. 2012; Camdali et al. 2004).

On the other hand, although entropy can help to explain the direction of energy transfers and conversion, hovewer its practical application in the evaluation of process efficiency of energy systems (for design and operation) is very limited. At this juncture, it is where the first and the second laws of thermodynamics need to complement each other by introducing another property known as exergy. Contrary to energy, which is always conserved, exergy is always destroyed in all irreversible processes. Exergy is defined as the maximum theoretical useful work (shaft work or electrical work) obtainable from an energy conversion system as the system is brought into thermodynamic equilibrium with the thermodynamic environment while interacting only with that environment (Moran and Shapiro 1992; Bejan et al. 1996). Bejan (2002) listed out the following attributes of exergy compared to its counterpart energy and entropy:

(i) It makes it possible to compare on a common basis different interactions (inputs, outputs, work, and heat), and
(ii) By performing exergy accounting in smaller and smaller subsystems, people are able to draw a map of how destruction of exergy is distributed over the engineering system of interest. In this way, people would be able to pinpoint components and mechanisms (processes) that destroy exergy the most.

In regard to energy sustainability, Luis and Van der Bruggen (2014) point out that social, environmental and economic factors play a role in the critical evaluation of a process and exergy could be considered as the property that joins together those three cores of sustainability. Thus, this study utilized the advantage of exergy analyses to evaluate performance of MCC cement dry rotary kiln in the aforementioned perspective. A substantial number of publications indicated that energy is the main part of production cost for most chemical and processing industries as discussed in Chapter Two. Thus, energy cost should be minimized and exergy analyses can be used to optimize the process from this perspective. Hinderink et al. (1999) argued that degree of sustainability of the process industry can be viewed in the following three parameters:

(i) Thermodynamic efficiency (exergy efficiency);
(ii) Use of renewable resources (at least to produce the fraction of exergy that will be destroyed during the production process), and
(iii) The extent to which circles (reuse, recycling) have been closed.

Thus, looking into perspectives of sustainability in industrial processes, exergy analyses can be applied to minimize use of natural resources, since the thermodynamic imperfection of the process can be detected and quantitatively assessed. Improvements of the detected imperfections through various exergetic variables, in turn, can lead into reduction of fuel and raw materials used for production. The impact of fuel and raw material reduction will be reflected into low emissions of CO_2 from the kiln system to the environment since CO_2 results from both calcination of $CaCO_3$ from raw materials and fuel combustion. Furthermore, reduction of raw materials and fuel used will conserve the natural environment and extend the period of their availability for future use. Additionally, increasing exergy efficiency of cement production process consequently, will lead into cheaper production processes and higher competitiveness. Introduction of alternative fuels from renewable energy resources to the kiln system and heat recovery from the waste energy streams from the kiln system will both contribute to degree of sustainability to cement production processes.

3.7.1. Energy and Exergy Analyses

In order to carry out the analysis properly, reviews of theories underlying energy and exergy analysis are presented in this subsection. The extensive review on past studies of exergy application in evaluating cement production processes are presented in Section 2.9.2. Detailed exergy analyses are presented in Chapter Five.

3.7.1.1. Mass, Energy and Exergy Balances

The exergy balance was applied to sources of exergy input and output of the predefined kiln system. Since the kiln system was assumed to be an open system operating under steady state conditions, the mass balance is given by:

$$\sum_{i=1} \dot{m}_i = \sum_{j=1} \dot{m}_e \tag{3.1}$$

whereby $\dot{m}_i$ [kg·s^{-1}] stands for input flows and $\dot{m}_e$ [kg·s^{-1}] stands for output flows across the kiln system boundary. The energy balance is given by:

$$\dot{Q} - \dot{W} = \sum_{e=1} \dot{m}_e \cdot h_e - \sum_{i=1} \dot{m}_i \cdot h_i \tag{3.2}$$

where, Q [kW] is the rate of heat transfer, $\dot{W}$ [kW] is rate of work, $\dot{m}$ [kg·s^{-1}] is mass flow rate and h [kJ·kg^{-1}] is specific enthalpy. Neglecting kinetic and potential energies, the control volume energy balance rate at steady state for the k-th component (Bejan et al. 1996) is:

$$\dot{Q}_{CV.k} - \dot{W}_{CV.k} + \left(\sum_{i=1} \dot{m}_i \cdot h_i \right)_k - \left(\sum_{e=1} \dot{m}_e \cdot h_e \right)_k = 0 \tag{3.3}$$

The total specific exergy of material streams is given by:

$$e = e^{\mathrm{PH}} + e^{\mathrm{KN}} + e^{\mathrm{PT}} + e^{\mathrm{CH}} \tag{3.4}$$

Kinetic and potential exergy is negligible for cement kiln system and thus, Eq. (3.4) reduces to:

$$e = e^{\mathrm{PH}} + e^{\mathrm{CH}}$$

Specific physical exergy of a material stream is given by:

$$e^{\mathrm{PH}} = (h - h_0) - T_0 \cdot (s - s_0) \tag{3.6}$$

Physical exergy associated with the *j*-th material stream is:

$$\dot{E}_j^{\mathrm{PH}} = \dot{m}_j \cdot e_j^{\mathrm{PH}} = \dot{m}_j \cdot \left[(h_j - h_0) - T_0 \cdot (s_j - s_0) \right] \tag{3.7}$$

Whereby h [kJ·kg^{-1}] is the specific enthalpy and s [kJ·kg^{-1}·K^{-1}] is the specific entropy. The subscript 0 refers to reference environment.

Cement production processes in the kiln system involve flow of solids and mixture of gases at various temperature and pressure profiles. The process also involves physiochemical reactions of various types. In due regard, chemical exergy of an ideal mixture of N ideal gases is given by:

$$\bar{e}_{\mathrm{MIG}}^{\mathrm{CH}} = \sum_{l=1}^{N} x_l \cdot \bar{e}_l^{\mathrm{CH}} + \bar{R} \cdot T_{\mathrm{o}} \sum_{l=1}^{N} x_l \cdot \ln(x_l) \tag{3.8}$$

The chemical exergy of multicomponent material stream is given by (Hinderink et al. 1996):

$$\bar{e}^{\mathrm{CH}} = L_o \sum_{i=1}^{n} x_{0,i} \cdot \bar{e}^{\mathrm{CH,ol}} + V_o \sum_{i=1}^{n} y_{0,i} \cdot \bar{e}^{\mathrm{CH,ov}} \tag{3.9}$$

whereby L_o [kmole·s^{-1}] and V_o [kmole·s^{-1}] represent liquid and vapor phase flow of n components in a stream, respectively. Then, $\bar{e}^{\mathrm{CH,ol}}$ [kJ·kmole^{-1}] and $\bar{e}^{\mathrm{CH,ov}}$ [kJ·kmole^{-1}] stand for standard chemical exergy of the liquid and gaseous phase components, respectively, while $x_{0,i}$ [–] and $y_{0,i}$ [–] stand for mole fractions of the i-th component of specified stream. Eq. 3.9 can be extended to include solid phase flow of n components in a stream respectively.

The chemical exergy of substances is tabulated by Morris and Szargut (1986). Exergy of the heat transfer across the boundary of the kiln system is given by:

$$\dot{E}_{\mathrm{Q}} = \dot{Q} \cdot \left(1 - \frac{T_0}{T} \right) \tag{3.10}$$

The kiln system is assumed to be an open system at steady state steady flow and thus, exergy balance is given by (Bejan et al. 1996):

$$\sum_{j=1}\dot{E}_{\mathrm{Q},j}+\dot{W}_{\mathrm{CV}}+\sum_{i=1}\dot{E}_{i}-\sum_{e=1}\dot{E}_{e}-\dot{E}_{\mathrm{D}}=0 \tag{3.11}$$

$\dot{E}_{\mathrm{i}}$ [kW] and $\dot{E}_{\mathrm{e}}$ [kW] are the total exergy transfer rates at the inlet and outlets, respectively. For the sign convention in all equations, it was assumed that work supplied to a system is positive. Likewise, the exergy balance rate of the control volume at steady state for the *k*-th component of the energy system can be given by (Bejan et al. 1996):

$$\sum_{j=1}\dot{E}_{\mathrm{Q},k,j}+\dot{W}_{\mathrm{CV}}+\sum_{i=1}\dot{E}_{k,i}-\sum_{e=1}\dot{E}_{k,e}-\dot{E}_{\mathrm{D},k}=0 \tag{3.12}$$

3.7.1.2. Exergy of Fuel and Product

The value of exergy destruction for the overall energy system can be calculated using the "Fuel-Product" concept. The product exergy represents the desired results (expressed in terms of exergy) generated by the system being considered and is denoted by $\dot{E}_{\mathrm{P}}$ [kW] (Tsatsaronis 2007). The fuel exergy represents resources (expressed in terms of exergy) expended to provide the product exergy: The fuel exergy is denoted by $\dot{E}_{\mathrm{F}}$ [kW]. The term "fuel exergy" is not limited to fossil fuels but represents, in general, the exergetic resources used to drive (to "fuel") the process being considered.

From the exergy balance for the total energy systems:

$$\dot{E}_{\mathrm{F,tot}}=\dot{E}_{\mathrm{P,tot}}+\dot{E}_{\mathrm{L,tot}}+\dot{E}_{\mathrm{D,tot}} \tag{3.13}$$

Using the same concept for component level, exergy balance can be expressed as:

$$\dot{E}_{\mathrm{F},k}=\dot{E}_{\mathrm{P},k}+\dot{E}_{\mathrm{D},k} \tag{3.14}$$

Exergy destruction is the exergy destroyed due to irreversibilities within a system, but exergy loss represents the exergy transfer to the system surroundings. If boundaries of a system or component are set where the temperature is equal to the reference environment temperature, exergy loss associated with heat transfer is equal to zero ($\dot{E}_{\mathrm{L},k}=0$).

The exergy efficiency is one of the most important criteria for evaluating the system or components from the thermodynamic point of view. The exergetic efficiency ε_k of a component is defined as:

$$\varepsilon_k=\frac{\dot{E}_{\mathrm{P},k}}{\dot{E}_{\mathrm{F},k}} \tag{3.15}$$

For the overall system:

$$\varepsilon_{tot} = \frac{\dot{E}_{\mathrm{P,tot}}}{\dot{E}_{\mathrm{F,tot}}} = 1 - \frac{\dot{E}_{\mathrm{D,tot}} + \dot{E}_{\mathrm{L,tot}}}{\dot{E}_{\mathrm{F,tot}}} \tag{3.16}$$

With the total exergy destructions $\dot{E}_{\mathrm{D,tot}}$ [kW] is equal to the sum of exergy destructions within the components $\dot{E}_{\mathrm{D,tot}} = \sum \dot{E}_{\mathrm{D},k}$

The exergy efficiency of clinker production considers the chemical exergy accumulated in the product, in this case, the chemical exergy of clinker. There are three input flows of exergy: exergy of the fuel, exergy of the raw meal feed, exergy of the combustion air. Also there are three exit exergy flows: exergy of the exit gas, the exergy of the clinker and the exergy of the heat loss through the kiln walls. The raw meal and the air enter the kiln at ambient temperature. From an exergy balance the following is obtained:

$$\dot{E}_{\mathrm{F}} = \dot{E}_{\mathrm{a}} + \dot{E}_{\mathrm{rm}} = \dot{E}_{\mathrm{g}} + \dot{E}_{\mathrm{Ck}} + \dot{E}_{\mathrm{w}} \tag{3.17}$$

where $\dot{E}_{\mathrm{F}}$ [kW] is the exergy of supplied fuel, $\dot{E}_{\mathrm{rm}}$ [kW] is the exergy of raw meal feed to the kiln system, $\dot{E}_{\mathrm{a}}$ [kW] is the exergy of the combustion air, $\dot{E}_{\mathrm{g}}$ [kW] is the exergy of the exit gases, $\dot{E}_{\mathrm{CK}}$ [kW] is the exergy of the clinker and $\dot{E}_{\mathrm{W}}$ [kW] is the exergy of the heat loss through the kiln walls. The chemical exergy of the fuel can be calculated from the following equation: (Bejan et al.1996)

$$\bar{e}^{\mathrm{CH}} = -\Delta G + \left(\sum_{p} n \cdot \bar{e}^{\mathrm{CH}} - \sum_{r} n \cdot \bar{e}^{\mathrm{CH}} \right) \tag{3.18}$$

Whereby, ΔG [kJ] is the change in Gibbs function for reaction, regarding each substance as separate at temperature T_0 [K] and pressure p_0 [Pa]. The terms in curly brackets correspond to terms in curly brackets of Eq. 3.18, evaluated using known standard chemical exergies together with the *n*'s giving moles of the reactants and products per mole of the substance, whose chemical exergy is being evaluated. Furthermore, the fuel specific heat energy consumption is calculated using the equation:

$$q = \frac{\dot{m}_{\mathrm{f}} \cdot HHV}{\dot{m}_{\mathrm{cl}}} \tag{3.19}$$

Where q [kJ·kg^{-1}] is specific heat energy consumption, HHV [kJ·kg^{-1}] encompass fuel higher heating values, $\dot{m}_{\mathrm{f}}$ [kg·s^{-1}] is fuel flow rate and $\dot{m}_{\mathrm{cl}}$ [kg·s^{-1}] is clinker flow rate.

3.7.2. Concluding remarks

It can be concluded that the exergy-based methods backed up with modeling and simulation fit very well objectives of the research. Description of how the methods are implemented is presented. Exergy based methods were employed successfully in other related studies. Challenges of both exergy based method and modeling and simulations are highlighted. However,

advantages of both methods outweigh limitations and hence, proved to be very useful for evaluations of performance of energy systems.

Chapter Four – Kiln System Process Modelling

4.1. Mbeya Cement Production Processes Description

Recall, Mbeya Cement Company Limited (MCC) is one among eight cement manufacturing companies in Tanzania. The company is located in Mbeya region, in southern highlands. Then 14 % of MCC is owned by Lafarge international, a company with several cement manufacturing industries all over the world. The plant was built in 1978 and till now it has undergone several changes to meet both plant operational requirements and cement consumers' demands. The company current production capacity stands at 770 tons per day (tpd). The company's production capacity has been growing dramatically during the recent years as a result of growing demand for cement in the country. To meet potential growing demands, the company has short-term as well as long-term expansion programs (Fig. 4.1). It can be observed that clinker production will be increased from the current value of 770 tpd to1200 tpd.

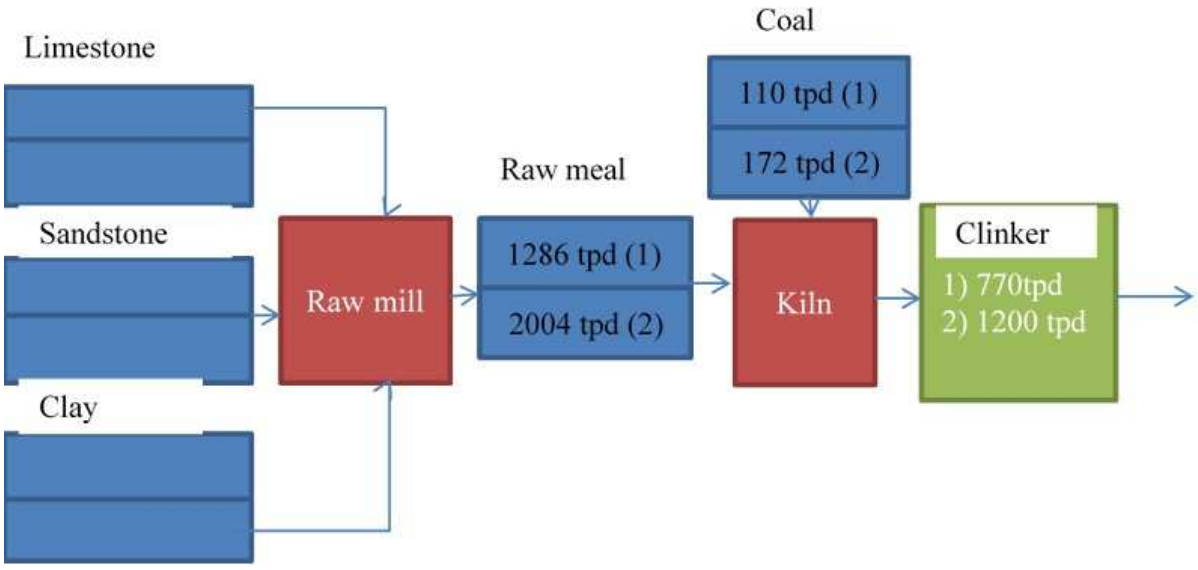

Figure 4.1. MCC Raw mill and kiln feed current and future expansion data:
1 - Stands for current data, and 2 - stands for future expansion

The major product of MCC is pozzolana cement (32.5N) and ordinary Portland cement (32.5N) is a minor product. In addition, 32.5N stands for the standard strength class of cement classifying its performance at 28 days. Cement is also tested at stages of 2 or 7 days, depending on the required performance of the product in order to establish an overall "strength class", which codifies standard strength with early strength. Other classes include 32.5R, 42.5N, 42.5R, 52.5N and 52.5R, where N and R stand for normal hardening and rapid hardening cement, respectively (Kurdowski 2014; Alsop et al. 2007; Kohlhaas 1983; Deolalkar 2016).

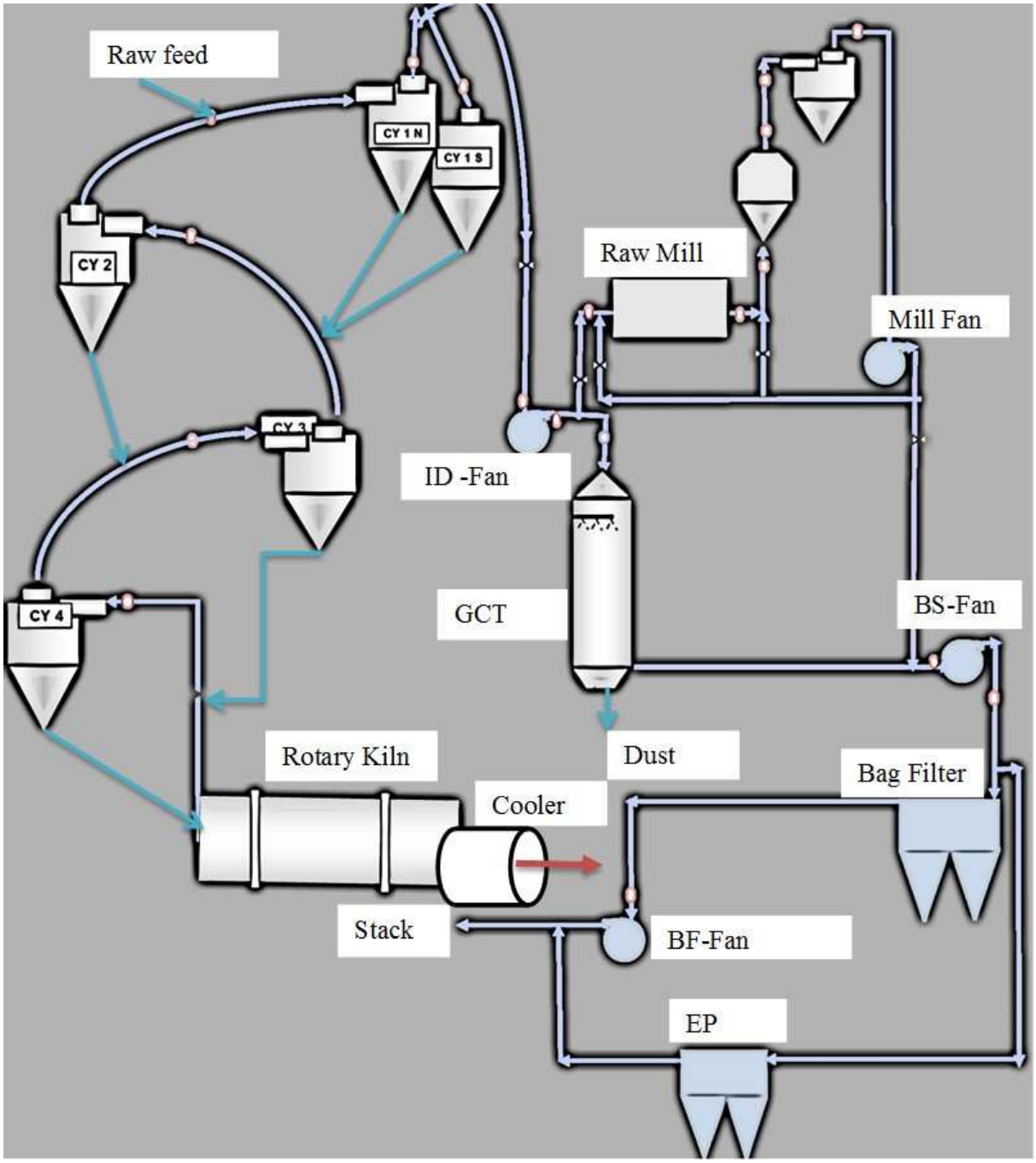

Figure 4.2. MCC Plant kiln system process flow sheet (MCC, 2013)

Strength class is the same for both pozzolana and ordinary Portland cement because the factory decided to have both products with the same strength class. Thus, they just manipulate the composition of raw feed of each type to make sure they end up with products of the same strength class or grade. Currently, coal is the only fuel used to provide heat energy demand for clinker burning processes. MCC uses three different types of coal fuel. Both, Mchenga and Erland are imported from neighbour country of Malawi, while Tancoal is obtained from Mbeya, Tanzania. Coal analysis is presented in Table 4.2, while ash analysis for Tancoal and Mchenga

coal mix is presented in Table 4.1 as part of raw meal mix design. MCC plant is a 4-stage pre-heater cyclone dry rotary kiln system (Fig. 4.2).

The MCC rotary kiln is with 58m long, 3.9 5m diameter, inclined at an angle of 3% of 10.8^0 and it rotates at 1.5rpm (Fig. 4.3 and Appendix 8).

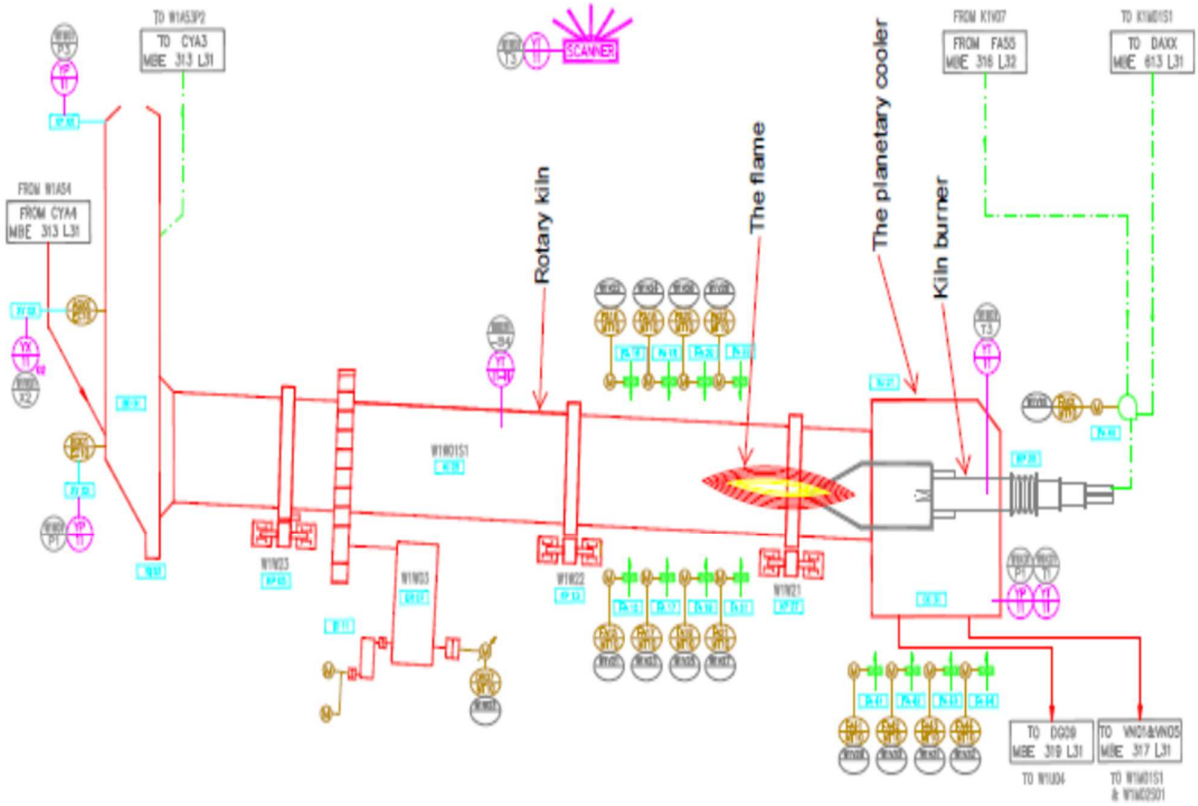

Figure 4.3. The MCC dry rotary kiln and planetary cooler (MCC, 2015)

Clinker phase formations are presented in Fig. 4.4. The specific heat requirement for clinker burning at MCC, primary air requirement, clinker cooling air and their flow rates are presented in Appendix 8. The type of clinker cooler employed at MCC is a planetary cooler. Specification data for the MCC planetary cooler are presented in Appendix 8. In general, the planetary cooler consists of a set of 9-11 well insulated steel pipe welded to the rotary kiln. Thus, there is no any addition motor drives needed to drive the planetary cooler. The latter is one of its advantages because it cuts down need for extra driving power as opposed to its counter grate cooler.

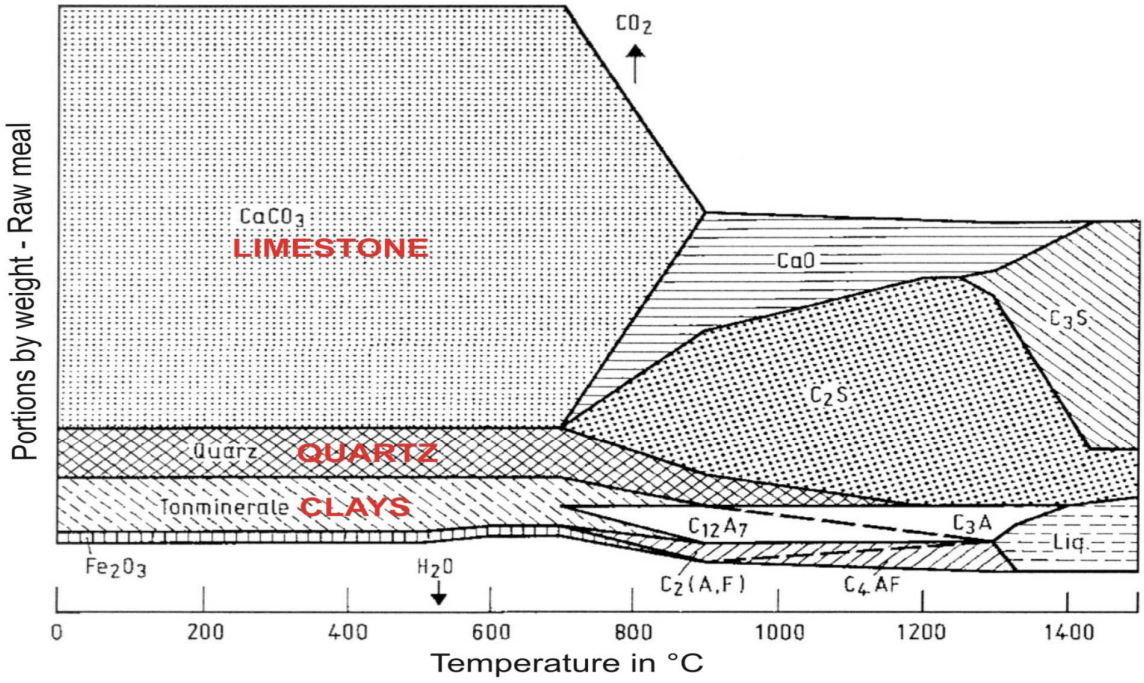

Figure 4.4. Clinker phase formations (Käänteet al. 2004)

4.2. MCC Rotary Kiln System Production Processes Model

In this section, there is presentation of the developed model. It includes the global flow sheeting of MCC Aspen Plus model as well as all sub-flow sheeting. Detailed descriptions of the model including the model blocks of Aspen Plus used (Fig. 4.5) and assumptions used for simulation (Section 4.2.2.) are presented. Also all data used for simulation and model description are presented.

4.2.1. Model Input Data

In this section, all necessary input plant data used for model simulation are presented. Generally, input data include coal flow rates as well as coal analysis, which encompass ultimate, proximate and ash analysis, respectively together with Particle Size Distribution (PSD) for coal and raw meal, raw meal flow rates $\dot{m}_{rm}$ [kg·s^{-1}], primary and secondary air flow rates $\dot{m}_{air}$ [kg·s^{-1}], raw meal chemical composition and MCC plant processes flow sheets. Table 4.1 presents raw material feeds analysis, raw mix and clinker chemical composition as well as ash analyses. Also Table 4.2 presents coal properties. In order to simulate solids in Aspen Plus, particle size distributions (PSD) should be specified. Therefore, Table 4.3 presents PSD for raw meal feed used at MCC plant, which was used in this study. Table 4.4 presents raw meal, coal and air flow rates, respectively

Table 4.1. Raw material feeds, raw mix and clinker chemical compositions data

Substance	Limestone / %	Clay / %	Sand stone / %	Pozzolana / %	Gypsum / %	Raw mix / %	Clinker / %	Ash / %
SiO_2	4.46	42.04	82.03	59.01	14.39	12.78	22.24	54.7
Al_2O_3	1.38	22.5	7.38	18.96	2.05	3.19	5.14	22.5
Fe_2O_3	1.06	21.06	3.75	4.53	0.68	2.41	3.52	11.95
CaO	50.48	1.35	2.16	0.54	29.87	44.57	67.55	2.8
MgO	0.84	0.26	0.33	0.36	0.55	0.78	1.22	0.655
SO_3	0.45	0.12	0.33	0.32	34.66	0.02	0.01	2.9
K_2O	0.21	0.54	1.80	3.75	0.10	0.46	0.29	1.92
Na_2O	0.11	0.20	0.16	3.02	0.05	0.15	0.18	0.06
TiO_2	0.06	1.59	0.48	0.70	0.07	0.02	0.30	1.54
MnO	-	-	-	-	-	-	-	0.215
CO_2	-	-	-	-	-	-	-	-
H_2O	2.92	12.28	3.41	8.10	7.2	0.4	0.02	-
P_2O_5	0.01	0.04	0.05	0.03	0.01	0.02	0.04	0.085
Cl	-	-	-	-	-	-	-	-
LOI:(CO2)	41.16	10.68	2.94	7.38	18.19	36.22	0.22	-

Table 4.2. Coal mix analysis

Tancoal & Mchenga	Parameters	% wt	Erland & Mchenga	Parameters	% wt
Proximate analysis	Moisture	5.85	Proximate analysis	Moisture	3.62
	Ash	19.50		Ash	19.14
	VM	26.95		VM	24.00
	FC	47.70		FC	53.24
	Sulfur	0.92		Sulfur	1.39
Ultimate analysis			Ultimate analysis		
	Carbon	62.55		Carbon	65.10
	Hydrogen	4.28		Hydrogen	4.24
	Nitrogen	1.25		Nitrogen	1.33
	Oxygen	5.67		Oxygen	5.16
	HHV	22.35 $MJ \cdot kg^{-1}$	HHV		20.82 $MJ \cdot kg^{-1}$

Table 4.3. Raw meal particle size distributions (PSD)

Interval	Fraction	X = [% wt] Fraction
60mm	1.5	0.3334
50mm	1.0	0.2222
40mm	1.0	0.2222
30mm	1.0	0.2222
25mm		
17mm		
15mm		
Total	4.5	1.0

Table 4.4. Raw feed, coal and air flow rates

S/N	Item	Units	Quantity
1	Primary Air	$kg \cdot h^{-1}$	11,438
2	Secondary Air	$kg \cdot h^{-1}$	33,712
3	Coal	$kg \cdot h^{-1}$	4,158
4	Raw feed flow rate	$kg \cdot h^{-1}$	58,000
5	Current clinker output	$kg \cdot h^{-1}$	35,000

Technical parametric data for the rotary kiln system like kiln dimensions and capacity, clinker cooler dimensions and capacity are presented in Appendix 8. Also operational data like flow rates, specific fuel consumptions, efficiency, operating temperatures, cooling air loading and the like are presented in Appendix 8.

4.2.2 .Assumptions and Limitations

In engineering, thermodynamic analyses of energy systems or processes are very often idealized as being at steady state. The steady-state open system, also called the steady-state steady-flow system, is a system where mass and energy flows across its boundaries do not vary with time and the mass within the system remains constant. The predefined kiln system used for modeling cement production processes at Mbeya cement factory is considered as a steady state control volume system, steady flow process. Therefore, the following assumptions were made in formulating the model for this study:

(i) Uniform conditions exist and reactors are well mixed: Thus, inlet streams such as feed raw material mix, primary air and fuel are at constant flow rates, temperature, pressure and composition. Also it was assumed that kiln surface temperatures are kept constant.

(ii) The raw material feed and coal particles are homogeneous.

(iii) An adiabatic condition for reactors was assumed in order to monitor temperature changes in the reactors. However, such condition is not completely valid because approximately 8 % to 15 % of heat generated from the clinker burning processes is dissipated to the kiln surface (Caputo et al. 2011). Also Karellas et al. (2013) point out that significant heat loss of about 35 % 40 % of process heat is lost mainly by flue gases and ambient air stream used for cooling down the clinker.

(iv) Heat transfer between walls and particles is neglected.

(v) Variations of potential and kinetic energies are neglected.

(vi) All gas streams are assumed to be ideal gases.

(vii) Solids leave reactors at the same temperature like gases.

(viii) A fuel and primary air stream inter combustion chamber separately.

(ix) Chemical equilibrium was assumed for all chemical reactions taking place within the system. This assumption was justified due to the fact that physico-chemical processes taking place within the kiln system last for about a minute for the preheater tower cyclones stages and for about 20 to 60 minutes for the dry rotary kiln. Therefore, it was expected that time is long enough for completion of chemical reaction taking place to reach its equilibrium.

(x) It was assumed that there was no pressure drop for all reactors representing rotary kiln referred to down streams in this thesis. However, pressure drops were taken into consideration for the preheater tower cyclones simulation to properly mirror real process in a real plant.

(xi) In real dry process, cement production process with cyclone preheater without pre-calciner, 20-40 % of the feed is calcined at the kiln inlet (ICR, 2005). Based on this fact, it was assumed that 30% of calcination takes place at the last stage of 4-stage cyclone preheater tower.

(xii) Primary and secondary air composition were assumed to be 79 % N_2 and 21 % O_2 by mole fraction.

(xiii) The kiln system was assumed to operate in direct mode, that is, the raw mill is off when the kiln system is in operation.

4.2.3. Choice of Thermodynamic Method and Model Selection

When building a simulation model, it is important to ensure that properties of pure components and mixtures are estimated appropriately. In Aspen Plus, the estimation methods are stored in what is called a "property method". A property method is a collection of estimation methods to calculate several thermodynamic and transport properties. In addition, Aspen Plus stores a large database of interaction parameters that are used with mixing rules to estimate mixtures' properties. Property methods can be selected from the data browser under the properties folder. When a property method is selected, several estimation equations for the different properties are put into effect. Also when a component is selected to be included in the simulation, many properties for such component would be loaded.

In Aspen Plus, property methods are categorized into various process types. However, since physical property methods for solid components are the same for all property methods, the property method for this study was selected based on conventional components in the simulation model. The IDEAL property method (ideal gas and Raoult's law) was considered as a good choice for the kiln system simulation, since the process involves conventional components like H_2O (g), N_2 (g), O_2 (g) and the like at low pressure and high temperature. The combustion gases in burning zone of cement production process have a temperature of up to T_{flame} =2000 °C and solids can reach a temperature of up to T_{flame} =1450 °C, while pressure in a rotary kiln system is below environmental pressure. Exhaust gases' temperatures at the preheater tower exit vary, depending on the number of stages for preheater cyclones. Generally, for 4-stage preheater cyclones, temperature ranges are T_{exh} =300 °C to T_{exh} =380 °C and they are T_{exh} =300 °C and T_{exh} = 260 °C for 5 and 6-stages, respectively.

For non-conventional components that are heterogeneous with solids that do not participate in chemical or phase equilibrium, the only physical properties that are calculated are enthalpy and density. Therefore, HCOALGEN and DCOALIGT models are used to calculate enthalpy and density of coal, a pattern that is the only heterogeneous component found in the simulation. HCOALGEN uses the proximate, ultimate and sulfur analyses to calculate the enthalpy of coal.

Aspen Plus uses stream classes to define the structure of simulation streams when inert solids are present. In this study, cement production processes, raw meal feed and coal involve several inert solids components. Also the processes involve fluids like combustion gases and

the like. Therefore, Conventional Inert Solid (CISOLID) sub-streams are used to introduce conventional solids components while MIXED sub streams are used to introduce conventional components in the simulation. Furthermore, Non-Conventional (NC) sub-streams are used to introduce non-conventional components in the simulation. Both the CISOLID and the NC sub-streams provide the option to include Particle Size Distribution (PSD) for the sub-streams. However, the sub-streams are combined in different stream classes like MIXN as well as CPSD stream class, which contains sub-streams MIXED and NCPSD. In this simulation, a combination of Mixed Conventional Inert Non-conventional Particle Size Distribution (MCINCPSD) is used. The choice is suitable since the simulation includes CISOLID and NCPSD solid with particle size distributions as well as conventional components. Defining sub-stream NCPSD allows inclusion of component attributes like Proximate Analysis (PROXANA), Ultimate Analysis (ULTANAL) and Sulfur Analysis (SULFANAL) for coal combustion.

4.2.4. Model Description

In this section, a comprehensive description of the model used to model the kiln system is presented. The discussion starts with presentation of global flow sheet of MCC Aspen Plus simulation model (Fig. 4.5) followed by a generalized summary of all model blocks of Aspen Plus used for simulation (Appendix 1). A detail of each sub-process in cement production and how it was modeled is also presented.

4.2.4.1. Simulation of Coal Combustion Processes

In the following discussion, all Aspen Plus model blocks and streams are referred to Fig. 4.5. Combustion processes in the rotary kiln burner at MCC was modeled using Gibbs reactor (BURN) model of Aspen Plus. The model was based on Gibbs free energy minimization as well as chemical and physical equilibrium method was used. Furthermore, an adiabatic condition was assumed for combustion of coal in the kiln burner. However, the Gibbs free energy of coal cannot be calculated because it is a non-conventional component. Gibbs reactor (RGibbs) is used to model reactions that come to chemical equilibrium.

One of key calculations performed in process simulations involves phase equilibrium calculations. Phase equilibrium is calculated using fugacity coefficients, which are measure of tendency of the component to leave its phase. Equilibrium is achieved when fugacity of the component is equal in all phases. Therefore, specifying reaction stoichiometry is not required. However, thermodynamic specifications like temperature, pressure and heat duty should be specified (Appendix 1). Furthermore, all components listed on component specification sheet as potential products in the vapor phase or liquids, but a user can specify possible product by changing default setting by considering all components as possible products into identifying possible products.

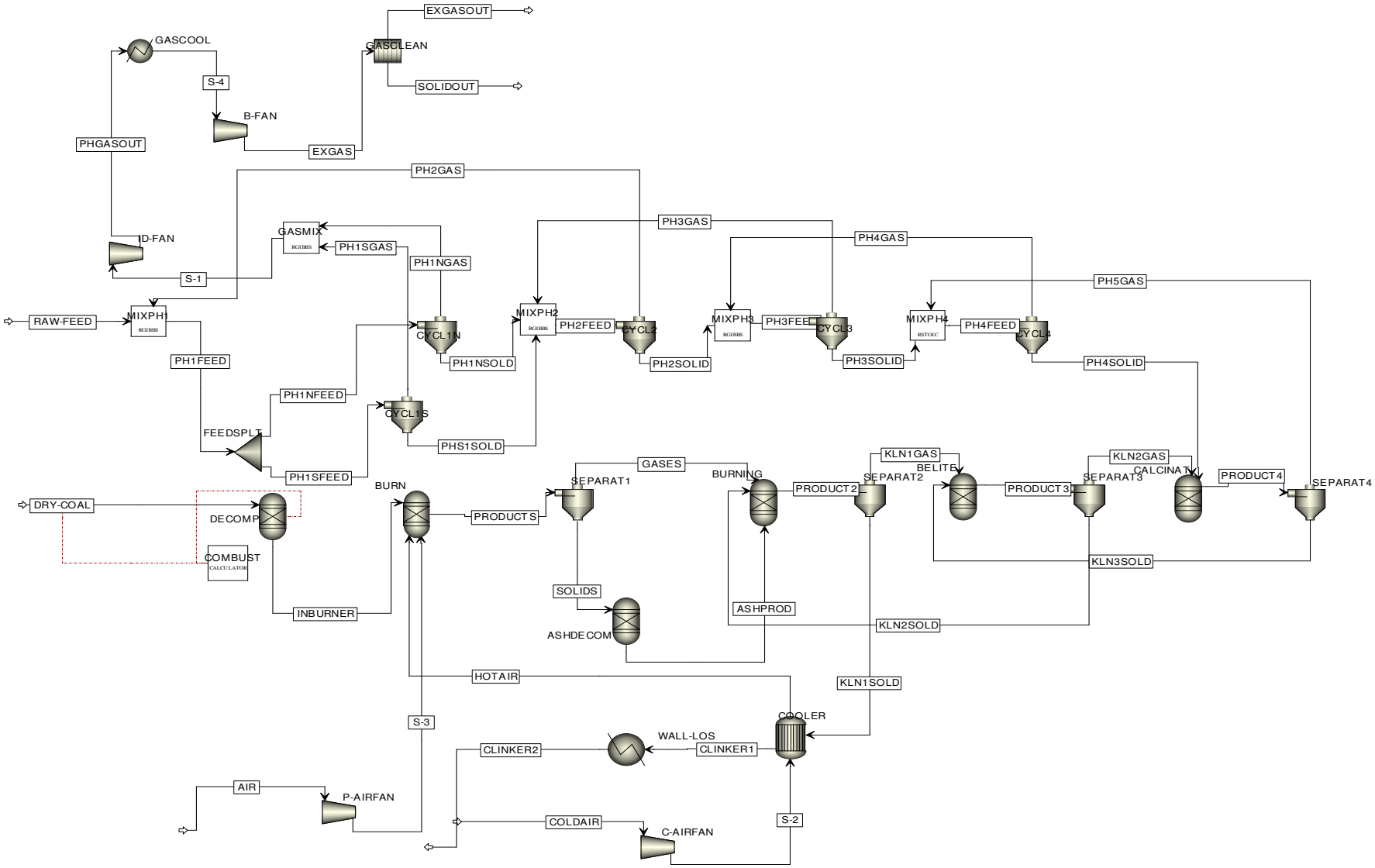

Figure 4.5. Global flow sheet of MCC Aspen Plus simulation

The coal composition and feed rate into the rotary kiln burner were kept constant throughout the simulation, and followed values for three types of coal analysis provided in Table 4.2. However, to study performance of dry rotary kiln system due to effect of varying coal mix, the coal mix flow rate (stream DRY-COAL) was varied to meet the clinker burning requirement temperature. Cooling air (stream COLDAIR) is used for heat recovery from hot clinker and as secondary combustion air, while primary air is very important for initiating combustion and for transporting pulverized coal to the kiln burner.

Before feeding the stream DRY-COAL to the Gibbs reactor BURN, the coal was decomposed into its constituents using yield reactor DECOMP. Yield reactor is used to simulate a reaction with known yield, and does not require reaction stoichiometry as well as kinetics. It is important to provide true yield distribution if data are known. However, there is a possibility of using Aspen Plus calculator block to compute actual yield distribution from component attributes for coal in the feed stream. In this simulation, a calculator block (COMBUST) was used to calculate actual yield distribution from the component attribute for coal. By defining the calculator block to calculate yields based on component attributes of the feed coal, it was easy to run different feed coals cases. It should be pointed out that for the yield reactor to calculate accurately the yield distribution, PSD for CIPSD and NCPSD sub-streams and the component attributes for the ash should be specified. Combustion gases and solid ashes (stream PRODUCTS) were separated using the Aspen Plus separator SSplit (SEPARAT1), which provides perfect separation. SSplit block separator mixes all of its feed streams, and then splits the resulting mixture into two or more streams according to sub-stream specifications.

Generally, in rotary kiln clinker burning, coal ashes are part of clinker product and therefore, it is considered during raw meal mix design. Based on this viewpoint, in this simulation, ashes (stream SOLID) were separated from combustion GASES and were carefully decomposed into their constituent elements using yield reactor model ASHDECOM. Since ash is a heterogeneous non-conventional component, it was necessary to decompose it so that Aspen Plus Gibbs model (BURNING) can consider it in clinker chemistry formation during clinker burning. Decomposed ash was transferred to BURNING using ASHPROD stream. Stream GASES from combustion burner BURN is used for supplying heat to solid material stream KLN2SOLD at the reactor BURNING. The stream KLN2SOLD represents solid products (BELITE or di-calcium silicates-C2S ($2CaO*SiO_2$) formed between free lime from calcination and silica (Eq. 4.2).

Normally, Aspen Plus estimates the heat of coal combustion based on its PROXANAL, ULTANAL and SULFANAL but there is an option for user specified input whereby the user can enter the heat of combustion directly into the simulation by changing the HCOALGEN option codes field from 1 to 6. This is done during defining properties and it is done by navigating through Methods-NC Props/Property method sheet. Therefore, in this simulation, the heating value of coal was input directly to the simulation since it was known from data collected of coal analysis (Table 4.2).

4.2.4.2. Simulation of Clinker Burning Processes

Under this section, simulation of clinker burning process starting from calcination, Belite ($2CaO{\cdot}SiO_2$) or C_2S and Alite ($3CaO{\cdot}SiO_2$) or C_3S formation is presented. It is an extension of the preceding sub-section where combustion processes are described. In a real cement rotary kiln operation, combustion of fuel is used to supply heat demand of the kiln system. The major chemical reaction, which consumes a significant amount of thermal energy from combustion is calcination. Calcination is an endothermic reaction whereby limestone ($CaCO_3$) and $MgCO_3$ are decomposed to lime (CaO) and MgO, respectively with release of CO_2 (Eq. 4.1). In the preheating section ($T_{Pecalcin}$ =700°C ÷ 900 °C), calcination as well as an initial combination of alumina ferric oxide and silica with lime take place (Käänteet et al., 2003). Calcination is followed by exothermic reaction between calcium oxide and silica to form what is so called belite or di calcium silicates (C_2S) (Eq. 4.2). Belite formation takes place at temperatures between 900 °C and 1200 °C. In systems consisting of only CaO, SiO_2, Al_2O_3 and Fe_2O_3, with typical Portland cement compositions, melting of tri calcium aluminates (C_3A) and tetra calcium aluminoferite (C_4AF) crystal phases commences at the eutectic at T_{cry} =1338 °C (Teleschow 2012). However, the melting temperature of the above mentioned compound solely depends on homogeneity of raw feed mixture. Inhomogeneity of the raw meal will lower the melting point. Generally, at the temperature above T_{liq} =1250 °C a liquid phase appears and this promotes the reaction between belite and free lime to form alite (Eq. 4.3).

Simulation of kiln system in this study considered the following chemical reactions for processes of clinker formation:

$$CaCO_3 \rightarrow CaO + O_2 \quad (4.1)$$

$$2CaO + SiO_2 \rightarrow 2CaO.SiO_2 \quad (4.2)$$

$$2CaO.SiO_2 + CaO \rightarrow 3CaO.SiO_2 \quad (4.3)$$

$$3CaO + Al_2O_3 \rightarrow 3CaO.Al_2O_3 \quad (4.4)$$

$$4CaO + Al_2O_3 + Fe_2O_3 \rightarrow 4CaO.Al_2O_3.Fe_2O_3 \quad (4.5)$$

However, stoichiometry for each reactions listed above, was not inputted to the Gibbs reactor because the reactor uses principle of free energy minimization to calculate phase and chemical equilibrium of participating components. Gibbs reactor was chosen to model chemical reactions for clinkerization processes because it is the only reactor in Aspen Plus that can calculate phase and chemical equilibrium between solid solutions, liquids and gases. It should be emphasized that in a real kiln operation, formation of clinker phases listed above overlaps. However, for simplification of studying and demonstrating useful energy consumptions, clinker formation processes were perfectly separated using reactors and separators. It means that the rotary kiln was further divided into sub-zones where calcination, belite and alite formation take

place. It has been seen already that 30 % of calcination takes place at the final stage of the preheater cyclone. Therefore, the remaining 70 % of calcination was carried out in Gibbs reactor (CALCINAT). The solid stream PH4SOLID at = $T_{PH4SOLID}$ =836 °C from the 4-th-stage preheater cyclone was brought to CALCINAT. Thermal energy required at the reactor CALCINAT for calcination is supplied from hot combustion gases (stream KLN2GAS) coming from preceding lower stage of the burning zone (belite formation). The outlet of the reactor CALCINAT is the stream PRODUCT4, which contains product of calcination and combustion gases. The cyclone separator block (SEPARAT4) is used to separate solid products of calcination (stream KLN3SOLID), CO_2 from calcination as well as combustion gases (stream PH5GAS). The stream PH5GAS proceeds to the 4-th-stage preheater cyclone riser duct, while the solid stream KLN3SOLID proceeds to the lower stage of the rotary kiln at the Gibbs reactor (BELITE). At the BELITE reactor it is where formation of belite takes place. Belite formation is an exothermic reaction, but heat required for operation of the reactor BELITE was supplied by combustion gases (stream KLN1GAS). In the Gibbs reactor BELITE, CaO from calcination reacts with silica to form belite. The outlet stream PRODUCT3 from the reactor BELITE consists of belite C_2S and other unreacted solids constituting raw meal major oxides and combustion gases. The solid stream KLN2SOLID and gas stream KLN2GAS are separated from stream PRODUCT3 using SSplit separator (SEPARAT3). The solid stream KLN2SOLD proceeds to the lower rotary kiln stage (BURNING) where liquid phase and alite are formed. The combustion gases (stream KLN2GAS) proceeds to the next upper stage of rotary kiln where it is used to supply heat of calcination to the reactor CALCINAT. Combustion gases stream GASES provides heat required for the Gibbs reactor BURNING. Furthermore, decomposed ash components are also added to the reactor. In the BURNING reactor, C_3S that is a major component of clinker is formed from the reaction of C_2S and free lime together with C_4AF, which is in liquid form. C_4AF promotes further reactions to take place as well as facilitating clinker agglomeration. However, due to lack of C_4AF compound in Aspen one plus data base, its formation was not considered in simulation. The amount of free lime remaining after alite formation depends on burning temperature at the reactor BURNING, which, in turn, depend on the combustion gases temperature. Also the amount of free lime depends on other factors like raw meal composition and particle size distribution. Therefore, the product from the reactor BURNING (stream PRODUCT2) contains mainly combustion gases, Alite, free lime, and small amount of other oxides constituting raw meal mix. The separator SSplit (SEPARAT2) is used to provide perfect separation between combustion gases (stream KLN1GAS) and solid stream KLN1SOLID. Solid streams KLN1SOLID proceeds to the clinker cooler while combustion gases KLN1GAS supply heat to the preceded reactor BELITE.

4.2.4.3. Clinker cooling

Clinker coolers are used to cool hot clinker from approximately $T_{CLINKER1}$ =1400 °C to approximately $T_{CLINKER2}$ =100 °C to 200 °C. The clinker cooler recuperates the clinker heat by heating

up the secondary combustion air, maintain a minimum cooling velocity in order to avoid unfavorable mineralogical clinker phases and crystal sizes, facilitating clinker handling and storage. The types of clinker coolers employed in cement production processes include: grate coolers, rotary coolers and planetary coolers.

Planetary cooler is employed at MCC plant such that the following discussion about clinker cooling simulation will only refer to the planetary cooler: The planetary cooler is a set of tubes (9 to 11) fixed to kiln and hence, no separate drive required. Cooling of the clinker starts from the kiln and therefore, the kiln burner pipe is inserted into the rotary kiln so that a cooling zone behind a flame of d_{KLN} =1.5 m to 2.5m is created. In this zone, the temperature of clinker is dropped from $T_{CLINKER1}$ =1450 °C to approximately $T_{CLINKER1}$ =1200 °C. The temperature reduction is important for protection of an inlet opening, an elbow and the first section of the cooling tube. After this first cooling in the kiln internal cooling zone, the clinker is then further cooled by air in counter flow. It should be noted that the amount of cooling air equals the amount of secondary air. The air is heated up to approximately T_{HOTAIR} =700 °C, while clinker reaches typical temperatures from $T_{CLINKER2}$ =140 to 240 °C. A considerable amount of heat is also transferred to the environment since approximately three quarter of the cooler shell is not insulated.

The planetary cooler was simulated using a counter-current two-stream heat exchanger model (COOLER) and heater model (WALL-LOS). Cooling air (stream COLDAIR) is drawn into the COOLER by a cooling air fan (C-AIRFAN) in a counter-current with the incoming hot clinker (stream KLN1SOLD). The cooling air is heated up to a temperature of T_{HOTAIR} =772 °C, while the outlet clinker is cooled down to $T_{CLINKER1}$ = 787 °C. However, in a real cooler operation at MCC the clinker is cooled to $T_{CLINKER2}$ =245 °C and therefore, it was assumed that temperature of the outlet clinker of $T_{CLINKER1}$ = 787 °C contain the cooler heat losses through the cooler shell. Therefore, this scenario was simulated using the heater model (WALL-LOS), which is used to set the temperature of the outlet clinker at a temperature of $T_{CLINKER2}$ = 245 °C.

4.2.4.4. Raw Feed Preheating and Exhaust Gas Cleaning Simulation

In cement production processes, cyclones are used as gas-solid pre-cleaners of gases containing solid dusts and also serve as heat exchangers. They are connected in series with other high efficiency gas-solid cleaners like Bag Filter also known as fabric filter (FabFl) and Electrostatic Precipitator (ESP). Cyclones are flow devices in which the inlet gas containing solids is brought tangentially into a cyclone cylindrical body. A strong vortex is created inside the cyclone and any particles in the flow, if they are denser than the carrier gas, are subjected to centrifugal forces. Such forces move the particles radially outwards, towards the inside cyclone surface onto which the solid deposits. Finally, solid particles leave the cyclone through solid outlet at the bottom while gases leave the cyclone through gas outlet at the top of the cyclone. Cyclones arranged in series, can increase the separation efficiency of gas-solid, at the same time increasing pressure drops at the preheater cyclones stages hence affecting the performance of Induced Draft Fan (ID-Fan) which is used to suck out exhaust gases from the rotary kiln system. This

will affect negatively electrical power consumption and production capacity of the clinker in the rotary kiln system.

In this study, each preheater stage cyclones were modeled using combination of cyclones and RGibbs model blocks except for the 4-th-stage whereby a combination of cyclone and RStoic blocks are used. The 4-stage preheater models of Aspen Plus are connected in series with FabFl model GASCLEAN. The cyclones removes large particles, FabFl removes the smaller particles. The cyclones were specified by using design mode. In design mode separation efficiency is specified as well as pressure drops. Efficiency correlation selected was Shepherd & Lapple and the type was set to medium efficiency. The reason for this preference settings are due to the fact that this type represents real situation for industrial cyclones. The medium efficiency is sometimes known as conventional design. A conventional design cyclone lies between the high efficiency and high throughput. They are characterized by higher collection efficiencies than the high-through puts and lower pressure drops than the high efficiencies. Thus, these cyclones are employed in most of general designs. It should be noted that performance of a cyclone is assessed by the particle collection efficiency and low pressure drops are typically used as the top-most stage, where separation efficiency of 95 % ÷ 97 % is required (Alsop et al. 2007).

Normally, for a 4-stage preheater cyclone, the top-most stage consists of twin cyclones with high separation efficiency and low pressure drops connected in parallel. The simulation of the 4-stage, dry rotary kiln preheater cyclones starts with injection of raw meal at T_{rm} = 28.32 °C to the mixer Gibbs model of Aspen Plus (MIXPH1), which represents 1-st-stage riser duct. On the other hand, hot exhaust gases at T_{PH5GAS} = 958 °C from combustion and calcination enter the rotary kiln preheater cyclone system through the rotary kiln riser duct. Pre-mixing of raw meal and exhaust gases at T_{PH2GAS} = 610 °C from the 2-nd-stage are done in MIXPH1. The outgoing stream (PH1FEED) is mixture of exhaust gases and solid raw feed which is divided into two equal streams PH1SFEED and PH1NFEED using FSplit model (FEEDSPLT). The purpose of splitting the stream PH1FEED is to control pressure drop in 1-st-stage preheater cyclones CYCL1S and CYCL1N by reducing the mass flow inside the cyclones. In the 1-st-stage preheater cyclones, free water from raw meal is evaporated at T_{evp} =100 °C by temperature from hot gases PH2GAS. Also it was assumed that 95 % of solid particles are removed from exhaust gases. Thus, CYCL1S and CYCL1N particle separation efficiencies were set to 95 %. In practical, pre-cleaned exhaust gases from the twin parallel top-most cyclones are drawn out of the preheater cyclones using ID-FAN through a common duct, while solids proceed to the duct of the second stage preheater cyclones. The pre-cleaned gases streams from top-most cyclones were simulated using PH1SGAS and PH1NGAS streams, which are combined in the mixer (GASMIX) to form a stream S-1 in the inlet side of ID-FAN. Gibbs reactor GASMIX was used to set ID-FAN inlet temperature of pre-cleaned exhaust gas (S-1). When the plant is in compound operation, Pre-cleaned gases (ID-FAN outlet stream PHGASOUT) are directed to the raw mill for raw meal drying. But when the raw mill is off, pre-cleaned exhaust gases PHGASOUT are fed to the cooling tower

(GASCOOL) where they are cooled down to a temperature of about T_{EXGAS} = 150 ^{0}C. In real operation, Booster fan (BS fan) is used to draw out cooled pre-cleaned gas from the cooling tower to the Bag Filter where it is further cleaned. Therefore, the stream EXGAS was further cleaned in Bag Filter (GASCLEAN). The clean gas stream EXGASOUT is finally drawn out from GASCLEAN by fan to the environment at a temperature of about $T_{GASCLEAN}$ = 130 °C. The residue solid (stream SOLIDOUT) can be directed to raw mill depending on its chemical composition.

On the other hand, the solid streams PHS1SOLD and PH1NSOLD from the top-most twin cyclones proceeds to the 2-nd-stage cyclone riser duct where they are combined with hot gases (stream PH3GAS) from 3-rd-stage preheater cyclone using a mixer (MIXPH2) to form a stream PH2FEED interring the 2-nd-stage cyclone CYCL2. The 2-nd-stage cyclone (CYCL2) particle separation efficiency was set to 85 %. Evolution of raw meal combined water and sulfur takes place at stages two and three of preheater cyclones at temperature above T_{evln} = 500 °C (ICR 2005). The pre-cleaned gas (stream PH2GAS) proceeds to the preceded 1-st-stage preheater cyclones, while preheated raw meal (stream PH2SOLID) proceed to the proceeding 3-rd-stage preheater cyclone riser duct. The stream PH2SOLID at a temperature of $T_{PH2SOLID}$ = 610 °C is pre-mixed with stream PH4GAS at T_{PH4GAS} = 836 °C in the 3-rd-stage preheater cyclone riser duct (MIXPH3) to form a stream PH3FEED at $T_{PH3FEED}$ = 739 °C. At the 3rd stage, intermediate reactions are initialized. The stream PH3FEED is separated using cyclone (CYCL3) into solid stream PH3SOLID which precedes to 4-th-stage preheater cyclone riser duct; and gas stream PH3GAS which proceed to the preceded 2-nd-stage preheater cyclone. It was assumed that 75 % of solid particles were removed from gases at 3-rd-stage preheater cyclone. Thus, the solid particle separation efficiency of CYCL3 was set to 75 %. The solid stream PH3SOLID inters 4-th-stage preheater cyclone riser duct at MIXPH4 where it is mixed with hot exhaust gases at T_{PH5GAS} = 958 °C from rotary kiln riser duct to form a stream PH4FEED at a temperature of $T_{PH4PHEED}$ = 836 °C. Stoichiometric reactor was used for a mixer MIXPH4 to set the percentage of $CaCO_3$ decomposition (calcination) to 30 %. It should be pointed out that in practical, 20 % and 40 % of calcination takes place at the 4-th-stage cyclone of a 4-stage dry rotary kiln preheater cyclone without pre-calciner (ICR 2005). It was also assumed that 75 % of solid particles were removed in this stage and therefore, 75 % solid particles separation efficiency was set for CYCL4. The stream PH4FEED was separated into gas stream (PH4GAS), which proceed to the preceded 3rd -stage preheater cyclone riser duct and solid stream (PH4SOLID), which proceeds to the kiln calcinator (CALCINAT) where further calcination takes place.

4.2.5. Model Results and Validation

Validation of the model is very important to verify that the developed model behaves approximately the same as the real plant modeled. Thus, real MCC plant operating data were used to validate the model. Further validation of the model is done using parametric analysis (Section 4.2.6.) to verify if the model behaves the same as the real plant in responding to changes in various input plant parameters.

Table 4.5. Comparison of plant clinker and simulated clinker

Substance	Plant Clinker	Model clinker
SiO2 / % wt	22.24	22.03
Al2O3 / % wt	5.14	5.42
Fe2O3 / % wt	3.52	3.94
CaO / % wt	67.55	67.84
MgO / % wt	1.22	1.20
SO3 / % wt	0.01	0.07
K2O / % wt	0.29	0.74
Na2O / % wt	0.18	0.23
TiO2 / % wt	0.30	0.07
MnO / % wt	-	-
CO2 / % wt	-	-
H2O / % wt	0.02	-
P2O5 / % wt	0.04	0.03
C3S / % wt	70.00	71.89
C2S / % wt	30.00	32.45
C3A / % wt	10.00	11.02

It is indicated from Table 4.5 that the clinker produced from the simulation model is relatively in good agreement with the plant clinker produced. However, it could be noted that there was enrichment of minor elements (SO_3, K_2O and Na_2O) in the simulated clinker compared to industry produced clinker. Nevertheless, typical value of SO_3 in industrial clinker is 0.6 % (ICR 2005). The relatively slight deviation of these minor and other compounds of simulated clinker from plant clinker can be due to formation of minor compounds like Na_2SO_4, K_2SO_4, and $CaSO_4$ that were not considered in the simulation. Furthermore, C_4AF compound is not available in Aspen one plus data base and therefore, it was not considered in the simulated clinker.

Additionally, the simulated clinker assumed that C_2S was completely reacted with free lime to form C_3S and thus, there is no free belite content in clinker formed. Teleschow (2012) discusses in detail clinker phase formation. In general, Alite (C_3S) is the most important clinker phase in cement, since it controls mainly initial and ultimate strength of cement. Portland cement clinker consists of approximately X_A = (50-70) % wt, which contains X_{CaO} = (71-75) % wt, X_{SiO2} = (24-28) % wt and $X_{sub\text{-}oxides}$ = (3-4) % wt substituted oxides. From the simulated clinker, C_3S consisted 71.89 % of the clinker. Also Portland cement clinker consist of Belite consisted X_B = (15 ÷ 30) % wt ; with X_{CaO} = (60 ÷ 65) % wt, X_{SiO2} = (29 ÷ 35) % wt, and $X_{sub\text{-}oxides}$ = (4 ÷ 6) % wt mainly, Al_2O_3, Fe_2O_3, K_2O, Na_2O, MgO, SO_3 and P_2O_5. From simulated clinker, it was found that X_A = 32.45 % wt of the clinker. Also the clinker contained tricalcium Aluminate (C_3A), which is the most reactive component. This part of clinker phase constituted X_{Al} = (5 ÷ 10) % wt cement clinker, which consistuted X_{CaO} = 62 % wt and X_{Al} = 38 % wt. From the simulated clinker,

C_3A consisted X_A = 11.02 % wt of the clinker. The calcium Aluminoferrite constitutes X_{Al} = (5 ÷ 15) % wt of Portland cement clinker. The pure phase contains X_{CaO} = 46 % wt, X_{Al2O3} = 21 % wt and X_{Fe2O3} = 33 % wt. However, C_4AF was not considered in simulation and hence, its value was not calculated. It can be concluded from Table 4.5 and Appendix 10 that the simulated clinker obtained was within the range of industrial clinker compositions.

Table 4.6. Comparison of plant parameters vs model parameters

S/N	COMPONENT	PLANT	MODEL
1	$\dot{m}_{cl}$ / kg·s^{-1}	35,000	35,528.2
2	$P_{ID\text{-}FAN}$ / kW	670	670.099
3	T_{cl} / °C	245	245
4	T_{flame} / °C	2,000	2,128
5	T_{HOTAIR} / °C	800	772
6	O_2 Back end / %	3	1.76
7	$T_{KLN\text{-}feed}$ / °C	836	836
8	$T_{riser\ duct\ gases}$ / °C	958	958
9	T_{PHT} / °C	396	380
10	P_{BF} / kW	132	132.06
11	T_{exh} / °C	138	138
12	$\dot{m}_{primary\ air}$ / kg·s^{-1}	11,438	11,438
13	$\dot{m}_{cooling\ air}$ / kg·s^{-1}	33,712	33,712
14	O_2 PHT exhaust gas / %	3.77	2.56
15	$\dot{m}_{KLN\ feed}$ / kg·s^{-1}	58,000	58,000
16	$\dot{m}_{coal}$ / kg·s^{-1}	5,000	4,158

In general, most of the model parameters presented in Table 4.6 were in good agreement with the real operating data of the plant. However, a few parameters deviated slightly from real operating data of the plant due to various reasons. There was relatively significant deviation of simulated model O_2 % in preheater exhaust gas from plant data. The difference can be contributed to in-leakages air from environment to the kiln system that was not accounted for during simulation. Normally, for optimum useful energy consumption, the percentage oxygen at preheater cyclone exit and kiln back end should be maintained at 2 % ÷ 3 % and 1.5% ÷ 2 % respectively (ICR 2005). An increase in O_2 of more than 2 % to 3 % at the preheater exit flue gases suggests excessive in-leakage air. Therefore, it can be concluded that from the plant data given for percentage oxygen at the preheater cyclone exit O_{2PHT} = 3.77 %, the useful energy consumption of the plant was not optimum. It implies that specific fuel consumption was high to compensate cooling caused by in filtrated air. This was further confirmed in model parametric study in Section 4.2.6.1. Additional fuel burn, in turn, will lead into more chemical irreversibility in the kiln and more CO_2 emission to the environment.

Table 4.7. Gases streams from MCC kiln system Aspen simulation model

	EXGASOUT	GASES	PH1NGAS	PH1SGAS	PH4GAS	PH5GAS	S-1
T / °C	138.6	2,128.5	410	410	836	958	380
p / bar	0.025	0.867	0.806	0.806	0.858	0.867	0.817
Mass VFrac	1	1	0.951	0.951	0.842	1	0.951
Mass SFrac	0	0	0.049	0.049	0.158	0	0.049
H / kW	77,661.90	6,792.48	42,110.06	42,106.79	188,450.00	193,840.00	84,883.67
Total flow, $kg \cdot s^{-1}$	67,678.59	48,500.23	35,646.18	35,645.20	111,248.00	107,608.00	71291.39
$\dot{m}_{H2O}$/ $kg \cdot s^{-1}$	2,071.31	1,805.75	1,035.66	1,035.66	1,841.66	1,841.66	2,071.31
$\dot{m}_{N2}$/ $kg \cdot s^{-1}$	34,685.57	34,479.83	17,342.78	17,342.78	34,683.04	34,683.04	34,685.57
$\dot{m}_{O2}$/ $kg \cdot s^{-1}$	1,893.42	2,168.44	946.72	946.72	1,890.50	1,890.50	1,893.42
$\dot{m}_{NO2}$/ $kg \cdot s^{-1}$	0.002	0.25	0.002	0.002	0.04	0.04	0.002
$\dot{m}_{NO}$/ $kg \cdot s^{-1}$	0.002	440.59	0.002	0.002	5.41	5.41	0.002
$\dot{m}_{S}$/ $kg \cdot s^{-1}$	trace	0.02	trace	trace			trace
$\dot{m}_{SO2}$/ $kg \cdot s^{-1}$	0.06	468.989	0.07	0.07			0.06
$\dot{m}_{SO3}$/ $kg \cdot s^{-1}$	11.40	0.24	5.65	5.65			11.40
$\dot{m}_{H2}$/ $kg \cdot s^{-1}$	trace	4.026	trace	trace	< 0.001	< 0.001	trace
$\dot{m}_{CO}$/ $kg \cdot s^{-1}$	trace	675.921	trace	trace	0.002	0.002	trace
$\dot{m}_{CO2}$/ $kg \cdot s^{-1}$	29,016.81	8,499.95	14,508.4	14,508.4	41,392.02	17,252.53	29,016.81

Also there was slight deviation of quantity of simulated clinker from the model to actual clinker produced at the factory. Such deviation could be due to performance of the preheater cyclones at the plant being low due to blockages (clotting) or clinker burning efficiency of the rotary kiln system. Furthermore, the model assumed cyclones efficiencies from 75 % to 95 % which could not be the case in the real plant. Thus, results obtained from the model indicated that if rotary kiln system burning efficiency and dust cleaning system are improved, the final product can be increased and significant amounts of raw material waste can be saved. Particular components or sub-systems, which contribute to inefficiency in the rotary kiln system are identified in Chapter Five (exergy analysis). It can be observed from Table 4.6 that secondary air temperature from the model deviated slightly from real operating data. However, the deviation was within the allowable range of secondary air temperature. The deviation could be due to type of selected model unit from simulators and the temperature approach used for simulation of heat exchanger. Another important parameter from the model, which deviates from the real plant data is temperature of combustion gases. The deviation could be due to the fact that the model did not consider imperfection of the real plant. This is properly explained in parametric study of the model (Section 4.2.6.1.). Deviation indicates an opportunity available of fuel saving if the current raw feed is kept constant or more clinker production at current fuel flow rate, if real plant imperfections are minimized. More fuel is burned to compensate fuel demand due to imperfection of real plant processes.

The preheater cyclone exit flue gase compositions and temperature presented in Table 4.7. (stream EXGASOUT) are in good agreement with the real plant data. It can be seen that CO_2 % in combustion gases (stream GASES) is 30.39 % of total emitted CO_2 from the plant processes and about 69.61 % of CO_2 originates from calcination of $CaCO_3$ from raw material. It can be observed that there are still combustible gases like H_2 and CO in combustion gases (stream GASES). The combustible gases did not originate from incomplete combustion, but rather, due to dissociations of CO_2 and H_2O gases at higher temperatures (T_{flame} = 2128 °C). However, there was just a trace amount of combustible gases at the PHT exit flue gases (stream EXGASOUT).

4.2.6. Parametric Study of the System Using the Model

There are several process parameters in a kiln system, which should be studied, both to observe trends that may indicate problems and provide necessary mean data for process analyses. The most important kiln controlling parameters are clinker production rate, fuel flow rate, specific heat consumption, secondary air temperature, kiln feed-end temperature, preheater exhaust gas temperature, ID-Fan pressure drop, Kiln feed-end % O_2, % down comer O_2, primary air flow as well as trip velocity m/sec, specific kiln volume loading, specific heat loading of burning zone cross-section area, cooler air including temperature, pressure and oxygen profile of preheater. However, the principal control variables are burning zone solid material temperature typical aim at T_{brn} = 1500 °C, feed-end gas temperature typical at T_{brn} = 1000 °C and feed-end oxygen typical at 2 % (ICR 2005). Control is managed by adjustments of kiln feed, fuel flow rate and ID fan speed.

The purpose of parametric analyses is to demonstrate the effect of changing any of the input or output parameters to the system behavior, process operation and its effect to energy use while maintaining the quality of clinker produced within acceptable values. Parametric analyses were carried out by varying coal flow rate, cooling and primary air flow rates. Other comparative parametric analyses which that carried out with this model were temperature versus fuel flow rate, fuel flow rate versus composition of combustion gases, fuel flow rate versus exhaust gas composition, coal moisture content versus combustion efficiency and air flow rate versus exhaust gases composition.

4.2.6.1. Combustion Temperature and its Effect on Clinker Production

From the thermodynamics of combustion of rotary kiln systems' point of view, increasing coal flow rate will increase burning temperature as well as clinker production rate.

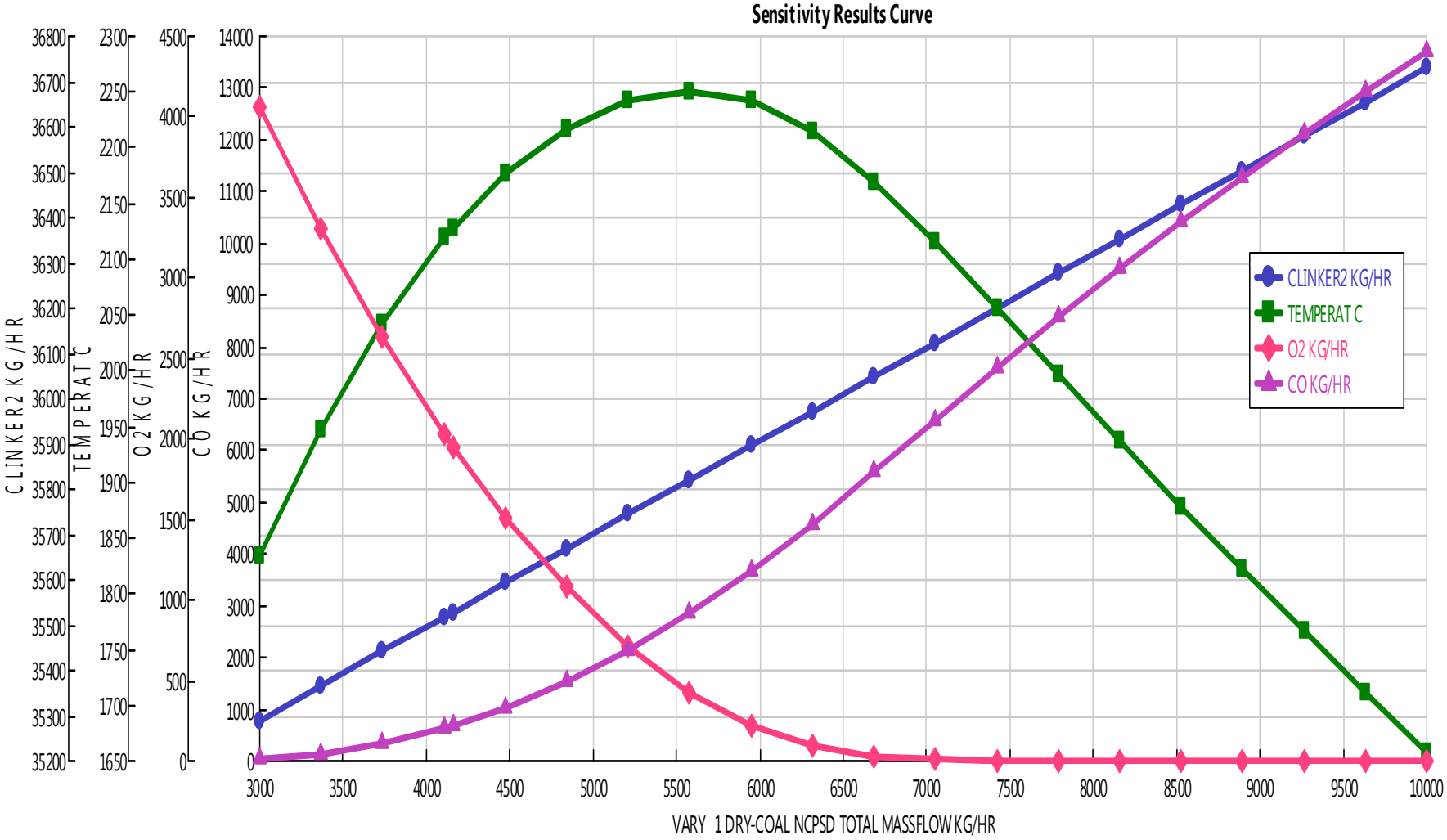

Figure 4.6. Coal flow rate vs. combustion efficiency and clinker production

However, increasing the fuel flow rate at stoichiometric conditions will reduce the flame temperature (Boateng 2008). Thus, under controlled conditions, flame temperature can be a useful measure of air fuel ratio, that is, how far they were deviated from stoichiometric conditions and whether the combustion was fuel-lean or fuel-rich (Boateng 2008). It should be emphasized that kiln stability, fuel efficiency, clinker finish grinding power consumption and cement quality all greatly depend upon provision of kiln feed and fuel with minimal variation, both of chemistry and flow rate. In order to maintain flame temperature at any set of conditions, fuel and air flow rate is varied proportionately. However, at MCC, only the coal flow rate is varied while the primary and secondary air is kept constant. This is done in accordance to kiln burning operation control principles (ICR 2005). It can be observed from Fig. 4.6 that maximum temperature is achieved at $\dot{m}_{coal}$ = 5580 kg·h^{-1}. The value achieved is T_{flame} = 2250 °C at $\dot{m}_{O2}$ = 431kg·h^{-1}, equivalent to 0.9 % O_2, which is below the recommended value of 1 % to 2 %). Increasing $\dot{m}_{coal}$ beyond 5580 kg·h^{-1}, flame temperature decreases from T_{flame} =2250 °C to 1660 °C at stoichiometric air. Nevertheless, it should be pointed out that transformation of clinker phases mainly, calcium silicates and calcium aluminate, requires excess air. Any lack of O_2 either results in incomplete formation or formation of other phases. Other risks include improper feeding of the main flame and improper burning of clinker. When it comes to energy efficiency, excess air required by the main flame should not be overly excessive. Depending on the type of kiln, characteristics of raw meal, and other influences, O_2 content at the kiln inlet should range between 1 % and 2 %. Generally, reducing O_2 content at the kiln inlet leads to reduced heat consumption in the range of 25 kJ·kg^{-1} to 75 kJ·kg^{-1} clinker output.

Also it can be observed from Fig. 4.6 that clinker production increases linearly with increasing coal flow rate. That could be due to temperature increase, which accelerates calcination as well as contribution of ash content to the amount of clinker formed. However, it was observed that even at stoichiometric condition, clinker production still increases with increasing coal flow rate because the lowest temperature reached is T_{flame} = 1660 °C, which is still sufficient for calcination process to proceed. This gives an indication that even below the minimum combustion gases flame temperature of T_{flame} =1800 °C mentioned in literature, there might be possibility of a significant amount of clinker burning. It should be noted that the current operating coal flow rate at MCC is $\dot{m}_{coal}$ =5000 kg·h^{-1}, which gives a burning zone flame temperature of combustion gases of T_{flame} =2230 °C. It gives an indication that there is an opportunity of fuel saving because suitable combustion gases temperature for clinker burning found in literature are from T_{flame} =1800 up to T_{flame} =2000 °C (CEMBUREAU 1999). It can be observed from Fig. 4.6 that these temperatures can be achieved at $\dot{m}_{coal}$ = 3000 kg·h^{-1} (T_{flame} =1835 °C) and $\dot{m}_{coal}$ = 3737 kg·h^{-1} (T_{flame} =2043 °C), respectively. This can provide a minimum potential coal saving of about $\dot{m}_{coal}$ =1263 kg·h^{-1}, which approximates to 76,126 tons per year at current kiln feed of 58,000 kg·h^{-1}. It should be pointed out that the current specific energy consumption of the kiln system is 4200 kJ·kg$_{cl}^{-1}$ at a clinker throughput of $\dot{m}_{CLINKER}$ = 35,000 kg·h^{-1}.

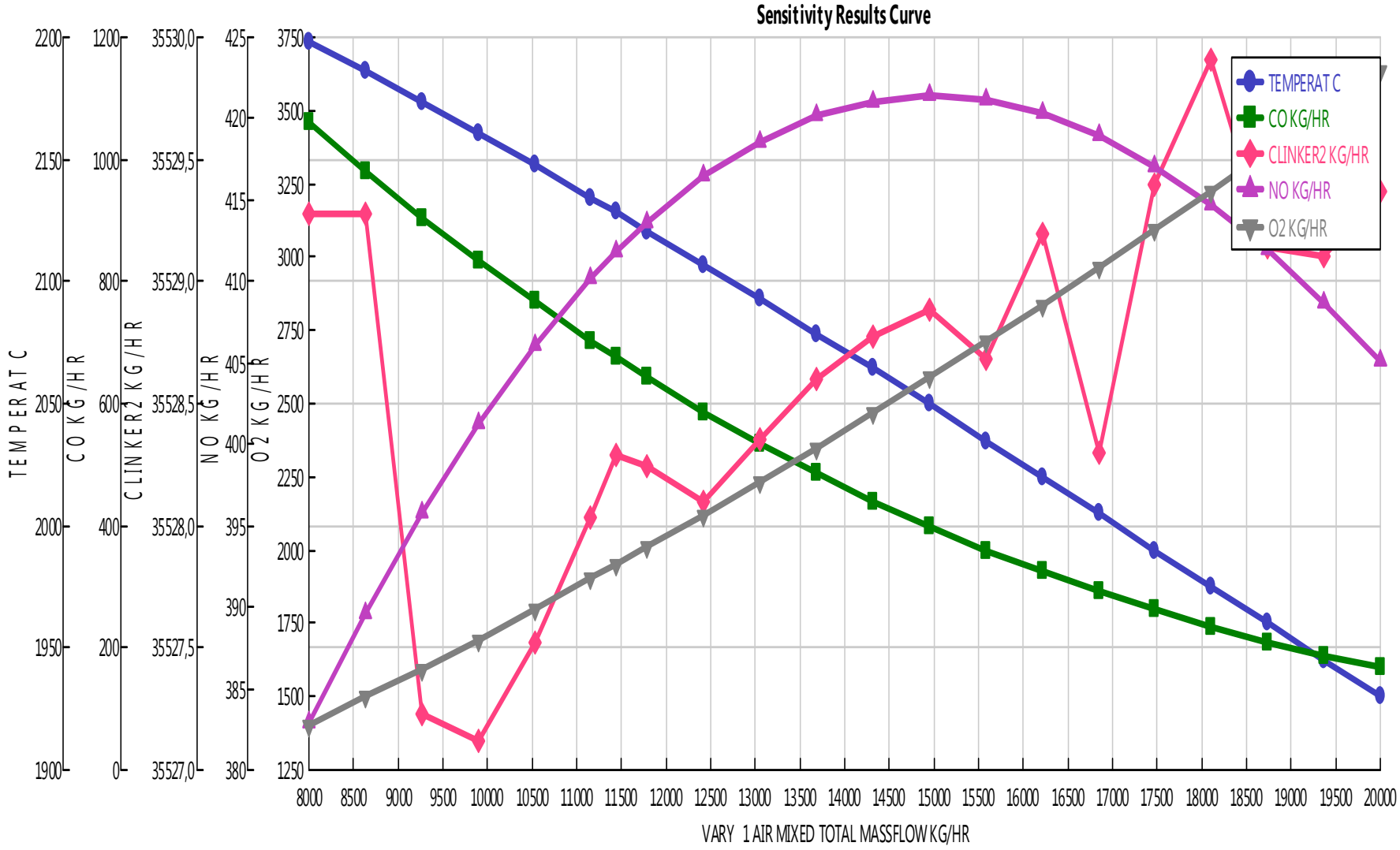

Figure 4.7. Primary air vs. clinker production, O_2, NO, CO and flame temperature

By considering coal input of $\dot{m}_{coal}$ = 3737 kg·h^{-1} to the kiln, this is equivalent to specific useful energy consumption of 2350.88 kJ·kg$_{cl}^{-1}$, which gives clinker output of $\dot{m}_{CLINKER}$ = 35,441.5 kg·h^{-1}. It gives specific energy saving of about 1849.12 kJ·kg$_{cl}^{-1}$, with relatively higher clinker throughput. Here the specific useful energy consumption was calculated using Eq. 3.19.

However, it should be cautioned that such fuel saving is only possible if the plant runs without any heat losses.

Also it can be observed from Fig. 4.6 that increasing the coal flow rate above an optimum value will lower combustion efficiency, which is shown by an increase in carbon monoxide (CO). This is explained by fact that increasing the coal flow rate at constant supply of combustion air results into a dramatic decrease in O_2 as indicated in Fig. 4.6. The decreases in O_2, in turn, result into incomplete combustion of coal.

4.2.6.2. Variation of Primary Air and its Impact on clinker Production

It was already been mentioned that traditionally, rotary kiln burning operation control is done by adjustment of raw feed; fuel flow rate and ID fan speed. However, Oxygen target level is very important not only for the complete combustion of fuel, but also for better clinker burning conditions. The set parameters during commission of the plant changes with time. Hence, there is necessity for plant process engineers to adjust parameters based on measured operating data. Furthermore, burners' age results into imperfect mixing of fuel and air, while calorific value of fuels varies, firing rate changes and weather changes from day to day. Any of these factors can change the amount of air required for safe and efficient combustion of fuel. Thus, it was necessary to do parametric study analysis to examine the optimum amount of primary air suitable for the kiln burning.

The right amount of oxygen for complete combustion is very important for thermal performance of a rotary kiln. However, a lot of oxygen means more combustion air into the system than expected, which, in turn, causes a significant amount of useful energy production from combustion of fuel to be used for heating up of excess air thereby cooling down the burning zone temperature as indicated in Fig. 4.7. The latter will result into kiln system heat losses. In other words, it can be stated that the higher the percent excess air, the greater the exergy destroyed of the thermal exergy of combustion gases. Fig. 4.7 indicates that varying primary air beyond 15,000 kg·h^{-1} clinker production is unstable or varies irregularly. Also it is indicated that NO emission increases but when primary air is beyond $\dot{m}_{air}$ =15,000 kg·h^{-1}, emission starts to decrease. The increase in NO emission below $\dot{m}_{air}$ =15,000 kg·h^{-1} primary air flow rate is due to increased amount of N_2 contained in primary air at elevated temperature, but above $\dot{m}_{air}$ =15,000 kg·h^{-1} the combustion temperature is cooled down by excess air volume at lower temperature. The NO_X level in the outgoing gases gives information about combustion processes. It should be pointed out that a high peak temperature in the combustion zone leads to higher NO_X level, among other things. Thus, for any given type of kiln, the amount of NO_X formed is directly

related to the amount of useful energy consumed in the clinker burning process. Therefore, measures that improve energy efficiency of this process should reduce NO_X emissions as well.

Also it can be noted from Fig. 4.7 that CO decreases with increasing the primary air flow rate, indicating complete combustion is approached with excess air. It should be noted that increasing excess air at a certain point may improve combustion efficiency, but when it exceeds the acceptable value between 1 % and 2 % O_2 (10 % – 15 % excess air), combustion efficiency is lowered followed by unstable kiln operation indicated by irregular clinker production as shown in Fig. 4.7. Furthermore, it can be noted that O_2 increases with primary air increase. Exceeding the primary air above $\dot{m}_{air}$ =20,000 kg·h^{-1} brings errors to the simulation and the simulation fails to converge. The simulation fails to converge probably due to excessive air flow rate, which contributes to excessive mass flow rate above optimal values allowed to some components like cyclones thereby causing excessive pressure drops and blocking cyclone outlets due to overloading. Also an excessive air mass flow rate may cause problems to reactors due to excessive cooling.

4.2.6.3. Variation of Cooling Air and its Effect on Energy Use

In a rotary kiln system, it is very important to keep the secondary combustion air temperature at a constant acceptable level of between T_{flame} = 800 ˚C to 1000 ˚C (ICR 2005). This is very important for stable and smooth operation of the kiln. Furthermore, efficiency of clinker cooler and the kiln system at large is mainly constrained by heat recovered from hot clinker by secondary air. It is observed from Fig. 4.8 that excessive increase in cooling air flow rate will lower combustion temperature. Also increasing cooling air flow rate above optimal value will cause an unstable kiln operation, that is, varying cooling air flow rate will cause fluctuating secondary air temperature thereby causing cycling of kiln operation. The latter will result into irregular clinker production as indicated in Fig. 4.8. This phenomenon is also supported by finding by Kääntee et al. 2003 and Arad et al. 2008. Furthermore, it can be noted from Fig. 4.8 that increasing cooling air flow rate will lower CO emission while increasing NO emission and O_2 flow rate.

4.2.6.4. Coal Variation and its Effect on Combustion Emissions

In order to study contribution of coal burning and emissions to environment, coal flow rate was varied. It can be noted from Fig. 4.9 that CO increases exponentially with coal flow rate. It is also noted that CO_2 increases with coal flow rate up to $\dot{m}_{coal}$ =4800 kg·h^{-1} when it starts to decrease with increasing coal flow rate. Such decrease in CO_2 can be explained by the fact that further increase in coal flow rate will increase flame temperature, which, in turn, result into CO_2 dissociation to form CO.

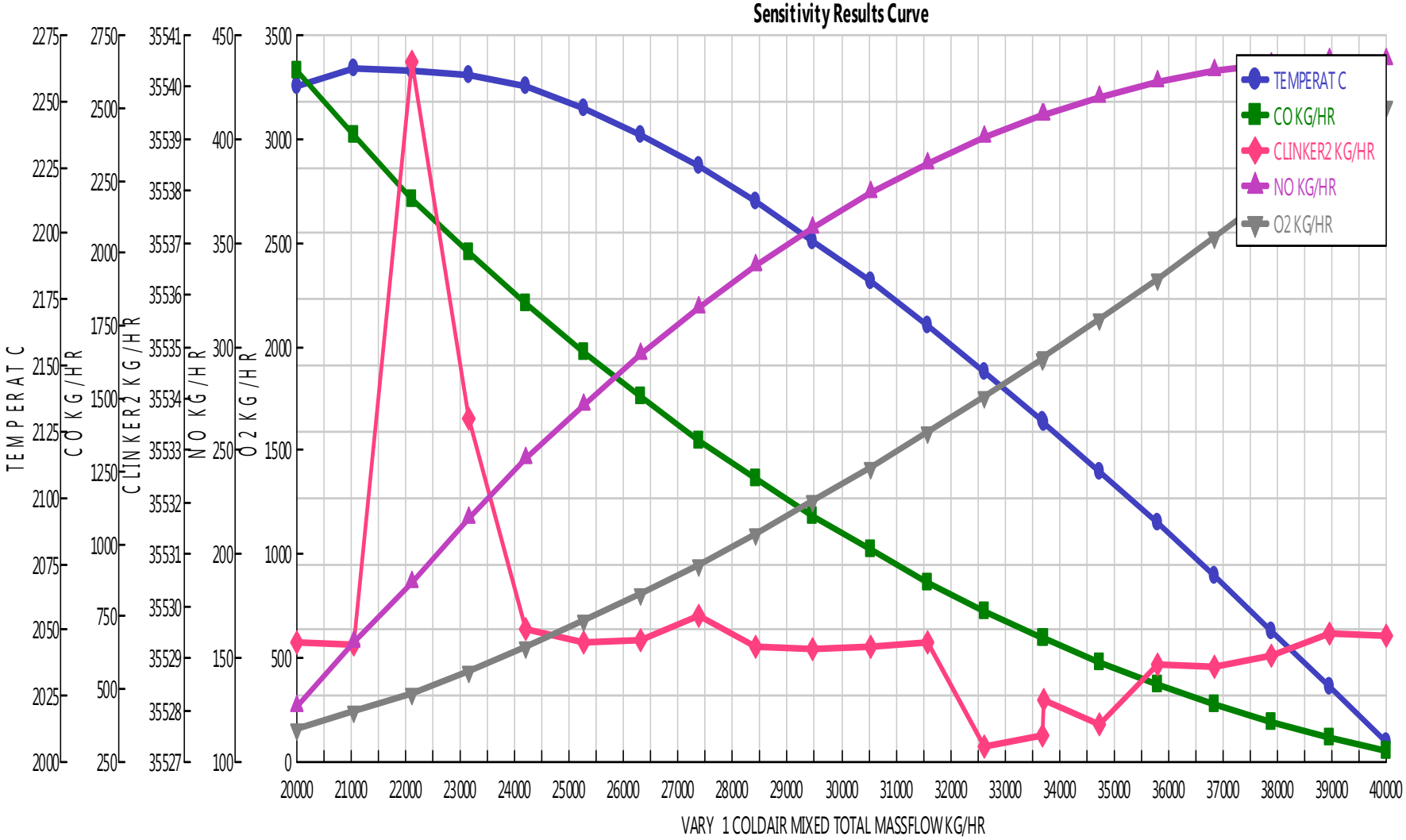

Figure 4.8. Cooling air vs. clinker production and combustion emissions

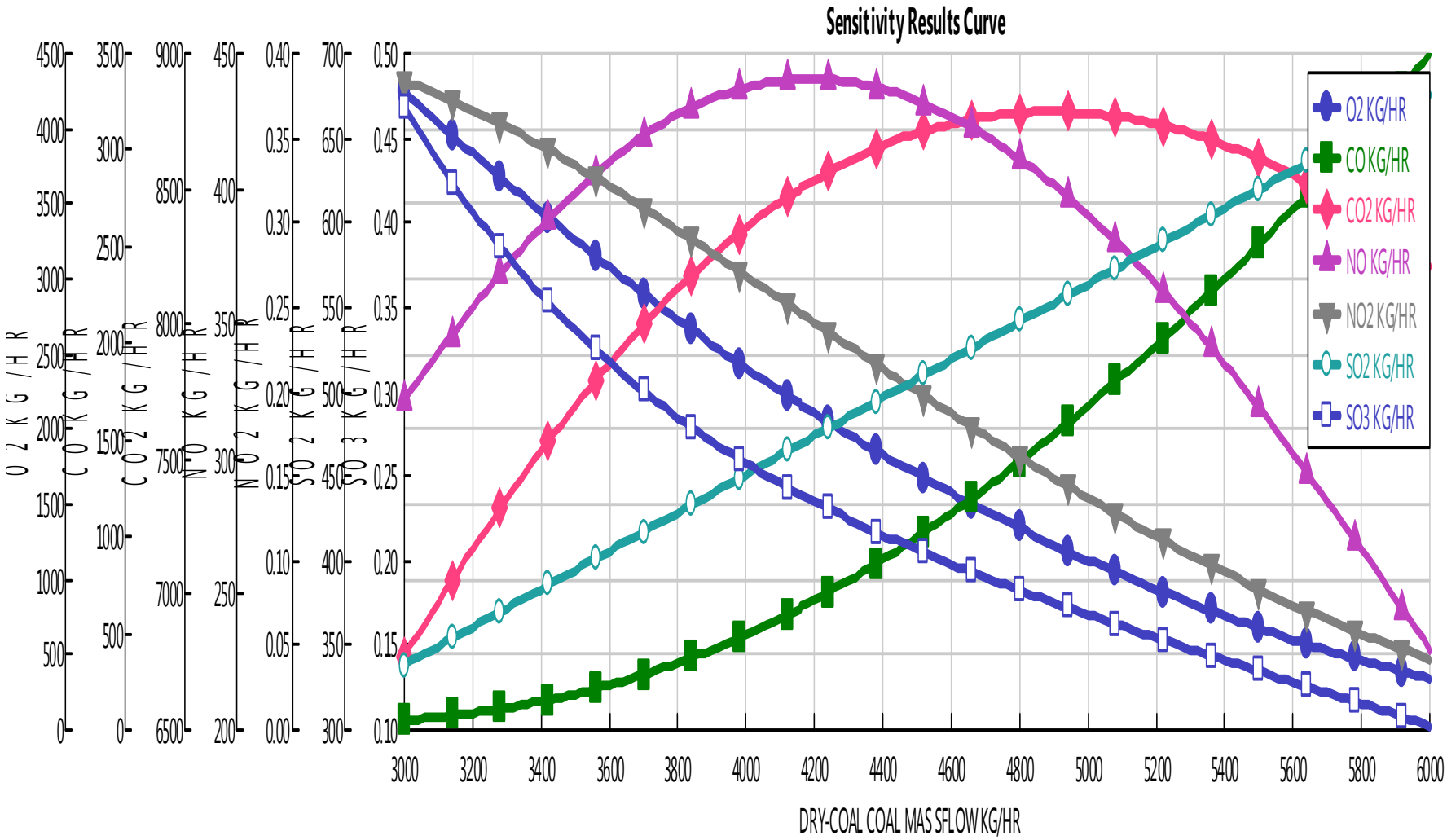

Figure 4.9. Coal flow rate vs. combustion gases composition

It is observed from Fig. 4.9 that NO_2 increases with decreasing coal flow rate, while NO increases up to coal flow rate of $\dot{m}_{coal}$ =4000 kg·h^{-1} where it starts to decline. The decrease in NO with increasing coal flow rate beyond $\dot{m}_{coal}$ =4000 kg·h^{-1} could be due to decrease in O_2 with increasing coal flow rate as shown in Fig. 4.9. Normally, it is expected that thermal NO_X emission should increase at elevated temperatures, but that depends on another factor, which is availability of oxygen and nitrogen from excess air.

4.2.6.5. Variation of Primary Air and its Effect on Combustion Emissions

Findings in Fig. 4.10 reveal that CO decreases with increasing primary air flow rate. The decrease in CO could be a result of more oxygen supply, which, in turn, facilitates complete combustion. It should be pointed out that presence of CO near the main flame has negative influence on clinker quality. NO increases with air flow rate up to primary air flow rate of $\dot{m}_{air}$ = 15000 kg·h^{-1} and starts to decrease with air flow rate increase. It is important to mention that NO in cement kilns has correlation to free-lime content in clinker and hence, it is used to determine clinker quality. NO_2 increases linearly with primary air flow rate, while O_2 increases with increasing primary air flow rate. It is also observed that CO_2 increases exponentially with primary air flow rate.

4.2.6.6. Variation of Primary Air and its Impact on Preheater Exhaust Gases

Primary air was varied to examine its effect on exhaust gase composition exiting in the upper most preheater cyclone. Nevertheless, kilns are frequently operated to the limit of the ID fan. In this case, low oxygen must be corrected by reducing both, fuel and raw feed. This implies that it is not allowed to increase excess air because in so doing, it will increase ID fan pressure drop thereby affect production capacity and power consumption. The oxygen level required at the kiln inlet will depend upon kiln stability and combustion efficiency. It is observed from Fig. 4.11 that NO, NO_2 and O_2 increase almost linearly with increasing primary air flow rate. It is further observed from Fig. 4.11 that CO decreases exponentially with increasing primary air flow rate. Moreover, CO_2 varies irregularly with increasing primary air flow rate. From $\dot{m}_{air}$ = 8000 kg·h^{-1} to 8500 kg·h^{-1} flow rate, CO_2 remains almost constant with increasing primary air flow rate. Above $\dot{m}_{air}$ = 8500 kg·h^{-1} primary air flow rate, CO_2 decreases with increasing primary air flow rate up to around $\dot{m}_{air}$ = 9800 kg·h^{-1} primary air flow rate. Above $\dot{m}_{air}$ = 9800 kg·h^{-1}, CO_2 increases irregularly with increasing primary air flow rate. Normally, CO_2 reaches its maximum value at the stoichiometric amount of air required for complete combustion. It should be pointed out that in cement rotary kiln; CO_2 is released from both decomposition of calcium carbonate ($CaCO_3$) and fuel combustion. While decomposition of $CaCO_3$ is constrained by rate of increase in air flow rate, CO_2 is enhanced by the same. Furthermore, there is an effect of CO_2 dissociation to CO at elevated temperatures. Thus, the resultant from the three effects could be the reason for an irregular flow of CO_2.

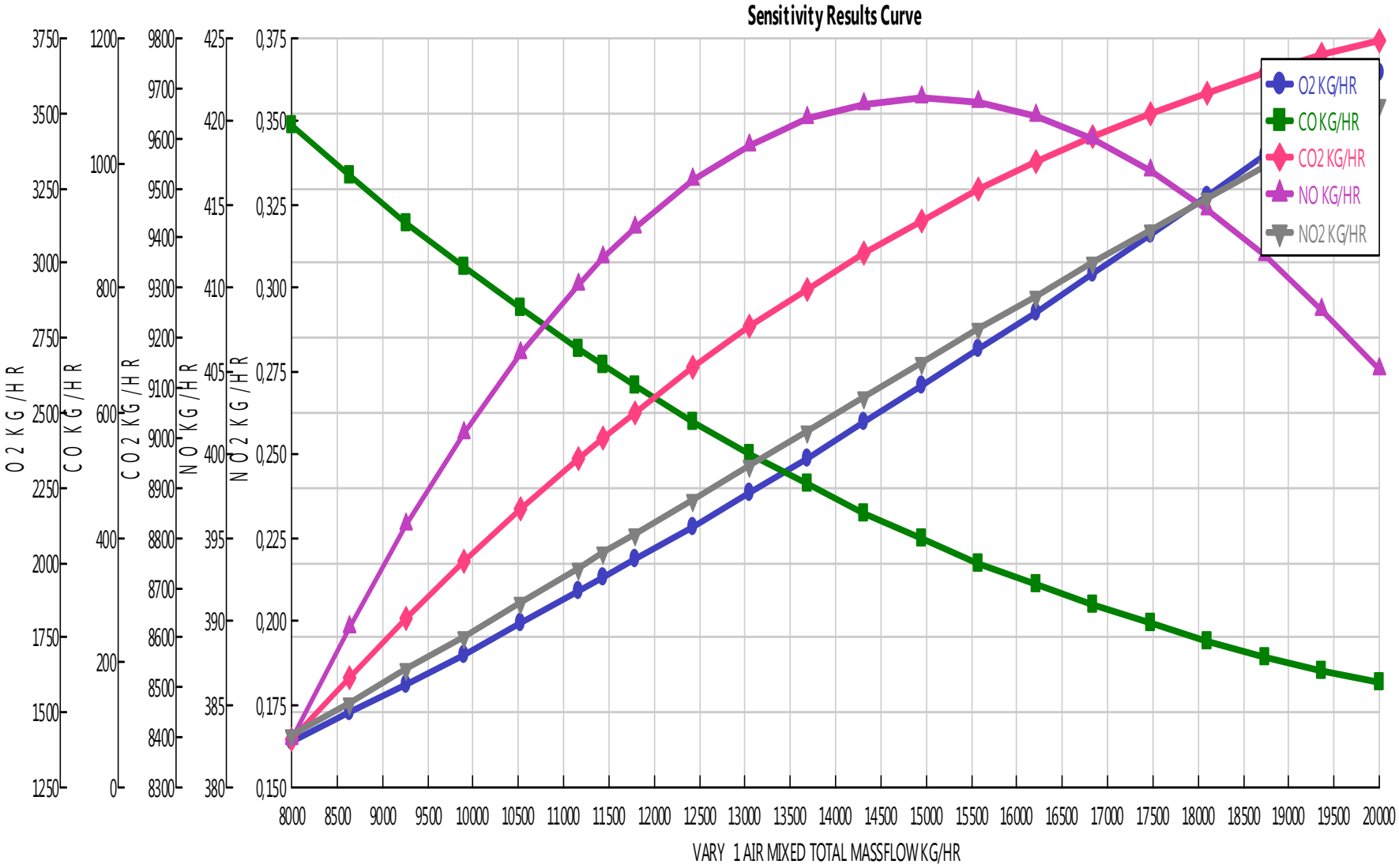

Figure 4.10. Primary air vs. combustion gases compositions

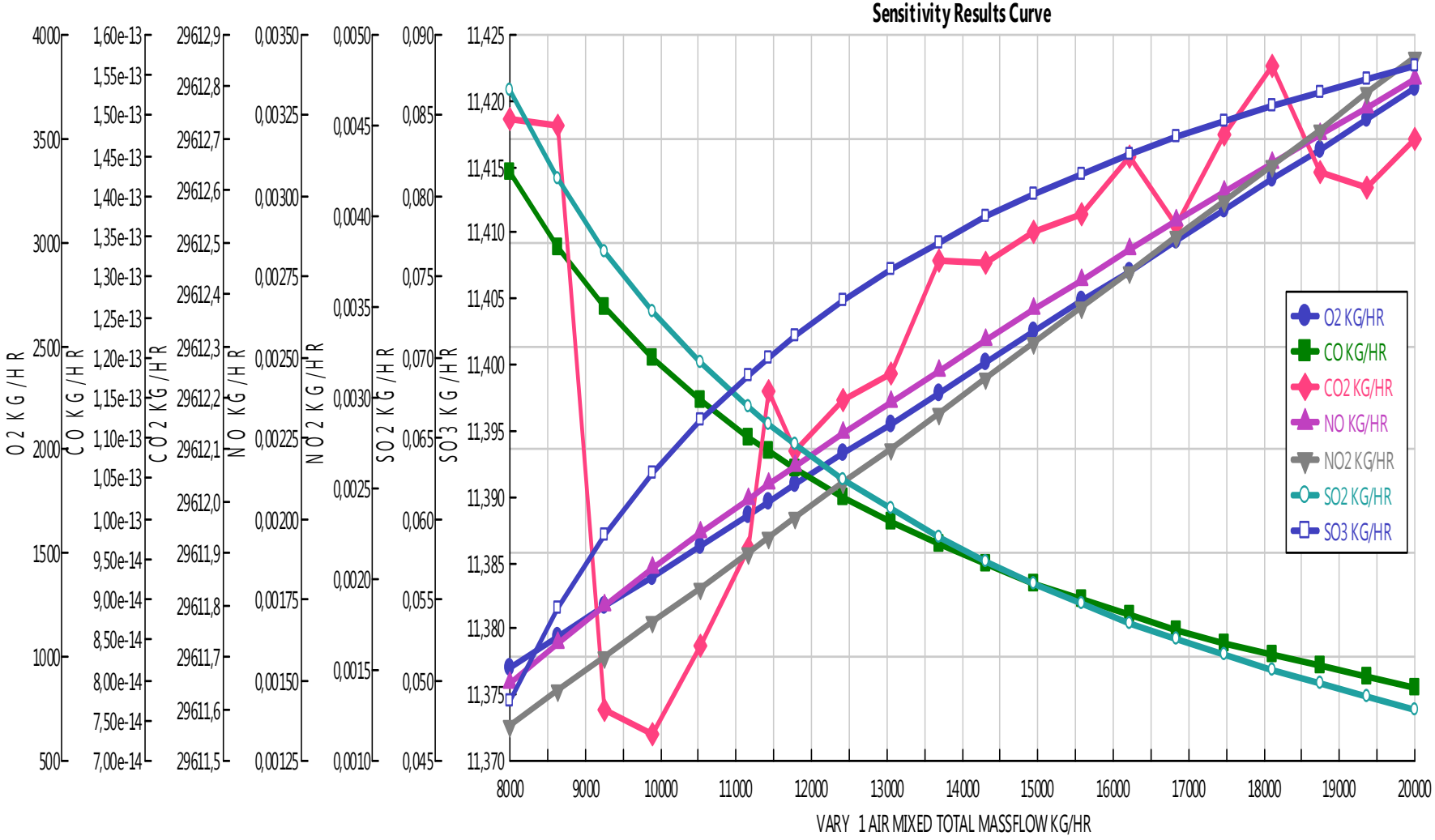

Figure 4.11. Primary air vs. exhaust gases compositions

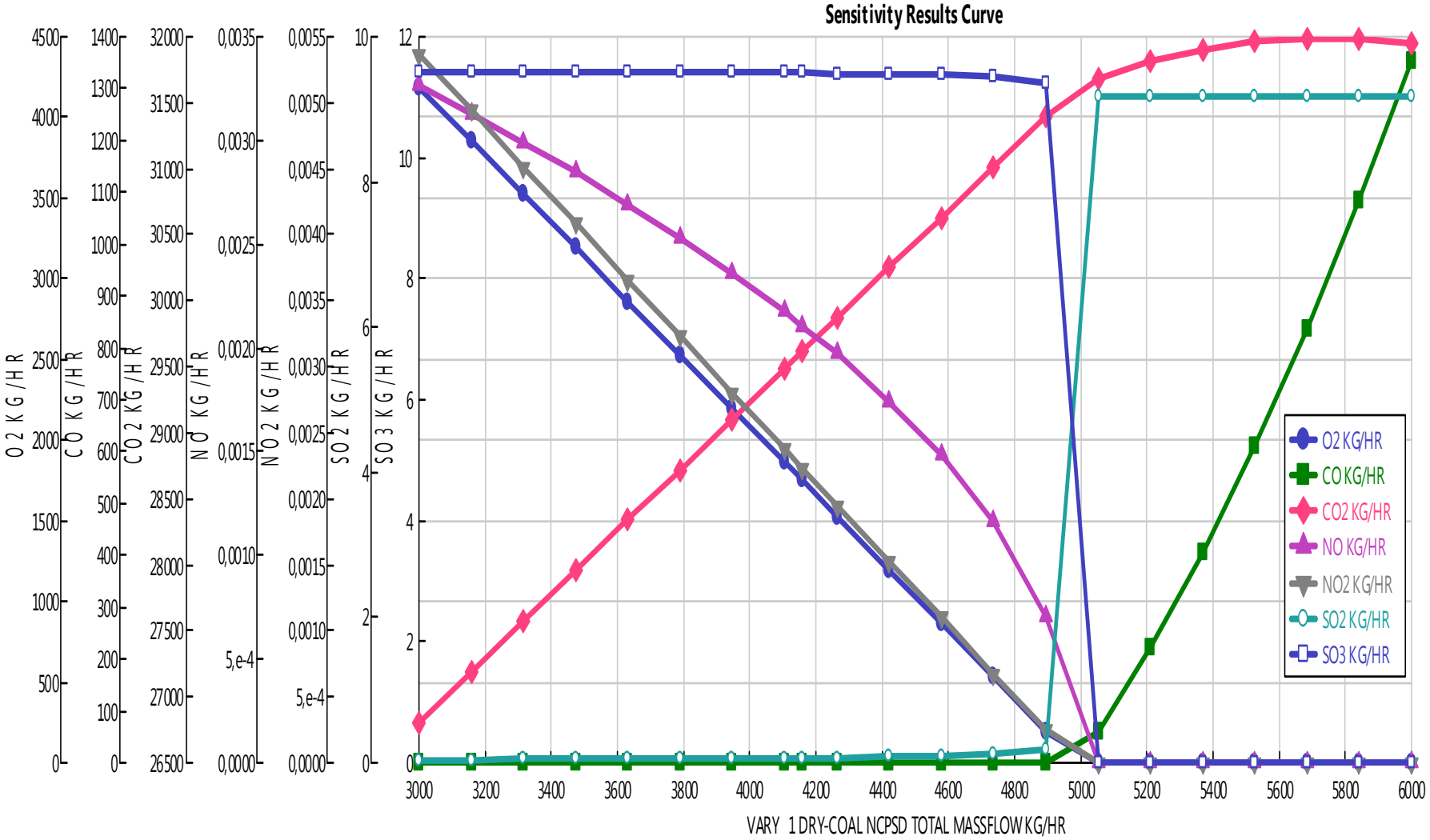

Figure 4.12. Coal flow rate vs. exhaust gas flow and composition

Generally, sulfur dioxide and sulfur trioxide emissions are greatly influenced by the amount of excess air used. Thus, SO_2 formation decreases with increasing air flow rate, while SO_3 increases with air flow rate. Emissions on NOx are mainly contributed to large quantity of excess air at elevated temperatures. However, raw material can be another source of NOx formation. Generally, NOx emissions are generated during fuel combustion by oxidation of chemically bound nitrogen in the fuel and by thermal fixation of nitrogen in the combustion air.

The amount of thermally generated NOx increases as flame temperature increases. NOx in the kiln systems are made up of 90 % NO and the remaining is NO_2. Most NOx are formed by thermal oxidation of atmospheric nitrogen at high temperatures. Threshold temperatures for thermal NOx formation fall between T_{thr} =1200 °C to 1600 °C. Hence, a considerable amount of NOx is formed in burning zone where flame temperatures are from T_{flame} =1800 °C to 2000 °C. Fuel NOx and raw feed NOx are negligible in a kiln system.

4.2.6.7. Variation of Coal and its Impact on Exhaust Gases Composition

Coal flow rate was varied to examine its impact in relation to emission contribution to the environment. It was observed that CO remains at constant flow rate of $\dot{m}_{CO}$ = 0 kg·h^{-1} with increasing coal flow rate up to $\dot{m}_{coal}$ = 4850 kg·h^{-1} where CO starts to increase exponentially. The findings suggest that at the current primary air and coal flow rates, the plant does not emit significant CO. The latter is confirmed in Table 4.7 stream EXGASOUT. It should be noted that CO above 1 % at the dust collector entrance should cause alarm and above 2 % should cause fuel and Electrostatic precipitator (ESP) together with Bag filters to shut off (ICR, 2005). This is done for safety because presence of CO and other combustible compounds like H_2 in exhaust gases can accumulate in ESP, Bag filters and ID fan to the extent of causing an explosion.

In addition, CO_2 increases exponentially with coal flow rate up to $\dot{m}_{coal}$ = 5600 kg·h^{-1} where CO_2 remains constant. Then NO decreases exponentially with increasing coal flow rate up to $\dot{m}coal$ = 5020 kg·h^{-1} where it remains at constant flow rate of $\dot{m}_{NO}$ = 0 kg·h^{-1}. NO_2 and O_2 decreases almost linearly with increasing coal flow rate up to $\dot{m}_{coal}$ = 5020 kg·h^{-1} where they remain constant at 0 kg·h^{-1}. Furthermore, SO_2 remains almost constant with increasing coal flow rate up to $\dot{m}_{coal}$ = 4850 kg·h^{-1} where it increases sharply (steeply) from $\dot{m}_{SO2}$ = 0.2 kg·h^{-1}to 10.3 kg·h^{-1} with increase of coal flow rate of $\dot{m}_{coal}$ = 4850 kg·h^{-1} to 5030 kg·h^{-1}. By increasing coal flow rate above $\dot{m}_{coal}$ = 5030 kg·h^{-1}, SO_2 remains constant at $\dot{m}_{SO2}$ = 10.3 kg·h^{-1}. In general, SO_2 increases with combustion temperature because SO_2 is more stable than SO_3 at higher temperatures and hence, high temperatures minimize SO_3 emissions. After all, SO_3 remains constant at around $\dot{m}_{SO3}$ = 10.6 kg·h^{-1} flow rate with increasing coal flow rate up to $\dot{m}_{coal}$ = 4850 kg·h^{-1} where it is observed to steeply decline to $\dot{m}_{SO3}$ = 0 kg·h^{-1}. In general, it can be noted that SO_3 decreases with increasing combustion temperature. It should be observed that over-fuelling results in preheater operating problems, an increase in exit gas temperature and CO in the exhaust gas.

4.2.6.8. Variation of Coal and its Impact on Sulfur Cycling in Cyclones

Coal flow rate was varied to observe impact of coal combustion and its contribution on sulfur cycling in the preheater cyclone. It is known that if the kiln is burned extremely hot or if the flame impinges on the load, sulfur cycle increases excessively until build-up or cyclone plugging occurs (CEMBUREAU 1999). It is observed from Fig. 4.13 that increasing coal flow rate above $\dot{m}_{coal}$ = 5000 kg·h^{-1} will result into sulfur increase.

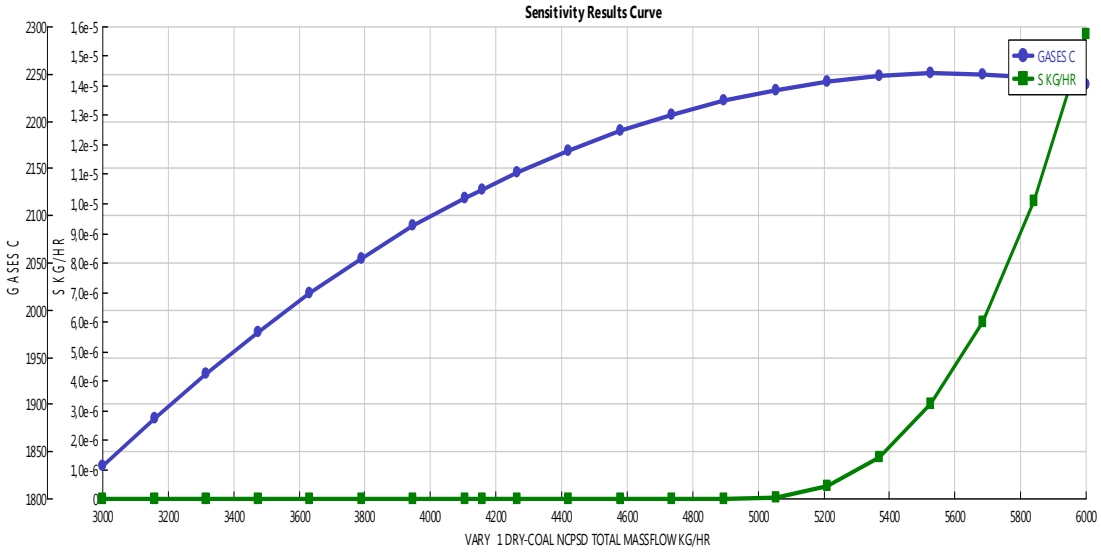

Figure 4.13. Variation of coal flow rate with sulfur

4.2.6.9. Effect of Coal Moisture Content on Combustion Temperature

It is observed from Fig. 4.14 that increasing the moisture content of coal will result into a lower combustion flame temperature.

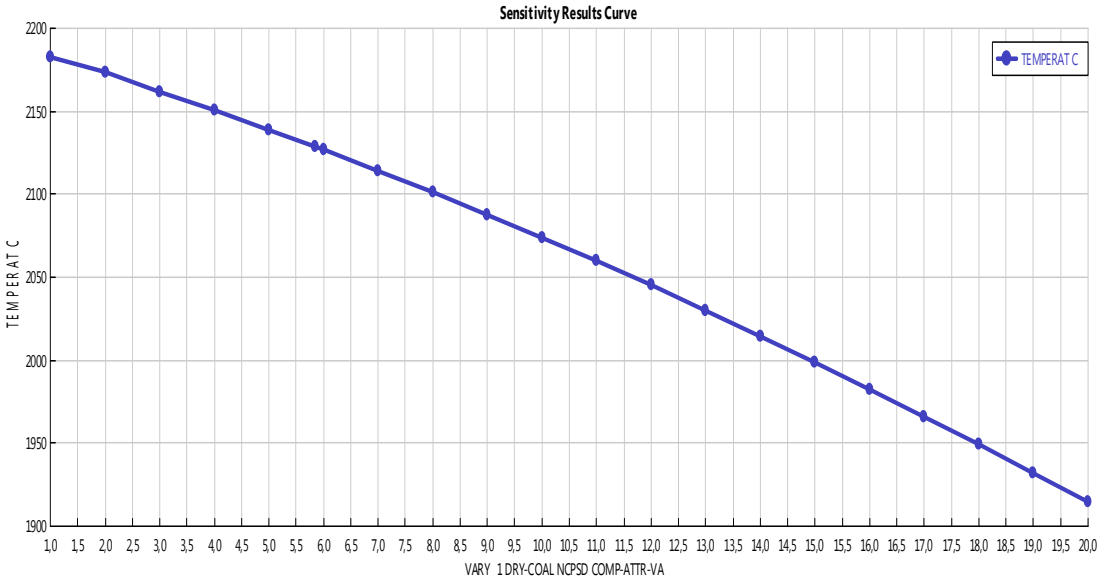

Figure 4.14. Coal moisture content vs. Combustion temperature

The raw coal at MCC has a moisture content of 8 %. Thus, it can be observed from Fig. 4.14 that at the coal moisture content of 8 % the combustion flame temperature of combustion gases is lowered to T_{flame} = 2100 °C. Therefore, it can be concluded that burning coal with higher moisture content in a rotary kiln will affect thermal efficiency of the kiln.

4.2.6.10. Effect of Air Preheating on Combustion and Kiln Performance

Fig. 4.15 presents combustion flame temperature in a kiln system as a function of primary air preheating for combustion process. Also Fig. 4.15 presents effect of preheating combustion primary air to cement clinker production. It was observed that primary air preheating from ambient temperature of T_0 =28 °C to T_{comb} =60 °C can increase the combustion flame temperature by only 4 °C. Also it is indicated in Fig. 4.15 that primary combustion air preheating from ambient temperature of T_0 =28 °C to T_{comb} = 60 °C has no significant impact to clinker production rate.

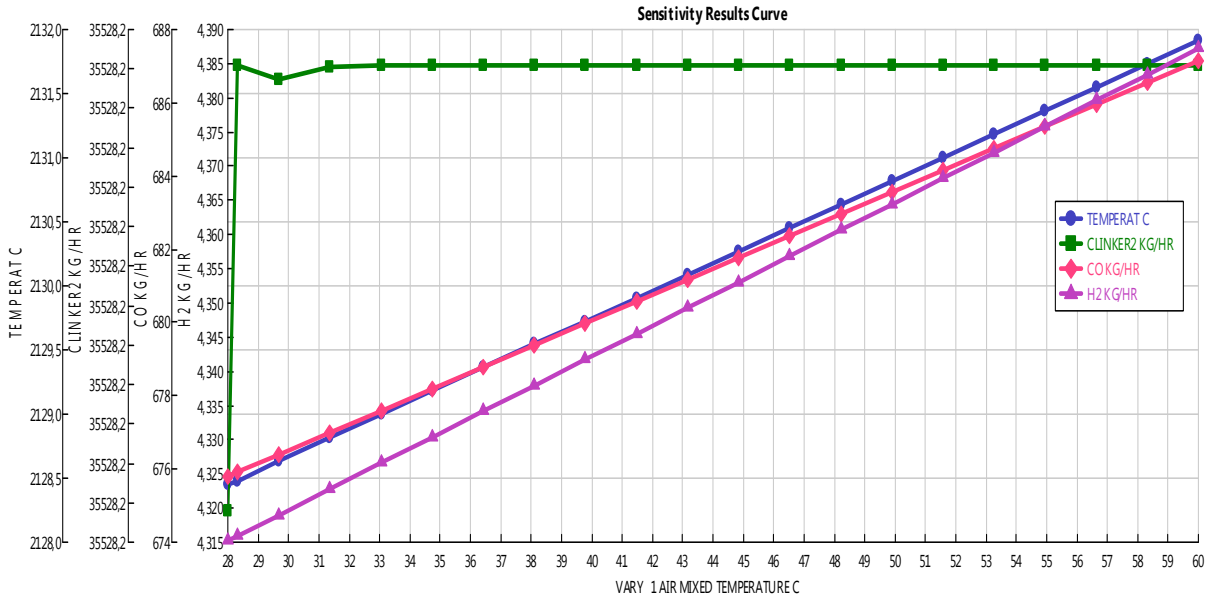

Figure 4.15. Primary combustion air preheating vs. combustion and kiln performance

4.2.7. Concluding remarks

In general, results obtained from the model indicate the importance of modeling and simulation in evaluation of cement production processes. The model generates vital information for evaluation of cement production processes. The constructed model proved to behave approximately the same as the real plant. That was demonstrated in both aspects: from model results data obtained against plant real operating data and from parametric analysis results obtained against real behavior of the cement plant subjected to change in various input parameters. Thus, the parametric analysis objectives were to improve kiln system performance and evaluate environmental performance of the plant due to emissions. It was shown from parametric

analysis that monitoring of flue gases in cement kiln system is very important for the following reasons:

(i) Monitoring flue gases for O_2 and combustibles allows the process to be operated more efficiently;

(ii) Maintaining air/fuel ratio within a specific range can be important for performance of the kiln system including quality of clinker produced;

(iii) Monitoring CO and combustibles can prevent build-up to levels that can cause an explosion in ESP, bag house as well as ID fans;

(iv) Significant reduction in emissions of NO_X together with other pollutants can be achieved by maintaining good combustion control, and

(v) Reliable flue gas analysis provides information for effective control of kiln system.

By monitoring and regulating exhaust gases, it is possible to improve combustion efficiency, which, in turn, leads to conserve fuels and lower expenses. Complete combustion will occur when proper amounts of fuel and air (fuel/air ratios) are mixed for correct amounts of time under appropriate conditions of turbulence as well as temperature. The amount of fuel supplied to the system depends on its calorific value, that is, the higher the calorific value, the lesser the amount of fuel required and vice versa. Also composition of exhaust gases depends on type of fuel used and amount of combustion air. Similarly, pre-heater exhaust gas temperature varies depending on number of stages and volume of exhaust gases. Volume and temperature of exit flue gases from preheater cyclone, in turn, affect fuel consumption in the kiln system. The volume of exit flue gases depends on amount of combustion air and infiltrating air in the kiln system. Results shown in Table 4.6 reveal that exit flue gases' temperature and volume at MCC preheater cyclone are above the optimum value. Therefore, heat recovery feasibility study can be performed based on exhaust gas conditions.

Results obtained from sensitivity analysis suggest that the maximum fuel flow rate possible at MCC kiln burner is $\dot{m}_{coal}$ = 5580 kg·h^{-1} (current $\dot{m}_{coal}$ = 5000 kg·h^{-1}). Increasing coal flow rate above $\dot{m}_{coal}$ = 5580 kg·h^{-1} would lower thermal efficiency of the kiln system. The current coal flow rate of $\dot{m}_{coal}$ = 5000 kg·h^{-1} gives a simulated burning zone gas temperature at T_{flame} =2230 °C, which is above typical plant temperature between T_{flame} =1800 °C and T_{flame} = 2000 °C, suggesting for an opportunity for fuel saving or more clinker production. The typical plant temperature values can be achieved using coal flow rates of $\dot{m}_{coal}$ = 3000 kg·h^{-1} and $\dot{m}_{coal}$ =3737 kg·h^{-1}, giving burning zone combustion gases temperature of T_{flame} =1835 °C and T_{flame} =2043 °C, respectively. The latter provides a minimum potential coal saving of about $\dot{m}_{coal}$ = 1263 kg·h^{-1}, which approximates to 76,126 tons per year at current raw feed. The current specific energy consumption of the kiln system is 4200 kJ·kg$_{cl}^{-1}$ assuming kiln coal supply of $\dot{m}_{coal}$ = 3737 kg·h^{-1}

will give specific energy consumption of 2350.88 $kJ \cdot kg_{cl}^{-1}$. The latter gives specific energy saving of about 1849.12 $kJ \cdot kg_{cl}^{-1}$. However, it should be noted that such fuel saving is only possible if the kiln system operates without losses.

It was observed from parametric analysis that the higher the excess air for combustion above optimal values, the greater the exergy destroyed due to thermal cooling of exergy of combustion gases. It should be noted that while increasing excess air at a certain point may improve combustion efficiency when exceeds the acceptable value of 1-2% O_2 (10-15% excess air), combustion efficiency is lowered followed by unstable kiln operation, which is indicated by irregular clinker production as shown in Fig. 4.7 and Fig. 4.8 Kääntee et al. (2003) observed that too large amount of secondary air fed to the burning zone interrupted clinker formation, the flame becomes unstable, the burning zone is cooled and a lot of dust is in circulation in the kiln and pre-calciner system. Furthermore, the findings by Kääntee et al. (2003) indicated that variation in the feed of secondary combustion air, changes the formation of clinker minerals. As the alite content goes down, the belite content grows rapidly. These changes was caused by the increase of oxygen. Arad and colleagues (2008) point out that non-uniform clinker product output suggests that large temperature gradients exist near and within the rotary kiln bed. Generally it can be concluded that, the demand of combustion air in the burning zone appears to have a large influence on the results.

Also increasing primary air above an optimal value at elevated temperatures will result into more NO_x emission. Thus, NO_x level can be used as an indicator to give information about combustion processes in the kiln system (Fig. 4.7).

Furthermore, increasing the cooling air volume above an optimal value lowers combustion gases temperature thereby lowering kiln thermal efficiency (Fig. 4.8). A parametric analysis was used to examine the effect of preheating the raw feed as well as the primary air used for combustion. It was observed that increasing the moisture content of coal and raw feed will result into lowering the combustion gas temperatures and therefore, affecting negatively the kiln thermal efficiency (Fig. 4.14). Thus, preheating of both raw feed and combustion air is very important for improving combustion processes in the kiln system as well as improving kiln thermal efficiency.

Chapter Five – Exergy Analysis of the MCC Process

5.1. Introduction

In this chapter, an exergy analysis of the kiln system is presented. The kiln system was divided into three major parts according to their functions in the real process of cement production, namely: Rotary kiln, preheater tower and clinker cooler.

The kiln system boundary and the three sub-systems boundary are presented in Fig. 5.1. The simplified schematic diagram for Mbeya Cement kiln system is presented in Fig. 5.2. All values given here together with subsequent calculations for exergy analysis are defined per kilogramme clinker produced. Useful streams and waste streams are defined to simplify the work of exergy analysis. Mass and energy balances, were calculated using the simulator. The exergy efficiency of the overall system and of each subsystem was calculated so as to identify potential areas for improvements.

The thermodynamic data and phase behaviour of the material stream in consideration were obtained from simulation by Aspen One Plus. All the required data for simulation are presented in Chapter Four, Tables 4.1 ÷ 4.4. Chemical exergy of process components were evaluated using reference environment model defined by Moris and Szagut (1986) that is presented in Table 5.1.

Table 5.1. Standard specific chemical exergy (source Morris and Szargut 1986)

Species	$\bar{e}_{CH}$ / kJ·kmol^{-1}	Species	$\bar{e}_{CH}$ / kJ·kmol^{-1}
Al_2O_3 (s,α)	200,400	$CaSO_4$ (s,α)	8,200
$Al_2O_3.SiO_2$ (s)	15,400	Fe_2O_3 (s)	16,500
CO (g)	275,100	H_2 (g)	236,100
CO_2 (g)	19,870	H_2O (l)	900
$CaCO_3$ (s)	1,000	H_2O (g)	9,490
$CaCO_3.MgCO_3$ (s)	15,100	K_2O (s)	413,100
CaO (s)	101,200	MgO (s)	66,800
$CaO.Al_2O_3$ (s)	275,400	$MgCO_3$ (s)	37,900
$2CaO.Al_2O_3$ (s)	460,400	N_2 (g)	690
$3CaO.Al_2O_3$ (s)	500,600	O_2 (g)	3,970
$CaO.SiO_2$ (s)	23,600	Na_2O (s)	296,200
$2CaO.SiO_2$ (s, β)	95,700	SO_2 (g)	313,400
$3CaO.SiO_2$ (s)	219,800	SiO_2 (s)	1,900
CaS	844,600	$Fe_2O_3.SiO_2$	18,400
$4CaO.Al_2O_3.Fe_2O_3$	667,000	NO_2	55,600
S (s)	609,600	NO	88,900

The chemical exergy of ideal gas mixtures was calculated using Eq. 3.8 and for pure multicomponent of the streams, it was calculated using Eq. 3.9. Streams components mole flow used for calculation of chemical exergies were obtained from simulation, and examples are presented in Appendices 2 and 3, respectively. Thus, the chemical exergy rates presented in Table 5.3 were obtained by multiplying the mole flow [kmole·h^{-1}] of each component from respective streams (Appendices 1 and 2) with standard chemical exergy from Table 5.1 in [kJ·kmol^{-1}].

To obtain exergy in [kJ·kg$_{cl}^{-1}$], results obtained in [kJ·s^{-1}] were divided by a factor of 9.87 [kg·s^{-1}] obtained from stream $\dot{m}_{CLINKER}$ = 35,528 kg·h^{-1}, which is the clinker produced per hour. Exergy flow rates of main process streams due to work rate were directly obtained from simulation and are presented in Table 5.2. The enthalpy rate, mass flow and physical exergy obtained directly from simulation are presented in Table 5.3 together with calculated chemical exergy.

Table 5.2. Exergy flow rates of main process streams due to work rate

Process drives	$\dot{W}$ /kW	$\dot{E}$/ kW	$\dot{e}$ / kJ·kg$_{cl}^{-1}$
Primary Air Fan	75	75	7.60
Cooling Air Fan	75	75	7.60
ID-Fan	670	670	67.88
Booster Fan	132	132	13.37

Examples of how chemical exergies were calculated for ideal gas mixtures and for solid multicomponent of streams are given for streams GASES and PH4SOLID presented in Appendices 4 and 5, respectively. An example is shown to demonstrate how chemical exergy was calculated for each component presented in Appendices 4 and 5, respectively. Chemical exergy of coal fuel was calculated using Eq. 3.18. The value of chemical exergy for coal fuel obtained using Eq. 3.18 is relatively comparable with the value obtained from simulation. The obtained values are presented in Table 5.3 for streams DRY-COAL and INBURNER. Coal was decomposed into its combustible elements as indicated in stream INBURNER. Therefore, chemical exergies for reactants were obtained from streams INBURNER, AIR and HOTAIR, while for product, they were obtained from combustion product (stream PRODUCT) and ASHPROD, all presented in Table 5.3. The change of Gibbs function values was obtained from simulation. Appendix 6 presents how ΔG values are calculated from reactants and products components obtained from respective streams mentioned above. Exergy balances for overall system, sub-systems and components together with exergetic variables' calculations are appended at the end of the thesis (Appendices 11 through 19).

5.2. Mass and Exergy Balances around the Processes

In this section, mass and exergy balances for the overall kiln system and of the sub systems are presented. All calculations are appended at the end of this thesis (Appendices 11 ÷ 19).

Table 5.3. Mass flow rates, and exergy flow rates of main process streams

Process streams	$\dot{m}$ / kg·h^{-1}	h / kJ·kg$_{cl}^{-1}$	$\dot{E}_{PH}$ / kW	$\dot{E}_{CH}$ / kW	$\dot{e}_{tot}$ / kJ·kg$_{cl}^{-1}$
RAW-FEED	58,000	12,664	0	0	0
DRY-COAL	4,158	579	0	34,598	3,505
INBURNER	4,158	135	0	32,172	3,260
AIR (4)	11,438	1	0	0	0
COLDAIR	33,712	3	0	0	0
EXGASOUT	68,244	8,058	4,811	2,963	788
SOLIDOUT	3,536	1,225	14	116	13
CLINKER2	35,528	12,324	472	10,911	1,153
CLINKER1	35,528	11,806	3,767	10,911	1,487
HOTAIR	33,712	748	3,764	0	381
PH4SOLID	40,324	12,909	4,936	10,097	1,523
KLN1SOLD	35,528	11,060	9637	10,799	2,071
PH5GAS	54,103	3,054	8,961	22,127	3,150
S-1 (PHT Exh.)	71,780	8,759	2,444	3,026	554
S-2 (In cooler)	33,712	2	42	0	4
S-3(Primary air)	11,438	1	43	0	4
S-4 (Exh.cooler)	71,780	9,270	3,811	3,026	693
EXGAS	71,780	9,283	3,724	3,016	683
PH3SOLID	71,345	23,379	7,600	2,345	1,008
PH3GAS	91,071	14,296	9,873	3,886	1,394
PH3FEED	16,242	37,675	17,479	7,103	2,491
PH4FEED	125,448	24,481	16,130	43,207	6,012
PH4GAS	85,124	11,572	11,189	13,207	2,472
GASES (Comb)	48,452	563.30	25,505	3,467	2,935
ASHPROD	856	229.31	682	172	87
PRODUCT2	83,980	11,974	24,558	11,843	3,688
KLN2SOLD	34,672	10,972	7,649	10,216	1,810
KLN1GAS	48,452	914	14,920	1,001	1,613
KLN3SOLD	34,672	10,871	5,036	13,671	1,895
PRODUCT3	83,124	12,252	19,660	11,843	3,200
KLN2GAS	48,452	1,281	12,011	969	1,315
PRODUCT4	88,775	13,925	13,998	36,039	5,070
PRODUCT	48,452	563	25,505	3,466	2,935
PH2SOLID	77,292	25,670	5,934	2,539	858
PH2GAS	80,929	11,329	6,369	3,313	981
PH2FEED	158,221	36,999	12,315	6,133	1,869
PHS1SOLD	33,576	11,366	1,276	1,103	241
PH1NSOLD	33,574	11,366	1,276	1,102	241
PH1SGAS	35,889	4,345	1,396	1,513	295
PH1NGAS	35,891	4,346	1,396	1,513	295
PH1SFEED	69,465	15,711	2,685	2,639	539
PH1NFEED	69,465	15,711	2,685	2,639	539
PH1FEED	138,930	31,422	5,369	5,279	1,079
PHGASOUT	71,780	8,827	2,975	3,026	608

5.2.1. System Boundary for the Overal Kiln System

The overall system boundary for the kiln system is presented in Fig. 5.1. It can be observed that input streams for the overall system are:

- Stream $\dot{m}_{\text{RAW-FEED}}$ = 58,000 kg·h^{-1}, at $T_{\text{RAW-FEED}}$ = 28 °C;

- Stream $\dot{m}_{\text{DRY-COAL}}$ = 4158 kg·h^{-1}, at $T_{\text{DRY-COAL}}$ = 28 °C;
- Stream $\dot{m}_{\text{AIR}}$ = 11,438 kg·h^{-1}, at T_{AIR} = 28 °C and
- Stream $\dot{m}_{\text{DRY-COAL}}$ = 33,712 kg·h^{-1}, at $T_{\text{DRY-COAL}}$ = 28 °C.

Other input streams crossing the overall system boundary were work supplied to the primary and cooling air fan. On the other hand there are only three output streams crossing the overall system boundary:

- Exhaust gases exposed to the environment $\dot{m}_{\text{EXGASOUT}}$ = 68,244 kg·h^{-1}, at T_{EXGASOUT} = 139 °C;
- Dust separated from exhaust gases $\dot{m}_{\text{SOLIDOUT}}$ = 3536 kg·h^{-1}, at T_{SOLIDOUT} = 139 °C and
- Clinker $\dot{m}_{\text{CLINKER2}}$ =35,528 kg·h^{-1}, at T_{CLINKER2} = 245 °C.

However, this study considered the stream PHGASOUT leaving the uppermost twin preheater cyclones (Fig. 5.2b) for evaluation of exergy lost to the environment. It should be pointed out that clinker is the main desired output from the kiln system.

Furthermore, there are driving power for kiln drives, but their effect is negligible compared to other exergy supplied to the rotary kiln (Kolip and Savas 2010; Farag 2012; Kolip 2010; Koroneos et al. 2005; Camdali et al. 2004). Based on the assumptions (iii) and (iv), adiabatic condition was assumed for combustion process in the rotary kiln burner and thus, exergy due to heat transfer was neglected in the exergy balance equations.

Simplified schematic diagrams for mass and exergy balances are presented in Fig. 5.2. Mass and exergy are presented per kilogram clinker, since clinker is the major required product from the cement kiln system. Exergetic evaluation of the overall kiln system and the three kiln subsystems was carried out first, followed by that of important individual components of the kiln system. The approach was chosen based on complexity of the real kiln system relative to the model used. Results obtained for each sub-system and overall system are tabulated first, followed by that of individual components. Detailed calculations are given within the Appendix.

In the simplified schematic diagrams of MCC kiln system, the names of simulated streams are given in brackets followed by real names of streams in the real cement plant kiln system processes.

5.2.2. Exergy of Fuel and Product Definitions for the Kiln System

In order to calculate the overall exergy efficiency of the kiln system, exergy of fuel and product for the overall system were defined followed by calculation of overall exergy destruction of the system. The thermodynamic data used for exergetic analysis were extracted from Table 5.3.

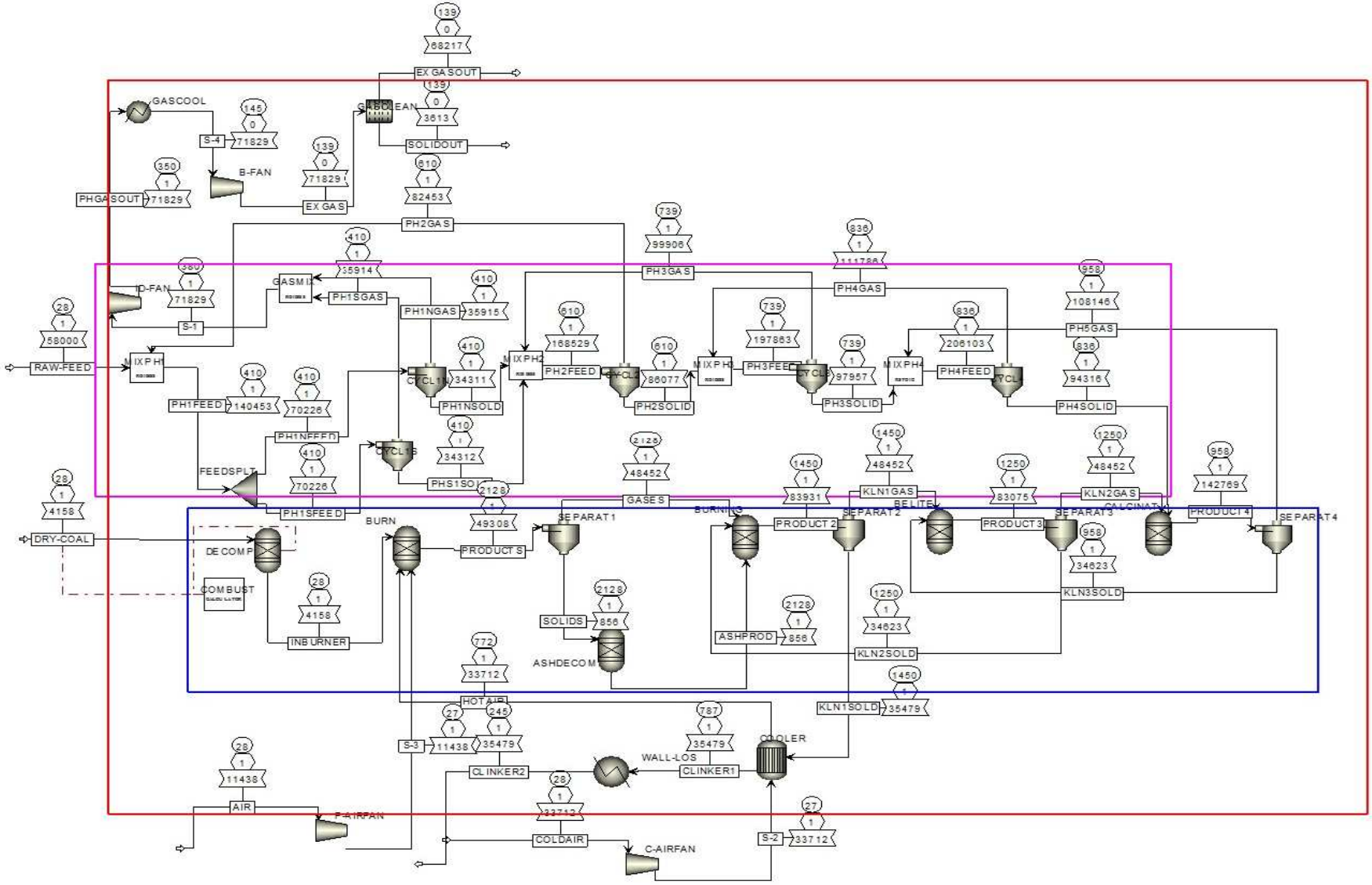

Figure 5.1. Global flow sheet of MCC kiln system boundary

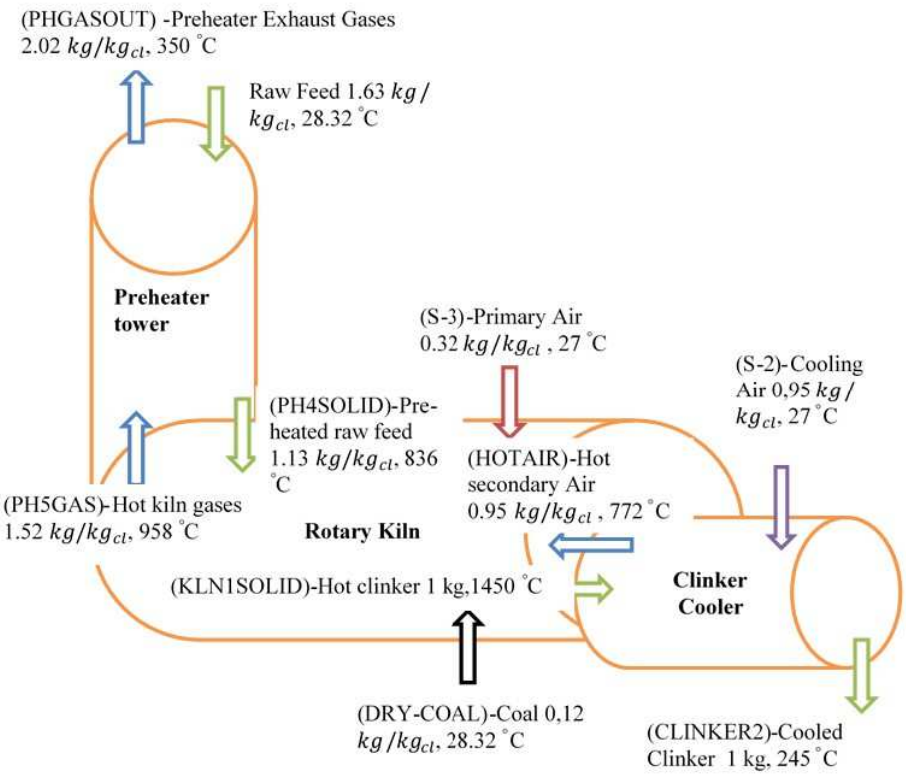

Figure 5.2a. Schematic diagram of MCC kiln system mass flows per kg clinker

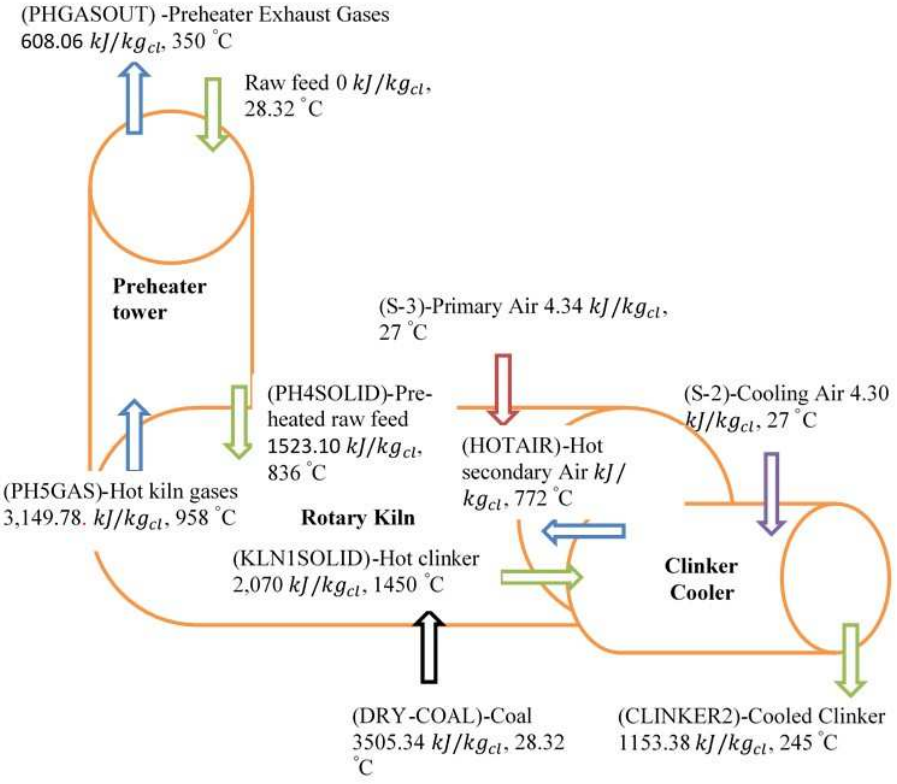

Figure 5.2b. Schematic diagram of MCC kiln system exergy flows per kg clinker

Recall, clinker is the major required product for kiln system of cement production processes. From the exergetic viewpoint, the exergy of stream $CLINKER_2$ represents the product for the total plant. The exergy rate of fuel was obtained from the stream DRY-COAL. Thus, the exergy of fuel and product are defined as:

$$\dot{e}_{F,SYS} = \left(\dot{e}_{DRY\text{-}COAL} + \dot{e}_{RAW\text{-}FEED} + \dot{e}_{S\text{-}3} + \dot{e}_{S\text{-}2}\right) \text{ and } \dot{e}_{P,SYS} = \dot{e}_{CLINKER} \text{ respectively} \quad (5.1)$$

However, the exergy destructions for the overall system are obtained by subtracting the sum of exergy of input streams from the sum of exergy of output streams.

$$\dot{e}_{D,SYS} = \dot{e}_{i,SYS} - \dot{e}_{e,SYS} = \left(\dot{e}_{DRY\text{-}COAL} + \dot{e}_{RAW\text{-}FEED} + \dot{e}_{S\text{-}3} + \dot{e}_{S\text{-}2}\right) - \left(\dot{e}_{CLINKER} + \dot{e}_{PHGASOUT}\right) \quad (5.2)$$

Overall exergy loss of the kiln system is given by stream PHGASOUT at 350 °C.

$$\dot{e}_{L,SYS} = \dot{e}_{PHGASOU} \quad (5.3)$$

$$\varepsilon_{SYS} = \frac{\dot{e}_{P,SyS}}{\dot{e}_{F,SyS}} \quad (5.4)$$

5.2.3. Exergy of Fuel and Product Definitions for the Rotary Kiln

The exergy destruction for the rotary kiln was calculated by equating the sum of exergy inputs and outputs of the streams. Nevertheless, the exergy definitions of fuels and products were also defined so as to calculate the rational efficiency for the rotary kiln.

$$\dot{e}_{D,RTK} = \dot{e}_{i,RTK} - \dot{e}_{e,RTK} = \left(\dot{e}_{HOT\ AIR} + \dot{e}_{DRY\text{-}COAL} + \dot{e}_{S\text{-}3} + \dot{e}_{PH4SOLID}\right) - \left(\dot{e}_{KLN1SOLD} + \dot{e}_{PH5GAS}\right) \quad (5.5)$$

$$\dot{e}_{F,RTK} = \left(\dot{e}_{HOT\ AIR} + \dot{e}_{DRY\text{-}COAL} + \dot{e}_{S\text{-}3}\right) \text{and } \dot{e}_{P,RTK} = \left(\dot{e}_{KLN1SOLD} - \dot{e}_{PH4SOLID}\right) \quad (5.6)$$

5.2.4. Exergy of Fuel and Product for the Preheater Tower

Taking the preheater tower as a heat exchanger, the exergy of fuel and product as well as exergy destruction were calculated from:

$$\dot{e}_{F,PHT} = \dot{e}_{PH5GAS} - \dot{e}_{PHGASOUT} \quad (5.7)$$

$$\dot{e}_{P,PHT} = \dot{e}_{PH4SOLID} - \dot{e}_{RAW\text{-}FEED} \quad (5.8)$$

$$\dot{e}_{D,PHT} = \dot{e}_{F,PHT} - \dot{e}_{P,PHT} = \left(\dot{e}_{PH5GAS} - \dot{e}_{PHGASOUT}\right) - \left(\dot{e}_{PH4SOLID} - \dot{e}_{RAW\text{-}FEED}\right) \quad (5.9)$$

5.2.5. Exergy of Fuel and Product for the Clinker Cooler

The planetary clinker cooler was modeled as cross flow heat exchanger. Thus, definitions for exergy of the fuel and product as well as exergy destruction are as follows:

$$\dot{e}_{\mathrm{F,PLC}} = \dot{e}_{\mathrm{KLN1SOLD}} - \dot{e}_{\mathrm{CLINKER_2}} \tag{5.10}$$

$$\dot{e}_{\mathrm{P,PLC}} = \dot{e}_{\mathrm{HOTAIR}} - \dot{e}_{\mathrm{S\text{-}2}} \tag{5.11}$$

$$\dot{e}_{\mathrm{D,PLC}} = \dot{e}_{\mathrm{F,PLC}} - \dot{e}_{\mathrm{P,PLC}} = \left(\dot{e}_{\mathrm{KLN1SOLD}} - \dot{e}_{\mathrm{CLINKER_2}}\right) - \left(\dot{e}_{\mathrm{HOTAIR}} - \dot{e}_{\mathrm{S\text{-}2}}\right) \tag{5.12}$$

The planetary cooler wall loss was modelled using the WALL-LOSS model. Hence, the wall loss can be estimated as:

$$\dot{e}_{\mathrm{L,WALL\text{-}LOS}} = \dot{e}_{\mathrm{CLINKER_1}} - \dot{e}_{\mathrm{CLINKER_2}} \tag{5.13}$$

5.3. Exergy of Fuels and Products for the Components

The models representing each *k*-th component for each sub-system are presented in Appendix 1. Therefore, exergy balances for each component were carried out based on principles guiding exergy balances of an individual component. For example, for the cooler, heat exchanger model is adopted, while for the kiln, burner combustion chamber model is applied. In general, eq. (3.12) was used for exergy balance for the *k*-th component. The exergy of fuel and product as well as exergy destruction calculations for each individual component were carried out first, and the thermodynamic data obtained from the exergetic analysis are presented in Table 5.4. Detailed calculations are appended at the end of the thesis.

WALL-LOSS: This component is treated as dissipative component.

$$\dot{e}_{\mathrm{D,WALL\text{-}LOSS}} = \dot{e}_i - \dot{e}_e = \dot{e}_{\mathrm{CLINKER_1}} - \dot{e}_{\mathrm{CLINKER_2}} \tag{5.14}$$

The flue gases from preheater tower are normally used to preheat raw feed when the kiln system is operated in a compound mode. However, in the simulation model of the kiln system, it was assumed that the raw mill was off and therefore, the flue gases passed through the cooler. The exergy of the fuel and product as well as exergy destruction were calculated based on the heat exchanger model:

$$\dot{e}_{\mathrm{D,GASCOOL}} = \dot{e}_{\mathrm{S\text{-}4}} - \dot{e}_{\mathrm{PHGASOUT}} \tag{5.15}$$

Combustion of coal in a rotary kiln takes place in the kiln burner here modelled as BURN and thus, the combustor model was used for definition of exergy of fuel and product as well as exergy destruction. The values for chemical and physical exergy used were obtained as shown in Table 5.3 and they were divided by 9.87 [kg·s^{-1}] to convert them from [kW] to [[kJ·kg], OXIDANT is the sum of exergy of streams HOTAIR and S-3.

$$\dot{e}_{\mathrm{D,BURN}} = \dot{e}_{\mathrm{F,BURN}} - \dot{e}_{\mathrm{P,BURN}}`$$

$$\dot{e}_{\mathrm{D,BURN}} = \left[\left(\dot{e}^{\mathrm{CH}}_{\mathrm{FUEL}} + \dot{e}^{\mathrm{CH}}_{\mathrm{OXIDANT}}\right) - \left(\dot{e}^{\mathrm{CH}}_{\mathrm{GASES}} + \dot{e}^{\mathrm{CH}}_{\mathrm{ASHPROD}}\right)\right] - \left[\left(\dot{e}^{\mathrm{PH}}_{\mathrm{GASES}} + \dot{e}^{\mathrm{PH}}_{\mathrm{ASHPROD}}\right) - \left(\dot{e}^{\mathrm{PH}}_{\mathrm{FUEL}} + \dot{e}^{\mathrm{PH}}_{\mathrm{OXIDANT}}\right)\right] \quad (5.16)$$

Clinker burning in a rotary kiln takes place in the burning zone of the kiln where heat exchange between combustion gases from the kiln burner and the compound from calcination of preheated raw feed takes place to form clinker. Thus, the cross flow heat exchanger was assumed for definition of exergy of fuel and product as well as calculation of exergy destruction:

$$\dot{e}_{\mathrm{D,\,BURNING}} = \left(\dot{e}_{\mathrm{F,\,BURNING}} - \dot{e}_{\mathrm{P,\,BURNING}}\right) = \left(\dot{e}_{\mathrm{GASES}} - \dot{e}_{\mathrm{ASHPRODUCT}} - \dot{e}_{\mathrm{KLN1GAS}}\right) - \left(\dot{e}_{\mathrm{KLN1SOLD}} - \dot{e}_{\mathrm{KLN2SOLD}}\right) \quad (5.17)$$

Calcination takes place in the reactor CALCINAT. Therefore the exergy destruction as well as fuel and product are given by:

$$\dot{e}_{\mathrm{D,\,CALCINAT}} = \left(\dot{e}_{\mathrm{F,CALCINAT}} - \dot{e}_{\mathrm{P,\,CALCINAT}}\right) = \left(\dot{e}_{\mathrm{PH4SOLID}} + \dot{e}_{\mathrm{KLN2GAS}}\right) - \left[\dot{e}_{\mathrm{PRODUCT4}} - \left(\dot{e}_{\mathrm{KLN3SOLD}} + \dot{e}_{\mathrm{PH5GAS}}\right)\right] \quad (5.18)$$

The 4-stage preheater cyclones consist of five cyclones. In the simulated model, the cyclones were presented using two components, a mixer followed by a cyclone so as to model properly the function of a real cyclone in the cement production. Details of the model are presented in Chapter Four. For proper definitions of exergy of fuel and products, the mixers are considered as heat exchangers with mixing (Tsatsaronis 1993). Thus, the exergy of fuel and products as well as exergy destruction are defined as follows:

$$\dot{e}_{\mathrm{P,MIXPH1}} = \dot{e}^{\mathrm{PH}}_{\mathrm{PH1FEED}} \quad (5.19)$$

$$\dot{e}_{\mathrm{P,MIXPH1}} = \left(\dot{e}^{\mathrm{TOT}}_{\mathrm{RAW\text{-}FEED}} + \dot{e}^{\mathrm{TOT}}_{\mathrm{PH2GAS}}\right) - \left(\dot{e}^{\mathrm{TOT}}_{\mathrm{PH1FEED}} - \dot{e}^{\mathrm{PH}}_{\mathrm{PH1FEED}}\right) \quad (5.20)$$

$$\dot{e}_{\mathrm{D,\,MIXPH1}} = \dot{e}_{\mathrm{F,\,MIXPH1}} - \dot{e}_{\mathrm{P,\,MIXPH1}} \quad (5.21)$$

$$\dot{e}_{\mathrm{P,MIXPH2}} = \dot{e}^{\mathrm{PH}}_{\mathrm{PH2FEED}} \quad (5.22)$$

$$\dot{e}_{\mathrm{P,\,MIXPH2}} = \left[\left(\dot{e}^{\mathrm{TOT}}_{\mathrm{PH1NSOLD}} + \dot{e}^{\mathrm{TOT}}_{\mathrm{PHS1SOLD}}\right) + \dot{e}^{\mathrm{TOT}}_{\mathrm{PH3GAS}}\right] - \left(\dot{e}^{\mathrm{TOT}}_{\mathrm{PH2FEED}} - \dot{e}^{\mathrm{PH}}_{\mathrm{PH2FEED}}\right) \quad (5.23)$$

$$\dot{e}_{\mathrm{D,\,MIXPH2}} = \dot{e}_{\mathrm{F,\,MIXPH2}} - \dot{e}_{\mathrm{P,\,MIXPH2}} \quad (5.24)$$

$$\dot{e}_{\mathrm{P,MIXPH3}} = \dot{e}^{\mathrm{PH}}_{\mathrm{PH3FEED}} \quad (5.25)$$

$$\dot{e}_{\mathrm{F,MIXPH3}} = \left(\dot{e}^{\mathrm{TOT}}_{\mathrm{PH4GAS}} + \dot{e}^{\mathrm{TOT}}_{\mathrm{PH2SOLD}}\right) - \left(\dot{e}^{\mathrm{TOT}}_{\mathrm{PH3FEED}} - \dot{e}^{\mathrm{PH}}_{\mathrm{PH3FEED}}\right) \quad (5.26)$$

$$\dot{e}_{\mathrm{D,\,MIXPH3}} = \dot{e}_{\mathrm{F,\,MIXPH3}} - \dot{e}_{\mathrm{P,\,MIXPH3}} \quad (5.27)$$

$$\dot{e}_{\mathrm{P,MIXPH4}} = \dot{e}^{\mathrm{PH}}_{\mathrm{PH4FEED}} \quad (5.28)$$

$$\dot{e}_{F,MIXPH4} = \left(\dot{e}^{TOT}_{PH3SOLD} + \dot{e}^{TOT}_{PH5GAS}\right) - \left(\dot{e}^{TOT}_{PH4FEED} - \dot{e}^{PH}_{PH4FEED}\right) \quad (5.29)$$

$$\dot{e}_{D,B\text{-}FAN} = \dot{e}_{F,B\text{-}FAN} - \dot{e}_{P,B\text{-}FAN} = \dot{W}_{B-FAN} - \left(\dot{e}_{S\text{-}4} - \dot{e}_{EXGAS}\right) \quad (5.30)$$

$$\dot{e}_{D,ID\text{-}FAN} = \dot{e}_{F,ID\text{-}FAN} - \dot{e}_{P,ID\text{-}FAN} = \dot{W}_{ID-FAN} - \left(\dot{e}_{PHGASOUT} - \dot{e}_{S\text{-}1}\right) \quad (5.31)$$

$$\dot{e}_{D,P\text{-}AIRFAN} = \dot{e}_{F,P\text{-}AIRFAN} - \dot{e}_{P-AIRFAN} = \dot{W}_{P-AIRFAN} - \left(\dot{e}_{S\text{-}3} - \dot{e}_{AIR}\right) \quad (5.32)$$

$$\dot{e}_{D,C\text{-}AIRFAN} = \dot{e}_{F,C\text{-}AIRFAN} - \dot{e}_{P,C\text{-}AIRFAN} = \dot{W}_{C-AIRFAN} - \left(\dot{e}_{S\text{-}2} - \dot{e}_{COLDAIR}\right) \quad (5.33)$$

Table 5.4. Data obtained from the exergetic analysis

Component	$\dot{e}_{F,K}$ /kJ·kg$_{cl}^{-1}$	$\dot{e}_{P,K}$ /kJ·kg$_{cl}^{-1}$	$\dot{e}_{D,K}$ / kJ·kg$_{cl}^{-1}$	$\dot{e}_{L,tot}$ / kJ·kg$_{cl}^{-1}$	ε_k / %
ID-FAN	68	54	14		79.4
B-FAN	13	10	3		74.0
P-AIRFAN	8	4	3		57.1
C-AIRFAN	8	4	3		56.6
CALCINAT	2,838	24	2,814		0.9
BELITE	298	85	213		28.6
COOLER	583	377	206		64.6
WALL-LOSS	1,487	1,153	334		77.7
BURN	2,890	2,267	623		78.4
BURNING	1,409	261	1,148		18.5
MIXPH2	1,255	1,248	7		99.4
MIXPH3	2,611	1,771	840		67.8
GASCOOL	693	608	85		87.8
Sub-systems (Figure 5.2.)					
Rotary kiln	3,891	547	194	3,150	14.7
Preheater	2,542	1,523	1,019		59.9
Cooler	917	377	540		41.1
Overall	3,514	1,153	1,753	608	32.8

5.4. Exergy Analyses Results Discussion and Conclusions

Recall, in cement production processes, the dry rotary kiln systems is normally made up of three major parts (sub-systems), namely, the rotary kiln, the clinker cooler and the preheater tower. In actual cement plant operations, rotary kiln, preheater tower and clinker cooler are considered as individual components of the kiln system. The kiln system of Mbeya cement is made up of the dry rotary kiln, the planetary clinker cooler and the 4-stage preheater cyclones. During modeling and simulation, the rotary kiln was further divided into imaginary reactors to

mirror actual reactions taking place in all major kiln regions, for example, combustion, calcination, clinker burning and belite formation.

However, most reactions overlap in real rotary kiln operations and hence, it is impossible to separate them completely. The purpose of dividing the rotary kiln into imaginary reactors is to demonstrate the contribution of each reaction in performance of the rotary kiln. Since the kiln zones are not physical components (reactors), the presentation of exergetic analyses results is shown in Table 5.4 and just considered their effect in contributing to imperfection of the rotary kiln. They were meant to give insights on what happens in the processes and the kind of reactions with major impact on contributing to irreversibility in the rotary kiln. Thus, they are not further considered in summing up their effect to give total exergy destruction individually as it is traditionally done.

Moreover, their effect was considered indirectly in calculating the exergy destruction of the rotary kiln sub-system as presented in Table 5.4. The approach was preferred to avoid complications and confusion that might have arose due to complexity of the system and processes in the kiln system. Nonetheless, other physical individual components like kiln burner, cyclones, fans like ID-FAN, Primary Air Fan, Cooler Air Fan and Booster Fan exergetic variables were calculated to evaluate performance of each individual component. They are presented in Table 5.4.

Thermodynamic data obtained from simulation and chemical exergy calculation are presented in Table 5.3. Results presented in Table 5.3 suggests that, chemical exergy contain large portion of overall clinker formation exergy (streams CLINKER1 and CLINKER2). Their chemical exergy value amounts to 10,912 kW, with their respective physical exergy of 472 kW and 3,766 kW. These are expected results since most of the clinker formation exergy results from chemical reactions. The results are in good agreement with published data (Appendix 9).

Results presented in Table 5.3 indicates that, compared to chemical exergy, physical exergy contributes significant portion of total exergy released with combustion gases. Their values are 3,466 kW and 25,505 kW respectively. Such results supports the theory that the main objective of combustion process is to convert the chemical exergy of input streams (fuel and oxidant chemical exergy), into physical exergy (Tsatsaronis et al. 2013).

Findings suggest that the rotary kiln has the highest exergy consumption rate among other kiln sub-systems. Additionally, it was found that from exergetic point of view, rotary kiln has the highest irreversibility compared to other kiln sub-systems. Compared to other physical and chemical reactions, Calcination process, which is an endothermic reaction consumes the largest part of the exergy input to the rotary kiln. This is an expected results based on most literatures that most of heat energy generated from kiln burner combustion process is used for calcination i.e. decomposition of calcium carbonate (Kääntee et al. 2003, Kääntee et al. 2004; Farag and Taghian 2015; Summerbell et al. 2016; Farag, 2012; Koroneos et al. 2005) The rotary kiln exergy destruction is mainly due to combustion reactions and chemical reactions as indicated in Table 5.4. The

findings indicate that calcination reaction destroys exergy the most, followed by clinker burning process reactions and combustion process, with exergy destruction amounting to $\dot{e}_{D,K}$ = 2,813.75 kJ·kg$_{cl}^{-1}$, 1,148.17 kJ·kg$_{cl}^{-1}$ and 623.42 kJ·kg$_{cl}^{-1}$ respectively. The rate of exergy destruction by chemical reactions during combustion can be reduced if the flame temperature is kept high with less temperature gradient in the combustor. The latter can be achieved by air preheating. Thus, heat recuperation from clinker cooler is very important for improving combustion efficiency in the kiln burner and is among the major controlling parameter for kiln system thermal performance (ICR 2005).

The reasons for higher exergy destructions in the clinker burning reactions could be due to heat exchange between finite temperature differences of gases T_{GASES} = 2128 °C and solids entering the burning zone at $T_{KLN2SOLD}$ = 1250 °C. Other reasons for high irreversibility in the clinker burning processes could be mixing of hot gases and solid materials at different compositions as well as temperatures. Furthermore, chemical reactions for formation of intermediate and major clinker compounds could be the major cause of irreversibility.

The exergetic efficiency of the rotary kiln is 14.1 %. This exergetic efficiency of the rotary kiln is very low, indicating poor performance of the rotary kiln. Also the exergy efficiency of the rotary kiln indicates an available potential for improvement measure for much better performance of the system. The exergetic analyses results for the rotary kiln are in good agreement with results found in most literatures. The results from literatures point out that the highest irreversibility in the cement rotary kiln system occurs in the rotary kiln and it is caused by chemical reactions, combustion and heat transfers (Appendix 9).

Findings suggest that the major causes of irreversibility in the clinker cooler at MCC were exergy loss with outlet cooled clinker to the environment at temperatures higher than that of the environment (245 °C). The second cause of irreversibility in the clinker cooler was exergy destruction due to heat exchange between cold secondary air and hot clinker from the rotary kiln. Another source of irreversibility in the clinker cooler was exergy loss with heat transfer through the cooler wall to the environment. The exergetic analysis results indicated that clinker cooler was found to have 41.1 % exergetic efficiency. The results obtained from the study are in good agreement with results found in most literatures (Appendix 9). Nevertheless, it should be mentioned that, in most pat studies, clinker coolers are in the third position in terms of poor performance, precided by rotary kiln and preheater tower cyclones. However, the slight deviation of the result from this study and most of the literatures are due to different types of clinker coolers used i.e grate coolers, rotary cooler and planetary coolers and their capacities.In the current study, the planetary clinker cooler was investigated. Planetary clinker coolers have the poorest efficiency compared to grate coolers and rotary coolers, hence this was an expected result.

Exergetic analyses results presented in Table 5.4 indicate that a significant amount of exergy was lost with the preheater exit flue gases and dusts $\dot{e}_L$ = 608.06 kJ·kg$_{cl}^{-1}$. This value is approximately equal to 17.3 % of fuel exergy input to the overall kiln system. This results are in good agreement with published literatures (Appendix 9), especially results obtained by Farag and Taghian (2015). In their study conducted for five Egyptian dry rotary kiln, they found that the preheater exhaust gases exergy ranges from 5 % to 8 % of total exergy input. The deviation of results obtained in the current study compared to Farag and Taghian (2015), could be mainly due to exhaust flue gases by pass ducts installed in the Egyptians kiln systems to avoid problems in the preheater tower due to presence of large quantity of sulfur and alkalis in their raw materials. The exergy lost with the by-pass flue gases ranges from 2.6 % to 8.8 %. Thus, if we sum the exergy lost due to exhaust flue gases from preheater tower and the by-pass duct, the obtained resultant exergy lost is approximately similar to what have been obtained in the current study. Additionally, the installations investigated by Farag and Taghian (2015) comprises of preheater cycolnes with precalciner. Moreover, the preheater cyclones stages ranges from four to five with grate coolers for four installations, while the remaining one has a rotary cooler. The investigated kiln system in this study, has four stage preheater cyclones without precaliciner, and the clinker cooler employed is planetary cooler.

It was assumed that 30 % of calcination of calcium carbonate takes place in the 4-th preheater cyclone stage and thus, calcination reaction and intermediated reactions contributed to significant exergy destruction. Another source of irreversibility was mixing of solid materials and flue gases of different compositions, temperatures and pressures. Preheater cyclones are ranked in the third place sub-system of the kiln system for contribution of imperfection with the exergetic efficiency of 59.9 %.

Overall performance of the kiln system was poor. Irreversibility of the overall kiln system is remarkably high 1,752 kJ·kg$_{cl}^{-1}$ representing about 49.9 % of the overall kiln system fuel exergy. The findings are in good agreement with published literature (Appendix 9). Farag and Taghian (2015), found that irreversibilities in the investigated kiln systems ranges from 1,652 kJ·kg$_{cl}^{-1}$ to 2396.4 kJ·kg$_{cl}^{-1}$ which represents 49.6 % to 53.3 % of the total exergy input.

The findings suggest that overall exergetic efficiency of the rotary kiln system was 32.8 %. The results are in good agreement with results found in most publications. Generally, values of exergetic efficiencies for overall system found in literature range between 8 % and 65 % as presented in Appendix 9. Causes of deviations from one study to another are discussed in detail in Section 2.9.2. of this thesis. The major causes of irreversibilities in the overall kiln system are chemical reactions of raw materials and combustion processes taking place in the rotary kiln sub-systems, exergy loss with exit flue gases, preheater cyclones and exergy destruction in the clinker cooler. Generally, the findings indicated higher potential for performance improvement of the overall kiln system because the exergy efficiency was below 50 %. Literature suggests

that with the Best Available Technology (BAT), the exergy efficiency of the overall kiln system should be around 50 %.

In general, it can be surmised that exergetic performance of the kiln components, sub-systems and overall kiln system was very low, suggesting potentiality for improvements. Hence, there is a need for improvement measures to be taken. Furthermore, findings from exergetic analyses confirmed the parametric results that there was possibility of saving substantial amount of coal fuel and specific energy consumption if performance of the rotary kiln system is improved. Measures for improving performance of the overall kiln system and sub-systems as well as implementation of some of these measures are discussed in Chapter Six of this thesis.

Chapter Six – Kiln System Improvement

6.1. Introduction

Exergetic performance of the kiln system is evaluated and discussed in Chapter Five. Exergetic variables for *k*-th component, sub-systems and overall rotary kiln system are calculated (Table 5.4). Components, processes and sub-systems with major exergetic inefficiency are pinpointed. Thus, in this chapter, improvement measures for avoidable part of irreversibility are suggested. Furthermore, this chapter provides suggestions on the manner to implement some of the improvement measures to demonstrate if they can really improve performance of individual components, sub-systems and the overall kiln system at large. However, implemented improvement measures are restricted to measures that do not involve technological change or replacement of equipment. The latter is only possible if further analyses like thermo economic and exergoeconomic are carried out to justify their implementation. Nonetheless, due to lack of information and scope of the work carried out in this research, it was not possible to conduct the two analyses. The suggested improvement measures are listed in the foregoing:

(i) Exergetic analyses results presented in Table 5.4 indicated that a significant amount of exergy is lost with preheater exit flue gases and dusts. Exergy analyses findings for preheater cyclones revealed that another source of irreversibility was mixing of solid material and flue gases of different compositions, temperatures and pressures. Irreversibility due to mixing in preheater cyclone unit can be minimized by maximizing the operational parameters and physical structure of cyclone system. Exergy loss due to flue gases and flue dust can be recovered by recycling flue gases for preheating the raw feed and coal fuel in the raw mill and coal mill, respectively. Furthermore, exergy loss with preheater flue gases and dust can be recovered for electrical power generation using steam turbine. Additionally, heat loss with exit flue gasses from the preheater and the kiln can be minimized through decreasing volume or temperature of exit flue gases. The latter can be achieved by optimization of geometric dimensions of preheater stages to improve collection efficiency and achieve good contact between gases and solid without increasing pressure drop. Also, reduction of in filtrated air to the kiln preheater and cooler can be achieved by providing better joints between ducts.

(ii) A strategy is needed to recover the exergy lost with clinker product at T_{CLINKER2} = 245 °C. The temperature of cooled clinker is higher than the standard temperature of T_{CLINKER2} 100 up to T_{CLINKER2} 200 °C mentioned in literature for the planetary cooler. Since there is a plan for expansion of the plant capacity, it could be thought of changing the clinker cooler to grate cooler, which is highly efficient especially for high capacity kiln system.

(iii) It was found that clinker burning reactions are the major cause of irreversibility in the rotary kiln. The exergy destroyed in the rotary kiln can be minimized by reducing the finite temperature gradient by insuring that optimum amount of excess air factor as well as coal fuel rate are controlled. The latter was investigated using parametric analysis. Furthermore, the burner should be properly controlled to make sure that the optimum amount of air factor is achieved so that maximum extraction of exergy contained in the product gases is achieved for clinker burning.

(iv) The findings imply that flue gas mixing in preheater cyclones causes relatively high exergy destruction as indicated in Table 5.4. In this case, exergy destructions are due to temperature and composition differences. It should be noted that operating conditions of cyclone separators can be improved by controlling in filtrated air in the preheater cyclones and monitoring for clogging. However, compositions cannot be easily changed. Furthermore, preheater cyclones were considered as heat exchangers. Thus, to improve performance of preheater cyclones, the temperature gradient between hot and cold streams could be improved by preheating raw feed.

(v) Also performance of preheater cyclones can be improved by ensuring that the kiln end feed is heated to the maximum value temperature of about $T_{PH4SOLID}$ =1000 °C from the current value of $T_{PH4SOLID}$ = 836 °C, while controlling the calcination level taking place in preheater cyclones. That could be possible if inclusion of the precalciner to the staged preheater cyclones is thought since there is a plan to burn alternative fuels to minimize both emissions and cost of coal fuels. However, before inclusion of precalciner is thought, analyses should be conducted to study benefits between use of exergy lost with preheater cyclones exit dusts for preheating raw feed and coal versus economics of coal fuels as well as emissions saved by installing a precalciner to burn alternative fuels.

(vi) Performance of primary air fan can be improved by preheating primary combustion air. Preheating of primary combustion air will also improve combustion processes. Irreversibility due to combustion in the rotary kiln can be reduced to a minimum value by working with the suitable excess air coefficient (near stoichiometric condition) and using high quality fuel. Decreasing excess air factor by minimizing false air amount would lead to decrease in specific fuel consumption in the kiln.

6.2. Proposal for Improvement Strategy

It is indicated in Table 5.4 that some components and sub-systems have higher irreversibilities (exergy destruction and exergy loss) than others. An avoidable part of irriversibilities can be minimized through development of processes or technology improvements as suggested in the foregoing discussion.

6.2.1. Case 1: Lowering Temperature of $T_{CINKER2}$ = 245°C to 200 °C

In this subsection, the effect of improving the cooling effect of clinker is discussed. The model was adjusted till temperature of the secondary combustion air (clinker cooling air) reached minimum temperatures at T_{HOTAIR} = 800 °C. The minimum temperature of the secondary combustion air gave the temperature of the cold outgoing clinker at $T_{CLINKER2}$ = 200 °C. Table 6.1 presents base case data when the cooled clinker stream was at $T_{CLINKER2}$ = 245 °C relative to other streams around the cooler and the rotary kiln that are related to each other.

Table 6.1. Thermodynamic data at T=200 °C for Clinker$_2$

Base case streams	T / °C	$\dot{e}_{tot}$ / kJ·kg$_{cl}^{-1}$	Case 1 streams	T / °C	$\dot{e}_{tot}$ / kJ·kg$_{cl}^{-1}$
CLINKER2	245	1,153	CLINKER2	200	1,137
CLINKER1	787	1,487	CLINKER1	779	1,470
S-2	34	4	S-2	34	4
GASES	2,128	2,935	GASES	2,141	2,955
ASHPROD	2,128	87	ASHPROD	2,141	87
AIR	28	0	AIR	28	0
S-3	46	4	S-3	46	4
COLDAIR	28	0	COLDAIR	28	0
KLN1SOLD	1,450	2,071	KLN1SOLD	1,480	2,101
KLN1GAS	1,450	1,614	KLN1GAS	1,480	1,65
HOTAIR	772	381	HOTAIR	800	409.4

Table 6.2. Data obtained from the exergetic analysis

Component	$\dot{e}_{F,K}$ /kJ·kg$_{cl}^{-1}$	$\dot{e}_{P,K}$ /kJ·kg$_{cl}^{-1}$	$\dot{e}_{D,K}$ / kJ·kg$_{cl}^{-1}$	$\dot{e}_{L,tot}$ / kJ·kg$_{cl}^{-1}$	ε_k / %
ID-FAN	68	54	14		79.4
B-FAN	13	10	3		74.0
P-AIRFAN	8	4	3		57.1
C-AIRFAN	8	4	3		56.6
CALCINAT	2,838	24	2,814		0.9
BELITE	298	85	213		28.6
COOLER	583	377	206		64.6
BURN	2891	2,287	604		78.4
BURNING	1,384	291	1,093		18.5
MIXPH2	1,255	1,248	7		99.4
MIXPH3	2,610	1,771	839		67.8
GASCOOL	693	608	85		87.8
Sub-systems (Fig. 5.2)					
Rotary kiln	3,919	578	191	3,150	14.7
Preheater	2,542	1,523	1,019		59.9
Cooler	964	406	558		41.1
Overall	3,514	1,138	1,769	608	32.8

Also Table 6.1 presents data in considering the effect of improving the clinker cooler (case 1) after model adjustment. Exergetic analysis data for case 1 as well as exergetic efficiencies for both base case (before improvement) and case 1 (after improvement) are presented in Table 6.2.

It was indicated in the base case that a substantial amount of exergy was lost with cooled clinker to the environment. Performance of the cooler can be improved by recovering more heat from hot clinker coming from the rotary kiln to the cooler. That can be achieved through heat recuperation by cooling air, which, in turn, is used as secondary combustion air in the kiln burner. Literature indicates that temperature output of cooled clinker using planetary cooler ranges from T_{CLINKER2} = (100 ÷ 200) °C. Also literature suggests that secondary air should be heated up from T_{HOTAIR} = (800 ÷ 1000) °C so as to improve performance of both the cooler and the rotary kiln (ICR 2005). Lowering temperature of outgoing clinker from the clinker cooler will reduce the temperature gradient between the cold clinker and the environment hence minimizing exergy lost with the cold clinker (stream $\mathrm{CLINKER_2}$). It is anticipated that exergy lost with the stream could be reduced to much lower values than expected if means are found for increasing efficiency of heat recuperation from hot clinker to secondary air.

However, maximizing secondary air temperature involves optimizing clinker bed depth and cooling air distribution to the recuperating zone. The latter would involve change of clinker cooler geometry or even replacing it with a large capacity or another type that is highly efficient. However, with adjustment made, there were only minor changes in both cooler geometry and other parameters. Further improvements can be achieved by replacing the planetary clinker cooler with grate cooler, which is greatly efficient. However, implementation of clinker cooler would mean further analyses to justify not only its economics potentiality but also technical viability.

Findings presented in Table 6.2 imply that cooling down output clinker from T_{CLINKER2} = 245°C ÷ 200 °C will raise the exergetic cooler efficiency by approximately 1 % from 41.11 % to 42.11 %. The exergetic efficiency of both the rotary kiln and clinker burning processes will be improved to 14.7 % and 21.0 % from 14.1 % and 18.5 %, respectively. Findings from the study indicated that there was relatively small improvement in combustion processes in the kiln burner from 78.4 % to 79.12 %. Furthermore, the findings indicated that although exergy destruction of individual components was decreased, overall system exergy destruction was increased thereby keeping the overall exergy efficiency of the system relatively constant. The reason for the latter can be explained in Eq. 5.2 and Eq. 5.4 used to determine the exergy distruction and exergy efficiency for the overall system.

From the Eq. 5.2, it can be observed that minimizing exergy lost with clinker stream $\dot{e}_{\mathrm{CLINKER2}}$ [$\mathrm{kJ \cdot kg_{cl}^{-1}}$] while keeping $\dot{e}_{\mathrm{F}}$ [$\mathrm{kJ \cdot kg_{cl}^{-1}}$] constant will simultaneously cause the value of exergy destroyed $\dot{e}_{\mathrm{D,SYS}}$ [$\mathrm{kJ \cdot kg_{cl}^{-1}}$] of the overall system to increase. From the Eq. 5.4 for calculating the

exergy efficiency of the overall system, it can be observed that minimizing the exergy lost with the stream $\dot{e}_{\mathrm{CLINKER2}}$ [kJ·kg$_{\mathrm{cl}}^{-1}$] while keeping the $\dot{e}_{\mathrm{F}}$ [kJ·kg$_{\mathrm{cl}}^{-1}$] constant will simultaneously lower $\varepsilon_{\mathrm{SYS}}$ [%] the exergy efficiency of the system. To counter the effect of increased exergy destruction of the overall system, it is better to reduce the fuel flow rate to the kiln burner, while monitoring the combustion gases temperature (stream GASES in Table 6.1) from T_{GASES} = 2141 °C to standard temperature of combustion gases suitable for clinker burning of T_{GASES} = 1800 °C ÷ 2000 °C. That can be justified by the fact that clinker burning exergy efficiency was improved due to improvement of combustion process in the kiln burner providing potential to reduce the fuel flow rate or supply more kiln feed to increase clinker production. In other words, minimizing exergy loss with clinker provides potential for minimizing extra fuel burned to compensate heat losses with clinker. This finding is supported by results from parametric analysis presented in Section 4.2.6.1., Fig. 4.6. From the study, it was found that if all irreversibilities in processes or individual components and the overall system at large are removed, about $\dot{m}_{\mathrm{COAL}}$ = 1263 kg·h^{-1} coal flow rate and specific energy use of about 1849.12 kJ·kg$_{\mathrm{cl}}^{-1}$ can be saved. However, due to presence of unavoidable irreversibilities in the system components and processes, only part of the fuel saving and specific energy use savings can be achieved.

6.2.2. Case 2: Preheating of Primary Air up to 60 °C

Table 6.3 presents thermodynamic data obtained from simulation for base case (before primary combustion air preheating) and case 2 (after preheating of primary combustion air).

It was found that preheating of primary combustion air will affect other related streams' thermodynamic performance as indicated in Table 6.3. Exergetic analyses data obtained after preheating primary combustion air are presented in Table 6.4. Both exergetic efficiencies of components and sub-systems before and after preheating primary combustion air are also presented in Table 6.4.

Table 6.3. Thermodynamic Data at T=60 °C for air stream

Base case streams	T / °C	$\dot{e}_{\mathrm{tot}}$ / kJ·kg$_{\mathrm{cl}}^{-1}$	Case 2 streams	T / °C	$\dot{e}_{\mathrm{tot}}$ / kJ·kg$_{\mathrm{cl}}^{-1}$
CLINKER$_2$	245	1,153	CLINKER$_2$	200	1,137
CLINKER$_1$	787	1,487	CLINKER$_1$	822	1,514
S-2	34	4	S-2	34	4
GASES	2,128	2,935	GASES	2,144	2,961
ASHPROD	2,128	87	ASHPROD	2,144	88
AIR	28	0	AIR	60	0
S-3	46	4	S-3	77	5
COLDAIR	28	0	COLDAIR	28	0
KLN1SOLD	1,450	2,071	KLN1SOLD	1,500	2,121
KLN1GAS	1,450	1,613	KLN1GAS	1,500	1,689
HOTAIR	772	381	HOTAIR	800	409

Findings imply that preheating of primary combustion air improves exergetic performance of various individual components, sub-systems as well as processes. It was found that preheating primary air from environment temperature at T_o = 28.3 °C to designed kiln firing temperature at T_{firing} = 60 °C will improve exergetic efficiencies of primary air fan, clinker burning processes, rotary kiln and clinker cooler by about 1.6 %, 4.4 %, 1.2 % and 0.05 % respectively.

Table 6.4. Data obtained from the exergetic analysis

Component	$\dot{e}_{F,K}$ /kJ·kg$_{cl}^{-1}$	$\dot{e}_{P,K}$ /kJ·kg$_{cl}^{-1}$	$\dot{e}_{D,K}$ / kJ·kg$_{cl}^{-1}$	$\dot{e}_{L,tot}$ / kJ·kg$_{cl}^{-1}$	ε_k / %
ID-FAN	68	54	14		79.4
B-FAN	13	10	3		74.0
P-AIRFAN	8	5	3		58.7
C-AIRFAN	8	4	4		56.6
CALCINAT	2,838	24	2,814		0.9
BELITE	298	85	213		28.6
COOLER	583	377	206		64.6
BURN	2,891	2,287	603		79.1
BURNING	1,359	311	1,048		22.9
MIXPH2	1,255	1,248	7		99.4
MIXPH3	2,610	1,771	839		67.8
GASCOOL	693	609	84		87.8
Sub-systems (Fig. 5.2)					
Rotary kiln	3,920	598	172	3,150	15.3
Preheater	2,542	1,523	1,019		59.9
Cooler	984	405	579		41.2
Overall	3,515	1,137	1,769	608	32.3

Although improvement in combustion process is relatively small it has a relatively large contribution to potential fuel savings. The potential fuel savings is indicated by the level of combustion gases temperature (stream GASES in Table 6.3). Findings from this study indicated that exergy destructions of individual components and processes are minimized, while the overall system exergy destruction was increased followed by relatively constant overall system exergy efficiency. Reasons for the latter are the same like in the first case study, although in this case, the exergy of fuel was relatively increased due to increase in exergy with stream $\dot{E}_{S\text{-}3}$ after preheating the primary air. Compared to the previous case study, primary air preheating seemed to bring relatively highly positive effects. Significant exergetic performance improvement is achieved in clinker burning process.

6.2.3. Case 3: Preheater Cyclones Exit Flue Gases Temperature

It is presented in Table 4.5 (model results and validation Chapter Four) that the preheater exit temperature of the plant is higher than normal. Findings also imply that the plant O_2 % in preheater exit gases indicated that excess air was relatively high above suggested standard values in literature. Both the high value of excess air and the high temperature above limits in the preheater exit gases is used as an indication of higher specific energy use beyond optimal, which, in turn, demands for more fuel burning. Additional fuel burning, in turn, will lead into more chemical irreversibility in the kiln and more CO_2 emission to the environment. This finding is further presented in Section 4.2.6.1. and results imply that more coal fuel was burned in the rotary kiln burner to compensate for inefficiencies in the kiln system. Moreover, results from exergetic analyses presented in Table 5.4 confirmed that a significant amount of exergy is lost with preheater exit flue gases and dusts. Findings on exergy analyses for preheater cyclones revealed that another source of irreversibility was mixing of solid material and flue gases of different compositions, temperatures and pressures.

Table 6.5. Thermodynamic data at T=350 °C for stream S-1

Base case streams	T / °C	$\dot{e}_{tot}$ / kJ·kg$_{cl}^{-1}$	Case 3 streams	T / °C	$\dot{e}_{tot}$ / kJ·kg$_{cl}^{-1}$
CLINKER$_2$	245	1,153	CLINKER$_2$	200	1,137
CLINKER$_1$	787	1,487	CLINKER$_1$	822	1,514
S-2	34	4	S-2	34	4
GASES	2,128	2,935	GASES	2,144	2,961
ASHPROD	2,128	87	ASHPROD	2,144	87
AIR	28	0	AIR	60	0
S-3	46	4	S-3	77	5
COLDAIR	28	0	COLDAIR	28	0
KLN1SOLD	1,450	2,071	KLN1SOLD	1,500	2,121
KLN1GAS	1,450	1,613	KLN1GAS	1,500	1,689
HOTAIR	772	381	HOTAIR	800	409
PH4SOLID	836	1,523	PH4SOLID	860	1,547
PHGASOUT	350	608	PHGASOUT	300	584

In the preceded discussion, several measures are suggested for improving both exergy lost with preheater exit flue gases and exergy destruction due to mixing in the preheater cyclones. In case 3, the model was adjusted to achieve the optimal temperature of the 4-stage preheater cyclone exit gases temperature at $T_{s\text{-}1}$ = 350 °C as suggested in literature (see ICR 2005). Thus, in this case study, there were efforts to minimize the temperature of preheater cyclone exiting flue gases and dust from $T_{s\text{-}1}$ = 396 °C of the operating plant data to $T_{s\text{-}1}$ = 350 °C by adjusting

the model. The thermodynamic data for streams are presented in Table 6.5, while the exergetic analysis results are presented in Table 6.6.

Table 6.6. Data obtained from the exergetic analysis

Component	$\dot{e}_{F,K}$ /kJ·kg$_{cl}^{-1}$	$\dot{e}_{P,K}$ /kJ·kg$_{cl}^{-1}$	$\dot{e}_{D,K}$ / kJ·kg$_{cl}^{-1}$	$\dot{e}_{L,tot}$ / kJ·kg$_{cl}^{-1}$	ε_k / %
ID-FAN	68	54	14		79.4
B-FAN	13	10	3		74.0
P-AIRFAN	8	5	3		58.7
C-AIRFAN	8	4	3		56.6
CALCINAT	2,838	24	2,814		0.9
BELITE	298	85	213		28.6
COOLER	583	377	207		64.6
BURN	2891	2,287	603		79.1
BURNING	1,359	311	1,048		22.9
MIXPH2	1,255	1,248	7		99.4
MIXPH3	2,610	1,771	839		67.8
GASCOOL	693	608	85		87.8
Sub-systems (Fig. 5.2)					
Rotary kiln	3,920	598	172	3,150	15.3
Preheater	2,565	1,547	1,019		60.3
Cooler	984	405	579		41.2
Overall	3,515	1,137	1,769	608	32.3

Results obtained from this study indicated that if the temperature of the preheater cyclone exit flue gas is improved from $T_{s\text{-}1}$ = (396 to 350) °C, the exergy loss could be improved by a factor of 24 kJ·kg$_{cl}^{-1}$. Also the exergetic efficiency of the preheater cyclones could be improved by a factor of 0.4 %. The exergetic efficiencies of both rotary kiln and clinker cooler sub-system are relatively improved from 14.1 % to 15.3 % and from 41.1 % to 41.2 %, respectively. The findings indicated that exergy destructions of rotary kiln and preheater tower sub-systems were relatively minimized. However, the overall system exergy destruction was relatively increased from $\dot{e}_D$ = (1,769 to 1,770) kJ·kg$_{cl}^{-1}$. Furthermore, exergetic efficiency of the overall system remained relatively constant. Reasons for such results can be explained in the Eq.5.9 5.2, and 5.4 used for calculating exergy destructions for preheater tower sub-system, the overall system and for calculating exrgetic efficiency for the overall system respectively.

Normally, minimizing exergy lost with preheater exhaust gases (stream PHGASOUT) will maximize exergy of preheated solid raw feed, leaving the preheater tower/entering the rotary kiln end (stream PH4SOLID) and hence, improving the thermal performance of the preheater

tower. If this positive effect is achieved at the preheater tower, it provides potential for minimization of fuel burnt at the kiln burner to compensate heat losses in various individual components and sub-systems. In this case, the minimized heat loss at the preheater tower should provide potential for minimizing fuel burnt at the kiln burner so that its benefit can be reflected at the overall kiln system level. Furthermore, by looking into Eq.5.2 used for calculating overall system exergy destruction, it can be seen that overall effect of minimizing exergy loss with both preheater exhaust gases and cooled clinker while keeping constant or increasing exergy with fuel will further contribute to higher overall system exergy destruction.

Nevertheless, the best way for improving exergetic performance of preheater cyclones and overall kiln system is to recycle exergy with exit flue gases and use it for preheating raw feed as well as coal fuel or generation of electrical power using steam turbine. Although common practice is to use exergy with preheater cyclone flue gases and dusts for preheating raw feed and coal fuel, collected data from the plant for the years 2011 and 2012 indicated that utilization factor for the raw mill was only 65.2 %. The latter implies that the kiln system was not run in compound operation for about 35 % of operating hours annually.

Once the kiln system is not run in compound mode (with the raw mill on), it implies that exit flue gases and dusts were passed through the cooler, where they were cooled down to a temperature suitable for gas cleaners (ESP) for cleaning the gas before they were exposed to the environment. Thus, it could be thought of making use of exergy with preheater cyclone exit flue gases for power generation during raw mill idle time. However, this could mean that a further study should be conducted to find out practical application of so doing.

In general, results obtained in this chapter suggest that, improvement of system components with the highest exergy destruction rate, with the objective of improving overall system efficiency, does not always lead to thermodynamic improvement. Such results are supported by literature for example Bejan et al. (1996). In the cogeneration system considered throughout this reference, the combustion chamber is the component with the highest exergy destruction rate (values tabulated in Table 6.2), whereby the exergy destruction rate for the base case is 25.75 MW, with the exergetic efficiency of 79.8 %, while the thermodynamically optimal design, these values are 23.81MW and 78.8 % respectively. Thus, it can be seen that although in the optimal design, the value of exergy destruction is reduced from 25.7 MW, to 23.8 MW, however the exergy efficiency droped to 78.8 % as well. Tsatsaronis (1999), concluded that an iterative approach in which the components are ranked according to their avoidable exergy destruction might provide an improvement of this iterative optimization procedure.

Chapter Seven – Summary, Conclusions and Future Work

This chapter presents summary of major results, conclusion and recommendations. The latter includes suggestions for future work.

7.1. Summary

Sustainability of cement production processes can be defined in many ways. Generally, its thermodynamics assessment involves consideration of factors such as energy and material use requirements; safety and health effects; ecological and environmental impacts; and societal as well as regulatory constraints. Both, thermodynamic and economic performance of cement kiln system and cement overall plant at large are largely dependent on their energy including material use requirements. The opposite is also true and thus, thermodynamic performance can be evaluated through energy and exergy balances around the processes. Fortunately, the processes' thermodynamic performance in terms of exergy destruction due to the reaction is one of the effective indicators of the thermal and material dissipations as a result of the reaction involved.

This study was focused on an investigation for performance of cement production processes relative to sustainable energy use. The main objective of the study was to improve the energy efficiency of cement industries in Tanzania. The study focused in searching for the appropriate methods which could be applied for improving performance of cement industries relative to sustainable energy use. Thus, the central research question was ``what is the potential for energy savings in cement industries in Tanzania. Additional research questions was:

(vii) Which factors affect useful energy consumptions of various equipment used in cement production processes?

(viii) How verification, monitoring and analysis of energy use in cement industries can be conducted?

(ix) How inefficiencies and energy losses in cement industries can be identified?

(x) How can energy be efficiently managed in cement industries in Tanzania?

In order to answer the research questions and achieving the main objectives of the study, two methodical approach was employed, namely modelling and simulation techniques as well as exergy-based methods. The model was developed, validated with real plant data. Additionally, sensitivity analysis of model parameters was conducted to gain more confidence on model performance in relation to real plant performance. Furthermore, data retrieved from the model were used for further investigation of the rotary kiln system performance using exergy based methods.

It has been noted from Table 4.6 that, the amount of oxygen percent in preheater tower (PHT) exit flue gases is 3.77 %, which is above the required value of 2 % to 3 % suggested in literature (ICR 2005). This findings suggest that there is excessive in-leakage air in the PHT. The effect of excessive in-leakage air in PHT, in turn necessitates more fuel burning in the kiln system, which will lead into more chemical irreversibility in the overall kiln system. More fuel burning will also cause more carbon dioxide (CO_2) emissions to the environment and higher operating costs.

It has also been proven in sensitivity analysis that, the kiln system uses more heat energy to compensate for heat loses. The major source of the heat loses are further revealed in exergy analysis Chapter Five.

From the temperature of combustion gases perspectives, in Table 4.6 and sensitivity analysis results, support that more coal fuel has been burned to compensate for heat losses due to various reasons. Specific sub-systems, components and processes with high irreversibilities, and consequently causes of irreversibilities has been indicated in Chapter Five exergy analysis.

Irregular variation of CO_2 emissions is seen in Table 4.7 as you move from one stage of PHT to another. Such results support the results obtained in sensitivity analysis. Presence of combustible components of coal fuel with flue gases in the stream GASES is due to decomposition of CO_2 to C and CO, and H_2O to H and O_2 at higher temperatures (Flaga and Seinfeld 1988). Thus, such results indicate that there is not incomplete combustion in the rotary kiln burner combustion processes.

Increase of coal fuel up to optimum value results into increase of flame temperature as well as amount of clinker produced (Fig. 4.6). Increase of clinker amount is due to both increase of rate of calcination i.e. decomposition of calcium carbonate ($CaCO_3$), at increased temperature and ash content of coal fuel. Ash content of coal is part of clinker produced in any cement rotary kiln which is fired using coal as a fuel.

From sensitivity analysis it has been found that, minimum potential coal saving is about 1,263[$kg \cdot h^{-1}$] and potential specific energy saving of about 1,849 [$kJ \cdot kg_{cl}^{-1}$]. Such amount of coal fuel saving represents a significant amount of operating cost minimization if it can be realized.

Analysis of PHT flue gases is very important for control and performance improvement of the dry rotary kiln system. Analysis of PHT flue gases conducted using sensitivity analysis indicates that optimum combustion air flow rates, cooling air flow rates as well as fuel flow rates to the kiln system is very important, not only for improving energy efficiency of the system but also for improving emissions to the environment (Figs. 4.8, 4.9, 4.10, 4.11 and 4.12). These findings are in good agreement with findings from literature that, air flow rate and fuel flow rate, type or fuel mix dominates the variation of cement plant performance (Summerbell et al. 2016, Kääntee et al. 2003). Summerbell et al. (2016) predicted reduction of both, energy consumption by 8.5 % and CO_2 emissions by 19.5 % using their mathematical model. Furthermore, they concluded that fuel mix and excess air ratio should be the focus of future research.

Sensitivity analysis results revealed that, burning coal with high moisture content in a dry rotary kiln burner lowers the thermal efficiency of the rotary kiln. Thus, preheating of coal fuel using heat energy from the PHT is of vital importance for the dry rotary kiln performance improvement.

Major results obtained from exergetic analysis indicates that Rotary kiln has lowest exergetic efficiency followed by the planetary clinker cooler (Table 5.4.). The exergetic analysis results are in good agreement with most exergetic analysis studies found in literature, that the main source of irreversibility in the dry rotary kiln system are chemical reactions and heat transfers taking place in the rotary kiln (Kolip and Savas 2010; Farag 2012; Farag and Taghian 2015).

7.2. Conclusions

From literature sources, it can be concluded that, in general, there is a problem of sustainable energy use in cement industries, globally, owing to limitations imposed to technologies, inefficient characteristic of equipment and processes as well as much reliance on fossil fuels. Other factors include, but not limited to, type of technology and raw materials used. However, there have been several efforts towards sustainable energy use in cement industries. Besides existence of BAT for cement production processes, there is still room for further improvements based on individual cement plant assessment. Arguments furthering energy efficiency improvement measures are: It has been indicated in literature that fossil fuels like coal will still dominate cement production processes at least for the next few decades. This implies that there is crucial need to improve performance of cement plants to avoid losses that result into demand for more fuel burning and hence, higher cost of production and more CO_2 emissions. Furthermore, demand for cement production is substantially increasing as the rate of development and need for more infrastructure increases. A comprehensive energy assessment should be a basis for energy efficiency initiatives. Energy efficiency initiatives are the most attractive solutions because they can lower maintenance cost, reduce waste, increase production yield and provide safer working conditions in a wide range of operations. Reducing energy wastes on energy intensive industries and promoting renewable energies are the best solutions towards sustainable energy systems.

From literature, there are several methods used for performance evaluation of cement production processes but the prominent one is energy audit. However, energy audit based on the first law of thermodynamics alone (mass and energy balance) has some limitations because it cannot identify real thermodynamic imperfection. Using the approach of the first law of thermodynamics alone has led most of past studies to draw wrong conclusions as discussed in Chapters Two and Three, Section 2.9.2 and Section 3.7 of this thesis. The current emerging method for performance evaluation of cement production processes is exergy based method. With this approach, it is possible to identify the real thermodynamic imperfection in each component, processes, sub-systems and the overall system at large. Also it is possible to pinpoint

the type, magnitude as well as causes of these real thermodynamic imperfections and suggest measures to minimize them. However, exergy based method application for complex energy systems like cement production processes needs computer based tools to simplify the analyses.

This study employed two approaches to respond to the central research question and achieve research objectives. The first approach involved modelling and simulation. Computer aided steady state modelling was used to predict performance of the cement dry rotary kiln. The purpose of modelling and simulation was to develop a model, validate it against real plant data, analyse it and use it to perform ``virtual experiments'' so as to predict performance of the plant as well as generate vital information for further analyses of the plant performance. The second approach encompassed use of information obtained from modelling and simulation to further analyse performance of the plant using exergy based method and propose improvement measures. In the second approach, mass and exergy balance together with exergetic variables of individual components, sub-systems and of the overall kiln system were carried out.

In the first approach, the model was successfully developed, validated against real plant data and it was used to evaluate performance of the plant. The developed model successfully delivered a comprehensive report of material, energy and exergy flow rates within the real plant processes. The model successfully determined the correlation between reactions and separation systems throughout the processes thereby reflecting real processes taking place in cement production processes. Also the model successfully investigated formation and separation of major product (clinker) and waste (flue dusts and gases) at sufficient level of accuracy as indicated in model results and validation (Section 4.2.5.). Furthermore, the model successfully used to evaluate performance of the plant when subjected to changes in various input variables such as combustion air, fuel flow rate, raw material and coal moisture content, and the like (Section 4.2.6.). Moreover, the model was successfully used to study how to eliminate wastes (both energy and material wastes) and minimization of emissions. It is indicated in Chapter Four Section 4.2.6.1. that if losses are minimized, a significant amount of fuel and specific energy consumption could be saved.

Based on the first approach, the following are concluding remarks: real plant data were entered into the model and predictions were found to be in good agreement with plant data (Tables 4.5, 4.6 and 4.7). Detailed information concerning temperature and pressure profiles, mass and energy balance as well as exergy flow rates was generated using the model (Sections 4.2.5. through 4.2.7. and Chapter Five, Table 5.3). Process modelling provides effective safe and economical ways for creating a detailed database of information about the process. The solutions indicated that such a model could be used to identify problems of kiln operations. The developed model is useful for assessing performance of the kiln system. The model allows assessments of individual components as well as sub-systems and the overall system at large. It is possible with the formulated model to investigate combustion processes, calcination, clinker

burning, and temperature profiles throughout the kiln system as well as evaluate emissions to the environment. The model may be used to improve the kiln system operation by facilitating identification of imperfections of individual major components, sub-systems and the overall system. Adequate graphical presentations of results were generated to facilitate determination of impact of the gas temperature and other important input variables changes on the kiln system operation (Sections 4.2.6.1. through 4.2.6.12.).

However, the developed model has the following limitations: the simulation model considered description of formation of silicates and aluminate phases from the four major compounds of CaO, SiO_2, Al_2O_3, and Fe_2O_3 of typical cement raw meals from the MCC plant (Table 4.1). However, the ferrite phase (C_4AF) and other clinker minor compounds were not considered in the simulation model due to lack of respective compounds in Aspen Plus data base. Thus, influence of minor and trace compounds on clinker phase formation as well as C_4AF was not addressed. However, the developed model is sufficient for evaluation of the processes since minor compounds, which are not included have little contributions in clinker chemistry formation as demonstrated in Chapter Four, Section 4.2.5. Nonetheless, further development of the model could be thought to have a comprehensive rigorous model by interfacing Aspen Plus data base with other software like FactSage and ChemApp so as to include the intermediate and minor compounds.

Based on the second approach, the following are concluding remarks: The specific objectives for the second approach are sufficiently met. The mass and exergy balance for each component, sub-system and the overall kiln system are presented in Chapter Five. Exergetic efficiencies for individual components, sub-systems and overall kiln system were calculated and presented in Table 5.4. Components and sub-systems with major exergetic inefficiencies and causes of these imperfections were identified and presented in Table 5.4 as well as discussed in detail in Section 5.4. Improvement measures are suggested and some of them were tested and presented in Chapter Six to demonstrate if they could really improve performance of components and subsystems.

Findings from exergy analyses suggest that the rotary kiln has the highest exergy consumption rate among other kiln system subsystems. From the exergetic point of view, the rotary kiln has the highest irreversibility compared to other kiln system as well as sub-systems with exergy efficiency of about 14.1 %. The rotary kiln exergy destruction is mainly due to chemical reactions, combustion reactions and heat transfer. Moreover, exergetic performance of subsystems indicated that the planetary clinker cooler had exergetic performance of about 41.1 %. Major causes of irreversibilities in the planetary clinker cooler were exergy loss with cooled clinker to the environment, exergy destruction due to heat exchange between cold cooling air and hot clinker from the rotary kiln and exergy loss due to heat transfer to the environment through the planetary cooler wall. Furthermore, findings indicated that the preheater tower was ranked

in the third place for poor performance in exergetic point of view with exergy efficiency of about 59.9 %. Major causes of imperfections in the preheater tower were exergy loss with preheater exit flue gases and irreversibility due to mixing of hot gases as well as cold raw feed. Furthermore, results indicated that the overall exergy performance for the kiln system was relatively low with exergy efficiency of 32.8 %. The overall exergetic performance of the kiln system suggests that there exists potential for performance improvements of the system. In general, it can be concluded that results obtained from exergetic analyses for the sub-systems and the overall kiln system are in good agreement with most results from other literature sources as presented in Appendix 9.

7.3. Recommendations and Future Work

(xi) The model can be extended for other cement production processes units such as raw mill, coal mill preparation unit as well as cement grinding.

(xii) The model can be extended to study use of alternative fuels relative to exergetic performance of the plant.

(xiii) The model can be further developed to have a rigorous model that would include more cement compounds for clinker chemistry phases and inbuilt calculation of chemical exergy simultaneously with physical exergy streams as well as its exergetic variables.

(xiv) Exergoeconomic and exergoenvironmental analyses could be conducted to further explore possible further improvements in terms of sustainable cement production. Advanced exergy-based methods could be applied as well.

References

Abdelaziz E A, Saiduri R, Mekhilef S (2011) A review on energy saving strategies in industrial sector. Renewable and sustainable energy 15:150-168

Abdollahi-Demneh F, Moosavian M A, Omidkhan M R et al. (2011) Calculating exergy in Flowsheeting Simulators: A HYSYS implementation. Energy 36:5320-5327

Ajith F P, Arjun C, Ramesh A (2014) energy and exergy analysis of a white cement kiln plant. International journal of mechanical engineering 3:87-94

Al-Ghandoor A, Al-Hinti I, Jaber J O et al. (2008) Electricity consumption and associated GHG emissions of the Jordanian industrial sector: Empirical analysis and future projection. Energy Policy 36:258–267.

Al-Mansour F, Merse S, Tomsic M (2003) Comparison of energy efficiency strategies in the industrial sector of Slovenia. Energy 28:421–40

Alsop P A, Chen H and Tseng H (2007) Cement Plant Operation Handbook for Dry –Process Plants. Trade ship Publications Ltd

Arad S, Arad V, Bobora B (2008) Advanced Control Schemes for Cement Fabrication and Automation in Construction. InTech. Available via http://www.intechopen.com. Accessed 12th February 2015

Aspen Plus V8.6, The software is a proprietary product of AspenTech, 2014, (http://www.aspentech.com)).

Ates S A, Durakbasa N M (2012) Evaluation of corporate energy management practices of energy management practices of energy intensive industries in Turkey. Energy 45(1):81-91

Atmaca A, Yumrutas R (2014) Thermodynamic and exergoeconomic analysis of a cement plant: Part II-Application. Energy Conversion and management 79:799-808.

Atul G S, Blamurugan S (2012) Cement plant simulation and dynamic data communication using LabVIEW and Matrikon OPC, Journal of theoretical and applied information technology. 43 (2)

Avami A, Sattari S (2007) Energy conservation opportunities: cement industry in Iran. International Journal of Energy 3:65–71.

Bejan A (2002) Fundamentals of exergy analysis, entropy generation minimization and the generation of flow architecture. International journal of energy research 26:545-565

Bejan A, Tsatsaronis G, Moran M (1996) Thermal Design and Optimization, Wiley & Sons Inc.

Benhelal E, Rafiel A (2008) Overview of process modeling software: utilizing alternative fuel in cement plant for Air pollution reduction. Ener-gy science and technology 4 (1):10-18

Boateng A A (2008) Rotary Kilns Transport Phenomenon and Transport Processes. Elsevier Inc.

Boyaghchi F A (2014) Thermodynamic and environmental impact assessment of calcium oxide formation in clinker production. International journal of environment research 8:85-92

Boyano H A, Morosuk T, Blanco-Marigorta A M et al. (2012) Conventional and advanced exergoenvironmental analysis of a steam methane reforming for hydrogen production. Journal of cleaner production 20:152-160

Brunke J, Blesl M (2014) Energy conservation measures for Germany cement industry and their ability to compensate for rising energy-related production costs. Cleaner production 82:94-111

Camdali Ü, Erisen A, Celen F (2004) Energy and exergy analyses in a rotary burner with precalcinations in a cement production. Energy conversion and management 45:3017-3031

Caputo A C, Pelagagge P M, Salin P (2011) Performance modelling of radiant heat recovery exchangers for rotary kilns. Applied Thermal Engineering 31:2578-2589

CEMBUREAU BAT (1999) Best Available Techniques for the Cement Industry. The European Cement Association, available via http//www.cembureau.be. Accessed 15 September 2014

Cement Plant Operational Handbook, 4th Edition (2005) ICR

CSI- Cement Sustainability Initiative report (2009). Available via www.wbcsdcement.org. Accessed 25 January 2014

CSI/ECRA- European Cement Research Academy (2009) Technology papers. Available via www.wbcsdcement.org. Accessed 25 January 2014

CTI, Challenges of Unreliable electrical Power Supply to Manufactures in Tanzania (2011) A Policy Research Paper submitted to Energy Sector Stakeholders for Advocacy to ensure Reliable Electricity supply to Manufactures.

Cziesla F, Tsatsaronis G, Gao Z (2006) Avoidable Thermodynamic Inefficiencies and Costs in an Externally Fired Combined Cycle Power Plant. Energy 31:1472-1489

Deolalkar S P (2016) Designing Green Cement Plants. Elsevier Inc.

Diji C J, Ekpo D D, Adadu C A et al. (2013) Exegoenvironmental evaluation of a cement manufacturing process in Nigeria. International journal of engineering re-search and development 7:25-32. Available via www.ijerd.com . Accessed 26 March 2014

Dimian A C (2003) Integrated Design and Simulation of Chemical Processses. Elsevier Science B.V.

ECRA -European Cement Research Academy (2012) Technical report phase III. Available via www.ecra-online.org. Accessed 25 January 2014

El-Halwagi M M (2012) Sustainable Design through Process Integration. Elsevier Inc.

Engin T, Ari V (2005) Energy auditing and recovery for dry type cement rotating kiln sys-tems: A case study. Energy conversion and manage-ment 46:551-562

Farag L M (2012) Energy and Exergy analyses of Egyptian cement kiln dry process cement kiln plant with precalciner characterized by that the whole kiln gas is diverted through by pass. International Journal of Advances in applied sciences 1:35-44

Farag L M, Ghorab H, El-Nemr A (2013) Evaluation of the operational behaviour of an Egyptian cement dry process kiln plant. Journal of ap-plied sciences research 9(7): 4245-4254

Farag L M, Taghian A G (2015) Energy and Exergy analysis of Egyptian cement kiln plants. International Journal of Innovative Science, Engineering and Technology 2(9)

Farzad A, Mohammad A, Mohammad R O et al. (2011) Calculating exergy in flowsheeting simulators: A HYSYS implementation. Energy 36:5320-5327.

Fidaros D K, Baxevanon C A, Dritselis C D, Vlachos N S (2007) Numerical modeling of flow and transport process in a calciner for cement production. Powder Technology 177:81-95

Flaga R C, Seinfeld J H (1988) Fundamentals of Air Pollution Engineering. Prentice-Hal, Inc. Englewood Cliffs, New Jersey.

Ghannadzadeh A, Thery R, Baudouin O et al. (2012) General methodology for exergy balance in ProSimPlus process simulator. Energy 44:38-59

Gutiérrez A S, Martínez J B C, Vandecasteele C (2013) Energy and exergy assessments of a lime shaft kiln. Applied Thermal Engneering 51:273-280

Gürtürk M, Oztop H F (2014) Energy and Exergy analysis of a rotary kiln used for plaster production. Applied thermal engineering 67: 554-565

Habert G, Billard C, Rossi C et al. (2010) Cement production technology improvement compared to factor 4 objectives. Cement and concrete research 40:820-826

Haskin C (2006) System engineering Handbook A guide for system life cycle processes and activity. INCOSE-TP.

Hassanbiegi A, Hongyou L, Christopher J W et al. (2012) International Best Practices for Preprocessing and Co-processing Municipal Solid Waste and Sewage Sludge in Cement Industry. Lawrence Berkeley National Laboratory

Heshama G I, Ally Y O, Mokhtar S E et al. (2012) Aspen Plus simulation model for emission and particulate matter for cement plant. Journal of environmental science and engineering A 1:620-628.

Hinderink A P, Kerkhof F P J M, Lie A B K et al (1996) Exergy analysis with simulator –I Theory; Caclulating exergies of material streams. Chemical Engineering Science 51(20):4701-4715

Hinderink A P, Kerkhof F P J M, Lie A B K et al (1996) Exergy analysis with simulator –II. Application; Synthesis gas production from natural gas. Chemical Engineering Science 51(20):4693-4700

Hinderink P, Van der kooi H J, De Swaan Arons J (1999) On the efficiency and sustainability of the process industry. Green Chemistry 1:176-180. doi: 10.1039/A909915H

Hökfors B (2014) Phase chemistry in process models for cement clinker and lime produc-tion. Dissertation, UMEA UNIVERSITET

Household Budget Survey (HBS), United Republic of Tanzania. TZA-NBS-HBS 2007 V 01

Hurl K, Kihwele S and Kyaruzi A (2012) Visions, scenarios and action plan towards next generation Tanzania power system. Energies 5:3908-3927

Ibrahim H G, Okasha A Y, Elatrash M S (2012) Emissions of SO2 , NOx , and PMs from cement plant in vicinity of Khoms city in Northwestern Libya. Journal of environmental science and engineering 1: 620-628

ICR 2005. Cement Plant Operational Handbook, 4th Edition.

IFC - International Finance Corporation World Bank Group (2014) Waste heat recovery for the cement sector: Market and supplier analysis.

IPCC (2007) Contribution of Working Group III to the Fourth Assessment Report of the Intergovernmental Panel on Climate Change. Summary for Policymakers. Available via http://www.ipcc.ch/SPM040507.pdf. Accessed 20 April 2013

Jijesh V P, Yohana S, Jose J K et al. (2015) Energy and exergy analysis in a cement plant. International journal of science, engineering and technology research 4

Junior L M (2003) Sustainable development and the cement and concrete industries. Dissertation, University de Sherbrooke, Quebec

Kääntee U, Zevenhoven R, Backman R et al (2003) Modelling a cement manufacturing process to study possible impacts of alternative fuels-part A. Available via https:/www.researchgate.net/publication/228405258. Accessed 14th September 2016

Kääntee U, Zevenhoven R, Backman R et al (2004) Cement manufacturing using alternative fuels and the advantages of process modelling. Fuel processing technology 85:293-301

Kabir G, Abubakar A I, El-Naftaly U A (2010) Energy audit and conservation opportunities for pyroprocessing unit of a typical dry process cement plant. Energy 35:1237-1243

Karellas S., Leontaritis D., Panousis G., Bellos E., Kakaras E. Energetic and exergetic analysis of waste heat recovery systems in the cement industry. Energy (2013), http://dx.doi.org/10.1016/j.energy.2013.03.097

Khurana S, Rangan B, Gaitonde U (2002) Energy balance and cogeneration for a cement plant. Applied Thermal Engineering 22:485–494

Kohlhaas B (1983) Cement engineer's Handbook. Wiesbadden; Berlin: Banverlag

Kol S, Chaube A (2013) Exergy analysis of Birla cement plant Satna: A case study. International journal of scientific and engineering research 4

Kolip A (2010) Energy and Exergy analyses of a serial flow cyclone stages precalciner type cement plant. Scientific Research and Essays 5:2702-2712

Kolip A, Savas FA (2010) Energy and Exergy analyses of a parallel flow, four –stage cy-clone precalciner type cement plant. International journal of the physics Sciences 5:1147-1163. Available via http://www.academicjournals.org. Accessed 20th February 2014

Koroneos C, Roumbas G, Moussiopoulos M (2005) Exergy analysis of cement production. International journal of Exergy 2

Kotas T J (1995) The Exergy Method of Thermal Plant Analysis. KRIEGER PUBLISHING COMPANY, MALABA

Kurdowski W (2014) Cement and Concrete Chemistry. Springer + Business Media B.V.

Küssel U, Reiter M, Abel D et al (2009) Observer-Based model predictive control of rotary kilns –Applications to limestone calcination. Paper presented at 7th Modelica conference, Como, Italy, 20-22 September 2009

Luis P, Van der Bruggen B (2014) Exergy analysis of energy intensive production process: Advancing towards a sustainable chemical indus-try. Available via Wileyonlinelibrary.com. Accessed 20 August 2015

Maasa M K, Marwa M(2012) Equity research cement sector local listed companies. Available via www.tanzaniasecurities.co.tz Accessed 30 June 2012

Madlool N A, Saiduri R, Rahim N A et al (2011) A critical review on energy use and savings in the cement industries. Renewable and sustainable enrgy review 15:2042-2060

Madlool N A, Saiduri R, Rahim N A et al. (2012) An exergy analysis for cement industries: An overview. Renewable and sustainable energy review 16:921-932

Mastorakos E, Massius A, Tsakiroglou C D et al (1999) CFD prediction for cement kilns including flame modeling, heat transfer and clinker chemistry. Applied Mathematical modeling 23:55-76

MEM -Ministry of Energy and Minerals (2003) National energy policy. The United Republic of Tanzania.

MCC-Mbeya cement company Ltd (2013) Plant process flow sheet

MCC-Mbeya cement company Ltd (2015) Plant kiln system flow sheet

Mejeoumov G G (2007) Improved cement quality and grinding efficiency by means of closed mill circuit modeling. Dissertation, Texas A&M University

Miculcic H, Vujanovic M, Fidaros D K et al (2012) The application of CFD modelling to support the reduction of CO2 emissions in cement industries. Energy 45:464-473

Mohamed A K, Khan M TE (2008) Contribution Analysis of Electrical Energy Management in Industrial and Commercial Sector: A Challenge to the Tanzania Utility industry. Journal of Energy in Southern Africa. (19) 1

Moran M, Shapiro H (1992) Fundamentals of Engineering Thermodynamics. Wiley & Sons Inc.

Morosuk T, Tsatsaronis G (2008) A new approach to the exergy analysis of absorption refrigeration machines. Energy 33:890-907

Morosuk T, Tsatsaronis G (2009) Advanced Exergy Analysis for Chemically Reacting Systems-Application to a Simple Open Gas-Turbine Sys-tem. International Journal of Thermodynamics 12:105-111

Morosuk T, Tsatsaronis G (2011) Comparative evaluation of LNG-based cogeneration sys-tem using advanced exergetic analysis. Energy 36:3771-3778

Morris D R, Szargut J (1986) Standard chemical exergy of some elements and compounds on the planet earth. Energy 11:733–755

Mujumdar K S, and Ranade V V (2006) Modelling of Rotary Cement Kiln Using a One-Dimensional Model. Chemical Engineering Research and Design, 3:165-177

Mwihava N C, Mbise H A (2005) Infrastructure and utilities as stimulants of economic development. Paper presented in annual engineer's day, Karimjee Hall, Dar es Salaam.

Napp T A, Ghambir A, Hills T P et al. (2014) A review of the technologies, economics and policy instruments for decarbonizing energy-intensive manufacturing industries; Renewable and sustainable energy reviews 30:616-640

Onut S, Soner S (2007) Analysis of energy use and efficiency in Turkish manufacturing sec-tor SMEs. Energy Conversion and Management 48:384–394

Parmar M, Solanki D, Vegada B (2016) Energy and Exergy analysis of cement rotary kiln. International Journal of Advanced Engineering and Research Development 3(4)

Penkuhn M, Spieker C, Spitta C et al (2015) Exergoeconomic assessment of a small-scale PEM fuel cell system. International journal of hydro-gen energy 40:13050-13060

Petrakopoulou F, Tsatsaronis G, Morosuk T et al (2011) Conventional and Advanced Ex-ergetic Analyses Applied to a Combined Cycle Power Plant. Energy. doi:10.1016/j.energy

PHDR -Poverty and Human Development Report Research on Poverty Alleviation (2009), United Republic of Tanzania

Rasul M G, Widianto W, Mohanty B (2005) Assessment of the thermal performance and energy conversion opportunities of a cement industry in Indonesia. Applied thermal engi-neering 25:2950-2965

Saidur R (2010) A review on electrical motors energy use and energy savings. Renewable and Sustainable Energy Reviews 14:877–898.

Saidur R, Rahim N A, Hasanuzzaman M A (2010) review on compressed air energy use and energy savings. Renewable and Sustainable Ener-gy Reviews 14:1135–1153.

Saidur R, Rahim NA, Ping H W et al. (2009) Energy and emission analysis for industrial motors in Malaysia. Energy Policy 37:3650–3658

Schneider M, Romeo M, Tschudin M et al. (2011) Sustainable cement production-present and future, Cement and concrete research 41:642-650

Sogut M.Z., Oktay Z. Hepbasli A. Energetic and exergetic assessment of a trass mill process in a cement plant, Energy conversion and manage-ment 50(2009)2316-2323

Som S.K., Dalta A. Thermodynamic irreversibilities and exergy balance in combustion processes. Progress in Energy and combustion science 34(2008)351-376

Sorgenfrei M and Tsatsaronis G (2016) Detailed exergetic evaluation of heavy-duty gas turbine systems running on natural gas and syngas. Energy conversion and management 107:43-51

Steenhof P (2006) Decomposition of electricity demand in China's industrial sector. Energy Economics 28:370–384

Subhes C B, Ussanarassamee A (2005) Changes in energy intensities of Thai industry between 1981 and 2000: a decomposition analysis. En-ergy Policy 33:995–1002

Summerbell D L, Barlow C Y, Cullen J M (2016) Potential reduction of carbon emissions by performance improvement: Acement industry case study. Cleaner production 135: 1327-1339

Teleschow S (2012) Clinker Burning Kinetics and Mechanisms. Dissertation, Technical University of Denmark (DTU)

Tesch S, Morosuk T, Tsatsaronis G (2016) Advanced exergy analysis applied to the process of regasification of LNG integrated into an air sep-aration process. Energy 117:550-561

Tsatsaronis G (1993) Thermoeconomic analysis and optimization of energy systems. Progress in energy and combustion science 19:227-257

Tsatsaronis G (2007) Definitions and nomenclature in exergy analysis and exergoeconomics. Energy 32:249-253

Tsatsaronis G and Park H (2002) On Avoidable and Unavoidable Exergy Destructions and Investment Costs in Thermal Systems. Energy Con-version and Management 43:1259-1270

Tsatsaronis G, and Morosuk T (2010) Advanced exergetic analysis of a novel system for generating electricity and vaporizing liquefied natural gas. Energy 35:820-829

Tsatsaronis G, Morosuk T, Koch D et al. (2013) Understanding the thermodynamic inefficiencies in combustion processes. Energy 62: 3-11

Tsatsaronis G. Strenghs and limitations of Exergy analysis (1999). Retrived March 2013. Available via https:/www.researchgate.net/publication/235928944

Utlu Z, Sogut Z, Hepbasli A etal. (2006) Energy and Exergy analyses of a raw mill in a cement production, Applied thermal engineering 26:2479-2489.

Valero A, Abadias A (2016) Thermoeconomic analysis of a cement production plant. Pro-ceedings of ECOS 2016-The 29th International Conference on efficiency, Cost, Optimization, Simulation and Environmental Impact of energy Systems. June 19th-23rd, 2016, Portoroz, Slovenia.

Wang J, Dai Y, Gao L (2009) Energy analyses and parametric optimizations for different cogeneration power plants in cement industry. Ap-plied Energy 86:941–948

Worrell E, Bernstein L, Roy J (2009) Industrial energy efficiency and climate change mitigation. Energy efficiency 2:109-123

Worrell E, Kermel K, Galitsky C (2013) Energy Efficiency Improvement and Cost Saving Opportunities for Cement Making. An energy star guide for energy and plant managers. United States Environmental Protection Agency

Worrell E, Martin N, Price L (2000) Potentials for Energy Efficiency Improvement in the US Cement Industry, Energy 25:1189-1214

Yang Y, Wang L, Dong C et al (2013) Comprehensive exergy based evaluation of parametric study of a coal-fired ultra-supercritical power plant. Applied energy 112:1087-1099

Yokota M. 7th GTT workshop 2005 Aachen German

Zunga N, Lopez-Pinto A (2011) Imara Africa Cement report Africa, the last cement frontier

Appendices

Appendix 1: Aspen Plus model assumptions of MCC kiln system

Sub-Processes	Aspen Model	Specification and Function
1. Calcination	RGibbs: CALCINAT	T = 958 °C; p = 0.8673 bar Completion of calcination
	RStoic: MIXPH4	T = 836 °C; p = 0.8610 bar Pre calcination of 30% of limestone
	Cyclone: SEPARAT4	Mode=Design; Efficiency correlation = User specified Efficiency = 0.75 Separates gases and solid calcination products
	Cyclone: CYCL4	Efficiency = 0.75; Pressure drop = 0.0095 bar Separates solids from gases
2. Burning Zone	RGibbs: BURN	Duty = 0 kcal·hr^{-1}; p= 0.8673 bar Coal combustion
	BURNING	T = 1450 °C; p=0.8673 bar Clinker burning
	BELITE	T=1250 °C; p = 0.8673 bar Formation of belite (C2S)
	RYield: DECOMP	T = 28.32 °C; p = 0.8673 bar Decomposing coal
	ASHDECOM	T = 2128 °C; p = 0.8673 bar Decomposing Ash
	Calculator: COMBUST	Calculates actual coal yield
	SSPlit: SEPARAT1	MIXED split fraction=1; CIPSD split fraction=0 NCPSD split fraction=0 Separates solid ash from combustion gases
	SEPARAT3	MIXED split fraction = 1; CIPSD split fraction =0 NCPSD split fraction=0
	Compr: P-AIRFAN	Type=Isentropic; Isentropic efficiency = 0.75; Mechanical efficiency =0.75 Used to model primary air inlet fan
3. Clinker cooling	HeatX: COOLER	Calculation=shortcut; Type=design; Flow =countercurrent Approach T = 15 °C Cooling clinker
	Heater: WALL-LOS	T = 245 °C; p = 0.8673 bar Set thermodynamic condition of streams CLINKER2 to T = 245 °C and CLINKER1 to quantify cooler losses
	Compr: C-AIRFAN	Type=Isentropic; Isentropic efficiency = 0.75; Mechanical η=0.75 Used to model cooler inlet air fan
4. Preheater Tower	Cyclone: CYCL1N	Mode=Design; Pressure drop = 0.0151 bar; Efficiency = 0.95 Pre cleaning exhaust gases
	CYCL1S	Mode=Design; Pressure drop = 0.0151 bar; Efficiency = 0.95 Pre cleaning of exhaust gases
	CYCL2	Mode=Design; Pressure drop=0.0087 bar; Efficiency = 0.85 Pre cleaning of exhaust gases
	CYCL3	Mode=Design; Pressure drop = 0.0083 bar; Efficiency = 0.75 Pre cleaning of exhaust gases
	RGibbs: MIXPH1	T = 410 °C; p = 0.8195 bar Calculation=Phase and chemical equilibrium. Mixing of solid and gases and Drying of free water from raw meal
	MIXPH2	T = 610 °C; p = 0.8390 bar Calculation=Phase and chemical equilibrium. Mixing of solid and gases and Evolution of combined water from raw meal
	MIXPH3	T = 739 °C; p = 0.8514 bar Calculation=Phase and chemical equilibrium. Mixing of solid and gases and Evolution of combined water from raw meal
	GASMIX	T = 380 °C; p = 0.8170 bar Calculation=Phase and chemical equilibrium. Combining gas streams PH1SGAS and PH1NGAS
	FSplit: FEEDSPLT	Split fraction = 0.5 Splits stream PH1FEED into two equal parts
	Compr: ID-FAN	Type=Isentropic; Isentropic efficiency = 0.85; Mech. efficiency = 0.85 Sucking out of exhaust gases from kiln system
	Heater: GASCOOL	T = 150 °C; p = 0.05 bar Simulates exhaust gas cooling tower
	FabFl: GASCLEAN	Model=Design; Pressure drop = 0.021 bar Cleaning of fine dust from gases

Appendix 2: Gaseous component streams' mole flows

	Units	CLINKER1	CLINKER2	EXGAS	KLN1SOLD	PH3SOLID	PH4SOLID	PRODUCT4	RAW-FEED	S-1	SOLIDOUT	PH5GAS
From		COOLER	WALL-LOS	B-FAN	SEPARAT2	CYCL3	CYCL4	CALCINAT		GASMIX	GASCLEAN	SEPARATE4
To		WALL-LOS		GASCLEAN	COOLER	MIXPH4	CALCINAT	SEPARAT4	MIXPH1	ID-FAN		MIXPH4
Substream: ALL												
Mass Flow	$kg \cdot h^{-1}$	35528.24	35528.24	71779.71	35528.24	71344.72	40323.56	88775.42	58000	71779.71	3536.055	56211.26
Temperature	°C	772.9009	245	138.5546	1450	739	836	958	28.32	380	138.5546	958.0002
Pressure	bar	0.86731	0.86731	0.04646	0.86731	0.848018	0.8580556	0.86731	0.86731	0.81701	0.02546	0.852614
Substream: CIPSD												
Component Mole Flow												
SIO2	$kmol \cdot h^{-1}$	0	0	7.569771	0	152.7304	114.5513	114.5512	122.121	7.569771	7.569771	171.5828
AL2O3	$kmol \cdot h^{-1}$	0	0	1.113444	0	22.46524	16.84944	16.84944	17.96288	1.113444	1.113444	25.24054
FE2O3	$kmol \cdot h^{-1}$	8.773971	8.773971	0.537089	8.773971	10.8365	8.12762	8.127618	8.664709	0.537089	0.537089	12.17521
CAO	$kmol \cdot h^{-1}$	4.961598	4.961598	0	4.961598	0	299.6283	428.0403	456.3262	0	0	641.1424
MGO	$kmol \cdot h^{-1}$	10.56288	10.56288	0.6887396	10.56288	13.89626	10.42251	10.4225	11.11125	0.68874	0.6887396	15.61144
SO3P	$kmol \cdot h^{-1}$	0.312854	0.3128543	0	0.3128543	0	0	0	0.1434208	0	0	0
K2O	$kmol \cdot h^{-1}$	2.806055	2.806055	0.1737954	2.806055	3.506559	2.629998	2.629997	2.803793	0.173795	0.1737954	3.93975
NA2O	$kmol \cdot h^{-1}$	1.31176	1.31176	0.0861311	1.31176	1.737812	1.303398	1.303398	1.389529	0.086131	0.0861311	1.952497
TIO2	$kmol \cdot h^{-1}$	0.301365	0.3013651	0.0089107	0.3013651	0.179785	0.134843	0.134843	0.1437537	0.008911	0.0089107	0.2019955
H2OP	$kmol \cdot h^{-1}$	0	0	0	0	0	0	0	12.74793	0	0	0
P2O5	$kmol \cdot h^{-1}$	0.081055	0.0810547	0.0050145	0.0810547	0.101174	0.0758824	0.0758824	0.0808969	0.005014	0.0050145	0.1136723
CACO3	$kmol \cdot h^{-1}$	0	0	28.28575	0	570.7035	128.4121	0	0	28.28575	28.28575	0
MGCO3	$kmol \cdot h^{-1}$	0	0	0	0	0	0	0	0	0	0	0
CO2S	$kmol \cdot h^{-1}$	0	0	0	0	0	0	0	472.5194	0	0	0
C2S	$kmol \cdot h^{-1}$	0	0	0	0	0	0	0	0	0	0	0
C3S	$kmol \cdot h^{-1}$	122.4147	122.4147	0	122.4147	0	0	0	0	0	0	0
C3A	$kmol \cdot h^{-1}$	18.75548	18.75548	0	18.75548	0	0	0	0	0	0	0

Appendix 3: Conventional Inert Solids (CIPSD) component streams' mole flows

	Units	CLINKER1	CLINKER2	EXGAS	KLN1SOLD	PH3SOLID	PH4SOLID	PRODUCT4	RAW-FEED S-1		SOLIDOUT	PH5GAS
From		COOLER	WALL-LOS	B-FAN	SEPARAT2	CYCL3	CYCL4	CALCINAT		GASMIX	GASCLEAN	SEPARATE4
To		WALL-LOS		GASCLEAN	COOLER	MIXPH4	CALCINAT	SEPARAT4	MIXPH1	ID-FAN		MIXPH4
Substream: ALL												
Mass Flow	$kg \cdot h^{-1}$	35528.24	35528.24	71779.71	35528.24	71344.72	40323.56	88775.42	58000	71779.71	3536.055	56211.26
Temperature	°C	772.9009	245	138.5546	1450	739	836	958	28.32	380	138.5546	958.0002
Pressure	bar	0.86731	0.86731	0.04646	0.86731	0.848018	0.8580556	0.86731	0.86731	0.81701	0.02546	0.852614
Substream: CIPSD												
Component Mole Flow												
SIO2	$kmol \cdot h^{-1}$	0	0	7.569771	0	152.7304	114.5513	114.5512	122.121	7.569771	7.569771	171.5828
AL2O3	$kmol \cdot h^{-1}$	0	0	1.113444	0	22.46524	16.84944	16.84944	17.96288	1.113444	1.113444	25.24054
FE2O3	$kmol \cdot h^{-1}$	8.773971	8.773971	0.537089	8.773971	10.8365	8.12762	8.127618	8.664709	0.537089	0.537089	12.17521
CAO	$kmol \cdot h^{-1}$	4.961598	4.961598	0	4.961598	0	299.6283	428.0403	456.3262	0	0	641.1424
MGO	$kmol \cdot h^{-1}$	10.56288	10.56288	0.6887396	10.56288	13.89626	10.42251	10.4225	11.11125	0.68874	0.6887396	15.61144
SO3P	$kmol \cdot h^{-1}$	0.312854	0.3128543	0	0.3128543	0	0	0	0.1434208	0	0	0
K2O	$kmol \cdot h^{-1}$	2.806055	2.806055	0.1737954	2.806055	3.506559	2.629998	2.629997	2.803793	0.173795	0.1737954	3.93975
NA2O	$kmol \cdot h^{-1}$	1.31176	1.31176	0.0861311	1.31176	1.737812	1.303398	1.303398	1.389529	0.086131	0.0861311	1.952497
TIO2	$kmol \cdot h^{-1}$	0.301365	0.3013651	0.0089107	0.3013651	0.179785	0.134843	0.134843	0.1437537	0.008911	0.0089107	0.2019955
H2OP	$kmol \cdot h^{-1}$	0	0	0	0	0	0	0	12.74793	0	0	0
P2O5	$kmol \cdot h^{-1}$	0.081055	0.0810547	0.0050145	0.0810547	0.101174	0.0758824	0.0758824	0.0808969	0.005014	0.0050145	0.1136723
CACO3	$kmol \cdot h^{-1}$	0	0	28.28575	0	570.7035	128.4121	0	0	28.28575	28.28575	0
MGCO3	$kmol \cdot h^{-1}$	0	0	0	0	0	0	0	0	0	0	0
CO2S	$kmol \cdot h^{-1}$	0	0	0	0	0	0	0	472.5194	0	0	0
C2S	$kmol \cdot h^{-1}$	0	0	0	0	0	0	0	0	0	0	0
C3S	$kmol \cdot h^{-1}$	122.4147	122.4147	0	122.4147	0	0	0	0	0	0	0
C3A	$kmol \cdot h^{-1}$	18.75548	18.75548	0	18.75548	0	0	0	0	0	0	0

Appendix 4: Stream GASES chemical exergy calculations

Components	Mole flow / kmol·hr^{-1}	$\bar{e}_{CHi}$ / kJ·kmol$_i^{-1}$	x_i / kmol$_i^{-1}$·kmol$_m^{-1}$	$\bar{e}_{CHi}\cdot x_i$ / kJ·kmol$_m^{-1}$	$x_i \cdot \ln x_i$ / kmol$_i^{-1}$·kmol$_m^{-1}$
H_2O	100.23	9,490	0.061170364	580.506757	-0.170915653
N_2	1230.83	690	0.751175491	518.311089	-0.21492331
O_2	67.77	3,970	0.041360028	164.19966339	-0.131749903
NO_2	0.005	55,600	3.0515E-06	0.16966339	-3.87537E-05
NO	14.68	88,900	0.008959203	796.473174	-0.042243306
S	0.00055	609,600	3.35665E-07	0.20462137	-5.00381E-06
SO_2	7.32	313,400	0.004467396	1400.0818	-0.024172853
SO_3	0.003	249,100	1.8309E-06	0.45607715	-2.41875E-05
H_2	1.99	236,100	0.001214497	286.74272	-0.008153434
CO	22.57	275,100	0.01377447	3789.35668	-0.059022755
CO_2	193.14	19,870	0.117873333	2342.14313	-0.25203024
Total	1638.5386			9878.64502	-0.9032794

subscripts: *i*-component; m-mixture

An example is shown for stream GASES to demonstrate how chemical exergy was calculated for each component. Eq. (3.8) was used. Where the values in appendix 4 above, together with the values of $\bar{R}$ and T_0 given in the Thesis, are used to calculate the chemical exergy for the strem GASES as follows:

$$\bar{e}_m^{CH} = \sum_{l=1}^{N} x_l \cdot \bar{e}_l^{CH} + \bar{R} \cdot T_0 \sum_{l=1}^{N} x_l \cdot \ln(x_l) = 9878.64502 + 8.31447 \times 301.32 \times (-0.9032794) = 7615.645\,\text{kJ} \cdot \text{kmol}_m^{-1}$$

$$\dot{E}_m^{CH} = \dot{n}_m \cdot \bar{e}_m^{CH} = 1638.53855 \times 7615.645 = 12478527.25\,\text{kJ} \cdot \text{h}^{-1} = 3466.258\,\text{kW}$$

For pure solid multi-component of the streams, the following equation was used in the example shown in Appendix 5 for stream PH4SOLID. The chemical exergy of multi-component material stream is given by (Hinderink et al. 1996) Eq. (3.9).

Appendix 5: Stream PH4SOLID chemical exergy calculations

Components	Mole flow / kmol·hr^{-1}	$\bar{e}_{CH}$ / kJ·kmol^{-1}	$\dot{E}_{CH}$ / kW	
SiO_2	114.55	1900	$114.55 \times 1900 = 217645$ kJ·h^{-1}	= 60.46 kJ·s^{-1}
Al_2O_3	16.85	200400	$16.85 \times 200400 = 3376740$ kJ·h^{-1}	= 937.98 kJ·s^{-1}
Fe_2O_3	8.13	16500	$8.13 \times 16500 = 134145$ kJ·h^{-1}	= 37.26 kJ·s^{-1}
CaO	299.63	101200	$299.63 \times 101200 = 30322556$ kJ·h^{-1}	=8422.93 kJ·s^{-1}
MgO	10.42	66800	$10.42 \times 66800 = 696056$ kJ·h^{-1}	= 193.35 kJ·s^{-1}
K_2O	2.63	413100	$2.63 \times 413100 = 1086453$ kJ·h^{-1}	= 301.79 kJ·s^{-1}
Na_2O	1.30	296200	$1.3 \times 296200 = 385060$ kJ·h^{-1}	= 106.96 kJ·s^{-1}
$CaCO_3$	128.41	1000	$128.41 \times 1000 = 128410$ kJ·h^{-1}	= 35.67 kJ·s^{-1}
Total				10096.4 kW

Appendix 6: ΔG for Streams INBURNER, PRODUCT, AIR and ASHPROD

Component	DGFORM /kJ·kmol^{-1}	Mole flow / kmol·h^{-1}	-ΔG/ kW =DGFORM · Mole flow
H_2O(l)	236760	15.14	3584546.4 kJ·h^{-1} = 995.71 kJ·s^{-1}
N_2	0		0
O_2	0		0
H_2	0		0
C	0	228.62	0
H_2O(g)	228590	106.26	24289973.4 kJ·h^{-1} = 6747.21 kJ·s^{-1}
NO_2	51328	0.005	256.64 kJ·h^{-1} = 0.0713 kJ·s^{-1}
NO	86570	13.56	1173889.2 kJ·h^{-1} = 326.08 kJ/s
CO	137150	23.52	3225768 kJ·h^{-1} =896.05 kJ·s^{-1}
CO_2	394370	205.1	80885287 kJ·h^{-1} =22468.14 kJ·s^{-1}
SiO_2	856288	7.86	6730423.68 kJ·h^{-1} =1869.56 kJ·s^{-1}
Al_2O_3	1562702	1.91	2984760.82 kJ·h^{-1} =829.1 kJ·s^{-1}
Fe_2O_3	742683	0.65	482743.95kJ/hr=134.1 kJ·s^{-1}
CaO	603487	0.43	259499.41 kJ·h^{-1} =72.08 kJ·s^{-1}
MgO	569196	0.14	79687.44 kJ·h^{-1} =22.14 kJ·s^{-1}
K_2O	322087	0.18	57975.66 kJ·h^{-1} =16.10 kJ·s^{-1}
Na_2O	376089	0.01	3760.89 kJ·h^{-1} =1.04 kJ·s^{-1}
TiO_2	889446	0.17	151205.82 kJ·h^{-1} =42.01 kJ·s^{-1}
P_2O_5	1372797	0.01	13727.97 kJ·h^{-1} =3.81 kJ·s^{-1}
Total - ΔG			34423.20 kJ·s^{-1}=3487.66 kJ·kg$_{cl}^{-1}$

DGFORM is the standard Gibbs free energy of formation at T = 25 °C obtained from simulation. It should be noted that the standard Gibbs free energy of formation (or Gibbs function of formation) of a compound equals change in the Gibbs function (ΔG) for the reaction in which the compound is formed from its elements and its values of stable elements are zero (Bejan et al. 1996). The term stable means that the particular element is in a chemically stable form.

$$\bar{e}^{\,\mathrm{CH}} = -\Delta G + \left\{ \sum_{p} n \cdot \bar{e}^{\,\mathrm{CH}} - \sum_{r} n \cdot \bar{e}^{\,\mathrm{CH}} \right\} = 3{,}505.34\ \mathrm{kJ \cdot kg_{cl}^{-1}}$$

$$\sum_{p} n \cdot \bar{e}^{\,\mathrm{CH}} = \mathrm{PRODUCT} + \mathrm{ASHPROD};\ \sum_{r} n \cdot \bar{e}^{\,\mathrm{CH}} = \mathrm{AIR} + \mathrm{HOTAIR} + \mathrm{INBURNER}$$

Appendix 7: Chemical exergy of stream INBURNER

Components	Mole flow / kJ·kmol^{-1}	$\bar{e}_{CH}$ / kJ·kmol^{-1}	$\dot{E}_{CH}$ / kW	
H2O	15.14	900	$15.14 \times 900 = 13626$ kJ·h^{-1}	=3.79 kJ·s^{-1}
N2	1.9589	690	$1.9589 \times 690 = 1351.641$ kJ·h^{-1}	= 0.38 kJ·s^{-1}
O2	1.2622	3970	$1.2622 \times 3970 = 5010.934$ kJ·h^{-1}	= 1.39 kJ·s^{-1}
H2	93.2061	236100	$93.2061 \times 236100 = 22005960.21$ kJ·h^{-1}	=6112.77 kJ·s^{-1}
C	228.62	410260	$228.62 \times 410260 = 93793641.2$ kJ·h^{-1}	= 26053.79 kJ·s^{-1}
Total				32172.12 kW

Appendix 8: Rotary kiln system essential data

Plant area (Name):	Unit	Kiln tube/ Burner
Type		UNAX-Rotary dry kiln
Burner type		Simple type
Nominal dimension	m	3.95×58
Preheater		4-stage
Kiln design efficiency	$kJ \cdot kg_{cl}^{-1}$	3472.72
Kiln design (rated) capacity	tpd	800.00
Raw meal /clinker factor	-	1.67
Diameter (Inside Shell)	m	3.95
Diameter (Inside Brick)	m	3.49
Slope (Inclination)		3% / 10.8^0
Rotation speed, n, Norminal	rpm	1.50
Utilization Factor (UF)	%	72.79
Reliability Factor (RF)	%	86.34
RF actual	%	91.00
Energy Consumption (Burning)	$kWh \cdot t^{-1}$	38.62
Energy consumption (clinker)	$kWh \cdot t^{-1}$	89.09
Fuel (100% Coal) consumption	$kJ \cdot kg_{cl}^{-1}$	4200
Pick up velocity	m/s	0.5-0.6
Firing air temperature	˚C	60
Maximum particle size	mm	0.09
Maximum temperature of kiln feed	˚C	90
Nominal flow rate of feed material	tph	70
Maintainance hours	hrs	0
Running days per week	days	7
Shift Pattern	hrs	24
Current running hours per day	hrs	22
Maximum running hours per day	hrs	22
Current throughput at 22 working hrs	tpd	55
% of rated capacity used at current RF	%	166
Clinker Cooler		
Type		UNAX-Planetary
Design capacity	tpd	800
Cooler air loading	$Nm^3 \cdot kg_{cl}^{-1}$	0,8
Year of upgrade		2003
Type		ESTANDA-Planetary
Upgraded capacity	tpd	900
Recommended peak loads	tph	41,4
Clinker outlet temperature from kiln	˚C	245
Maximum cooler shell temperature	˚C	440
Ea cooler nominal diameter	m	1,5
Ea cooler nominal length	m	13,2
Total number of coolers		10
Cooler tube discharge width	mm	650
Kiln shell -cooler tube distance	mm	560

Appendix 9: Recent results from exergy analysis in cement industry

Author	Objectives	Major Results
Farag and Taghian 2015	Energy and exergy analysis of five Egyptians dry rotary kiln with pre-calciners and flue gasses by pass	Energy efficiency of the rotary kiln systemy found to vary between η = (41.6 and 55.5) % Exergetic efficiencies for five kiln systems studied were ε = (26.8, 32.5, 28.1, 28.4 and 35.6) %. Irreversibility of the kiln systems ranges from 1,651.7 kJ· kg_{cl}^{-1} to 2396.4 kJ· kg_{cl}^{-1}, representing 49.6 % to 53.3 % of the total exergy input.
Gürtürk and Oztop 2014	Energy and exergy analysis of a rotary kiln used for plaster production	Energy and exergy efficiency of the rotary kiln systems are η = 69 % and ε = 16 % respectively. $\dot{e}_D$ = 66 % of total exergy input.
Parmar et al. 2016	Energy and exergy analysis of cement rotary kiln	Energy and exergy efficiencies are η = 51.90 % and ε = 38.29 % respectively. $\dot{e}_D$ = 61.71% of the total input exergy.
Kolip and Savas 2010	Energy and exergy analyses of a parallel flow, four stages cyclone precalciner type cement plant.	The first and second law efficiencies for the kiln system were 51 % and 28 % respectively. $\dot{E}_{L,SYS}$=72 %. Major heat loses are due to, stack gas stream, heat transfer from hot surface and cooler exhaust.
Atmaca and Yumrutas 2014	Exergoeconomic analysis of a 4-stage dry rotary cement plant.	The energy and exergy efficiencies of the plant are η = 59.37 % and ε = 38.99 % respectively. The exergetic efficiencies of the crusher, raw mill, pyro processing (preheater cyclone) tower, rotary kiln, coal mill, cooler, cement mill and packaging units are determined to be ε = (1.71, 16.37, 35.93, 38.72, 10.99, 59.98, 9.47 and 2.23) % respectively.
Farag 2012	To evaluate energy and exergy efficiency of Egyptian dry process cement kiln plant with precalciner characterized by that the whole kiln gas is diverted through by pass	The first and second law efficiencies were 40 % and 25.7 % respectively. $\dot{e}_{D,SYS}$ =51 % of total exergy input. $\dot{E}_L$ of bypass gases are the largest followed by those of the preheater exit gases. Preheater Pre-calciner ε_{PHT} = 37.7 %, η_{PHT} = 56.8 %, $\dot{E}_{D,PHT}$ =43.16 % of total exergy input Rotary kiln ε_{RTK} = 29.8 %, η_{RTK} = 74.2 %, $\dot{E}_{D,RTK}$ = 25.8 % of total exergy input Rotary Cooler ε_{RC} = 52 %, η_{RC}, 65.7 %, $\dot{E}_{D,RC}$ = 34.3 % of total exergy input
Kolip 2010	To carry out energy and exergy analyses for a four stage cyclone pre-calciner cement plant.	The overall system exergy and energy efficiencies is ε_{SYS} = 32 %, η_{SYS} = 54 % and $\dot{E}_{L,SYS}$ = 68 %. Maximum exergy destruction takes place in the kiln and calciner units with 38.54 % and 36.70 % respectively and it is mostly caused by combustion, chemical reaction and heat transfer to raw material during mixing. Preheating of raw feed causes 8.64 % irreversibility while clinker cooler causes 16.13 %. Recoverable exergy destructions are exergy destruction via waste heat caused by stack gas, stack dust, clinker and unused coolant outlet air. Recoverable exergy destruction is found as 18.5 % of the total irreversibility.

Author	Objectives	Major Results
Koroneos et al. 2005	The main objective was to examine cement production in Greece using the exergy analysis methodology	Exergy and energy efficiencies are: ε_{SYS} = 50.20 % and η_{SYS} = 68.8 %. $\dot{E}_{L,SYS}$ = 50 %, The biggest losses (30.90 %) are due to irreversibility in the preheating of feed, cooling of clinker and combustion of Pet coke. A largest portion of exergy loss is due to exhaust gases from the combustion of pet-coke, 15 %
Utlu et al. 2006	The objective was to perform energy and exergy analysis of a raw mill and raw material preparation unit in a cement plant in Turkey.	Overall exergy and energy efficiencies are ε_{RM} = 25.20 % and η_{RM} = 84.30 %
Madlool et al. 2011	The objective was to review exergy analysis, exergy balance and exergetic eff. for cement industry	It has been found that the exergy efficiency for cement production units ranges from ε = (18 to 49) %. ε_{SYS} = 28 % and ε_{RTK} = 25 %. Exergy losses due to irreversibility from the kiln are higher than other units.
Madlool et al. 2012	The study focused on the thermal performance of the clinker cooling system in a cement plant (grate cooler)	It was found that energy efficiency varies from η = (46.18 to 45.19) % while exergy efficiencies vary from ε = (54.55 to 55.62) % respectively at different ambient temperature
Camdali et al. 2004	The applications of energy and exergy analyses are examined for a dry rotary kiln with pre-calciner.	35.60 % of the total exergy is lost mostly due rotary kiln and secondly due to stack gases. The energy and exergy efficiency of the overall system are η = 97% and ε = 64.40 % respectively.
Diji et al. 2013	Exergoenvironmental evaluation of a wet-processes of cement production	Results show that the major process components impacting the environment were the kiln and limestone extraction processes. Exergy destructions due to process and combustion are the major source of environmental hazards in the process. *Sub-systems exergy efficiency* ε_{HC} = 86 %, ε_{rm} = 73 %, ε_{KLN} = 48 %, $\dot{E}_{D,SYS}$ = 95% of the process exergy, ε_{FM} = 68 % and ε_{SYS} = 55 %
Kol and Chaube 2013	Exergy analysis of preheater precalciner rotary kiln at Birla cement plant Satna.	Exergetic efficiency was calculated to be: ε_{PHT} = 58.2 %, ε_{RTK} = 77.82 %, ε_{RC} = 83.72 %
Boyaghchi 2014	The study investigated energetic and exergetic analysis of calcium oxide formation, CO_2 emissions, and environmental effects during clinker formation processes in a rotary kiln.	ε_{SYS} = 28.6 %, η = 53.4 %. The most irreversibility was due to fuel combustion and chemical reactions of calcination in the kiln which is found to be $\dot{E}_{D,RTK}$ = 40.6 % of inlet exergy. Results also shows 18.4 % of exergy input is lost by exhaust hot gases. Total emission was estimated at 157,228 kg·h^{-1} which is 31.3 % of it due to calcination and 0.9 % of it is due to fuel combustion.

Author	Objectives	Major Results
Jijesh et al. 2015	The objective of the study was to determine exergy utilization and their irreversibility Malabar cem. plant.	The major heat loss sources have been determined as preheater and cooler. Exergetic and energetic efficiency of the overall system was calculated to be: ε_{SYS} = 38.68% and η_{SYS} = 54.93 %
Ajith et al. 2014	To review the energy and exergy analysis of the white cement wet-type rotary kiln	Exergetic and energetic efficiency of clinker production are: ε_{SYS} = 8 % and η_{SYS} = 12.2 % The irreversibility loss of the process is about 73 % of total exergy input
Karellas et al. 2013	The aim of this paper is to examine and compare energetically and exergetically, two different WHR (waste heat recovery) methods: a water-steam Rankine cycle, and an Organic Rankine Cycle (ORC).	A parametric study proved, that the water steam technology is more efficient than ORC in exhaust gases temperature higher than T_{exh} =310 ^{0}C.
Sogut et al. 2009	The main objective of this study is to assess the performance of a trass mill in a cement plant based on the actual operational data using energy and exergy analysis method	Energy and exergy efficiency of the trasmill system was η = 74 % and ε =10.68 % respectively. Using energy recovery systems energy and exergy efficiencies can be improved to η =84 % and ε = 48 % respectivel.
Rasul et al. 2005	To asses thermal performance and energy conservation opportunities of a cement industry in Indonesia using energy and exergy balances.	The burning efficiency and the second law efficiency of the kiln system are 52.07 % and 57.07 % respectively. Cooler efficiency and heat recovery efficiency are 47.75 % and 51.2 % respectively. Cooler loss was 19% and it was mainly due to convection and radiation from the un-insulated cooler. System irreversibility about 20 % due to the conversion of chemical energy of coal fuel.
Atmaca and Kanoglu 2012	To reduce energy consumption of a raw mill in a cement factory using first and second law analysis approach.	The first and second law efficiency of the raw mill is 61.5 % and 16.4 % respectively. The first and second law efficiencies of the raw mill increases with ambient temperature and with decrease in the moisture content of the raw materials. Use of PHT exit gases in raw mill provides 6.7 % reduction in energy consumption.
Gutiérrez et al. 2013	To analyze the energy and exergy consumption processes in a lime vertical shaft kilns in order to identify the factors affecting fuel consumption	The overall energy and exergy efficiency was 71.6 % and 40.8 % respectively. Most irreversibility source is fuel combustion and exergy destruction due to internal heat and momentum transfer in the kiln accounting to 40 % of efficiency loss. Main exergy loss is the exergy loss with exhaust gases contributing to 10 %.

Appendix 10: Calculation of major clinker compounds' percentage

$$\text{Alite}(C_3S) = \frac{122.41}{170.27} \times 100 = 71.89\% \quad \text{(A10.1)}$$

$$C_2S = \frac{114.55}{353.03} \times 100 = 32.45\% \quad \text{(A10.2)}$$

$$C_3A = \frac{18.76}{170.27} \times 100 = 11.02\% \quad \text{(A10.3)}$$

Appendix 11: Exergetic variables calculation for the overall system

$$\dot{e}_{F,SYS} = \left(\dot{e}_{DRY\text{-}COAL} + \dot{e}_{RAW\text{-}FEED} + \dot{e}_{S\text{-}3} + \dot{e}_{S\text{-}2}\right) \text{ and} \quad \text{(A11.1)}$$

$$\dot{e}_{P,SYS} = \dot{e}_{CLINKER_2} \quad \text{(A11.2)}$$

Exergy destructions for the overall system are given by equating the sum of exergy of input streams to the sum of exergy of output streams:

$$\dot{e}_{D,SYS} = \dot{e}_{i,SYS} - \dot{e}_{e,SYS} = \left(\dot{e}_{DRY\text{-}COAL} + \dot{e}_{RAW\text{-}FEED} + \dot{e}_{S\text{-}3} + \dot{e}_{S\text{-}2}\right) - \left(\dot{e}_{CLINKER_2} + \dot{e}_{PHGASOUT}\right) \quad \text{(A11.3)}$$

$\dot{e}_{D,\,SYT}$ = 3513.98 – (1153.38 + 608.06) = 1,752.54 kJ·kg$_{cl}^{-1}$ (A11.4)

Overall exergy loss of the kiln system is given by stream PHGASOUT at 350^{0}C.

$$\dot{e}_{L,SYS} = \dot{e}_{PHGASOUT} = 608.06 \text{ kJ·kg}_{cl}^{-1} \quad \text{(A11.5)}$$

Overall efficiency of the kiln system is given by:

$$\varepsilon_{SYS} = \frac{\dot{e}_{P,SYS}}{\dot{e}_{F,SyS}} = \frac{1153.38}{3513.98} \times 100 = 32.82\% \quad \text{(A11.6)}$$

Appendix 12: Mass and exergy balances around the whole process

Input Items	$\dot{m}$ / kg·h^{-1}	T / ˚C	$\dot{e}$ / kJ·kg$_{cl}^{-1}$
RAW-FEED	1.63	28	0
DRY-COAL	0.12	28	3,505
S-2	0.95	27	4
S-3	0.32	27	4
Sum	3.02		3,514
Output Items			
CLINKER2	1.0	245	1,153
PHGASOUT	2.02	350	608
$\dot{E}_{D,\,SYT}$			1,752
Sum	3.02		3,514

Appendix 13: Exergetic variables calculation for the rotary kiln

The rotary kiln sub system is a bit complex system and contains several devices like kiln burner and the like. Therefore, exergy destruction for the rotary kiln was calculated by equating the sum of exergy inputs and outputs of the streams. Nevertheless, exergy definitions of fuels and products were also defined so as to calculate the rational efficiency for the rotary kiln:

$$\dot{e}_{\mathrm{D,RTK}} = \dot{e}_{\mathrm{i,RTK}} - \dot{e}_{\mathrm{e,RTK}} = \left(\dot{e}_{\mathrm{HOT\,AIR}} + \dot{e}_{\mathrm{DRY\text{-}COAL}} + \dot{e}_{\mathrm{S\text{-}3}} + \dot{e}_{\mathrm{PH4SOLID}}\right) - \left(\dot{e}_{\mathrm{KLN1SOLD}} + \dot{e}_{\mathrm{PH5GAS}}\right) \quad \text{(A13.1)}$$

$\dot{e}_{\mathrm{D,RTK}}$ = (381.36+3505.34+4.34+1523.10) – (2070.56 + 3,149.78) = 193.8 kJ·kg$_{\mathrm{cl}}^{-1}$ (A13.2)

$\dot{e}_{\mathrm{F,\,RTK}}$ = ($\dot{e}_{\mathrm{HOTAIR}}$ + $\dot{e}_{\mathrm{DRY\text{-}COAL}}$ + $\dot{e}_{\mathrm{S\text{-}3}}$) = (3505.34 + 381.36 + 4.34) = 3891.04 kJ·kg$_{\mathrm{cl}}^{-1}$ (A13.3)

$\dot{e}_{\mathrm{P,\,RTK}}$= ($\dot{e}_{\mathrm{KLN1SOLD}}$ – $\dot{e}_{\mathrm{PH4SOLID}}$) = (2070.56 –1523.10) = 547.46 kJ·kg$_{\mathrm{cl}}^{-1}$ (A13.4)

$$\varepsilon_{RTK} = \frac{\dot{e}_{\mathrm{P,RTK}}}{\dot{e}_{\mathrm{F,RTK}}} \times 100\% = \frac{547.46}{3891.04} \times 100\% = 14.07\% \quad \text{(A13.5)}$$

Appendix 14: Mass and Exergy balances around the rotary kiln

Input Items	$\dot{m}$ / kg·h^{-1}	T / ˚C	$\dot{e}$ / kJ·kg$_{\mathrm{cl}}^{-1}$
PH4SOLID	1.13	836	1,523
HOTAIR	0.95	772	381
DRY-COAL	0.12	28.32	3,505
(S-3)	0.32	27	4
Sum	2.52		5,414
Output Items			
KLN1SOLD	1.0	1450	2,071
PH5GAS	1.52	958	3,150
$\dot{E}_{\mathrm{D,RTK}}$			194
Sum	2.52		5,414

Appendix 15: Exergetic variables calculation for the preheater tower

Taking the preheater tower as a heat exchanger, exergy of fuel and product as well as exergy destruction was calculated from:

$$\dot{e}_{\mathrm{F,PHT}} = \dot{e}_{\mathrm{PH5GAS}} - \dot{e}_{\mathrm{PHGASOUT}} \quad \text{(A15.1)}$$

$$\dot{e}_{\mathrm{P,PHT}} = \dot{e}_{\mathrm{PH4SOLID}} - \dot{e}_{\mathrm{RAW\text{-}FEED}} \quad \text{(A15.2)}$$

$$\dot{e}_{\mathrm{D,PHT}} = \dot{e}_{\mathrm{F,PHT}} - \dot{e}_{\mathrm{P,PHT}} = \left(\dot{e}_{\mathrm{PH5GAS}} - \dot{e}_{\mathrm{PHGASOUT}}\right) - \left(\dot{e}_{\mathrm{PH4SOLID}} - \dot{e}_{\mathrm{RAW\text{-}FEED}}\right) \quad \text{(A15.3)}$$

$\dot{e}_{\mathrm{D,\,PHT}}$ = (3,149.78 – 608.06) – (1523.10 – 0) = 1,018.62 kJ·kg$_{\mathrm{cl}}^{-1}$ (A15.4)

Exergy efficiency for the preheater tower was calculated as:

$$\varepsilon_{\mathrm{PHT}} = \frac{\dot{e}_{\mathrm{P,PHT}}}{\dot{e}_{\mathrm{F,PHT}}} \times 100 = \frac{1523.10}{2541.72} \times 100 = 59.92\% \quad \text{(A15.5)}$$

Appendix 16: Mass and Exergy balances around the preheater tower

Input Items	$\dot{m}$ / kg·h^{-1}	T / ˚C	$\dot{e}$ / kJ·kg$_{cl}^{-1}$
RAW-FEED	1.63	28	0
PH5GAS	1.52	958	3,1508
Sum	3.15		3,150
Output Items			
PH4SOLID	1.13	836	1523
PHGASOUT	2.92	350	608
$\dot{E}_{D,\,PHT}$			1,019
Sum	3.15		3,150

Appendix 17: Exergetic variables' calculation for the clinker cooler

$$\dot{e}_{F,PLC} = \dot{e}_{KLN1SOLD} - \dot{e}_{CLINKER_2} \quad \text{(A17.1)}$$

$$\dot{e}_{P,PLC} = \dot{e}_{HOTAIR} - \dot{e}_{S\text{-}2} \quad \text{(A17.2)}$$

$$\dot{e}_{D,PLC} = \dot{e}_{F,PLC} - \dot{e}_{P,PLC} = (\dot{e}_{KLN1SOLD} - \dot{e}_{CLINKER_2}) - (\dot{e}_{HOTAIR} - \dot{e}_{S\text{-}2}) \quad \text{(A17.3)}$$

$\dot{e}_{D,\,PLC}$ = (2070.56 – 1153.38) – (381.36 – 4.30) = 540.12 kJ·kg$_{cl}^{-1}$ (A17.4)

$\dot{e}_{L,WALL\text{-}LOS}$ = $\dot{e}_{CLINKER1}$-$\dot{e}_{CLINKER2}$=1487.11 – 1153.38 = 333.73 kJ·kg$_{cl}^{-1}$ (A17.5)

Planetary cooler exergetic efficiency is given by:

$$\varepsilon_{PLC} = \frac{\dot{e}_{P,PLC}}{\dot{e}_{F,PLC}} \times 100 = \frac{377.06}{917.18} \times 100 = 41.11\% \quad \text{(A17.6)}$$

Appendix 18: Mass and Exergy balances around the clinker cooler

Input Items	$\dot{m}$ / kg·h^{-1}	T / ˚C	$\dot{e}$ / kJ·kg$_{cl}^{-1}$
KLN1SOLD	1.0	1450	2,071
S-2	0.95	27	4
Sum	1.95		2,075
Output Items			
CLINKER2	1.0	245	1,153
HOTAIR	0.95	772	381
Cooler wall loss			334
$\dot{E}_{D,C}$			206
Sum	1.95		2,075

Appendix 19: Exergetic variables calculation for the *k*-th Component

The models representing each *k*-th components for each sub-system are presented in Appendix 1. Therefore, exergy balances for each component were carried out based on principles guiding exergy balances of individual components. For example, for the cooler, heat exchanger model was adopted while for the kiln burner combustion chamber model was applied. In general, Eq. (3.12) was used for exergy balance for *k*-th component. Exergy of fuel and product as well as exergy destruction calculations for each individual component were carried out first, and then the thermodynamic data obtained from the exergetic analysis are presented in Section 5. Detailed calculations are appended at the end of the thesis.

WALL-LOSS: This component was treated as dissipative component.

$$\dot{e}_{\mathrm{D,WALL\text{-}LOSS}} = \dot{e}_i - \dot{e}_e = \dot{e}_{\mathrm{CLINKER_1}} - \dot{e}_{\mathrm{CLINKER_2}} \tag{A19.1}$$

$$\dot{e}_{\mathrm{D,\ WALL\text{-}LOSS}} = 1487.11 - 1153.38 = 333.73\ \mathrm{kJ\cdot kg_{cl}^{-1}} \tag{A19.2}$$

$$\varepsilon_{\mathrm{WALL-LOSS}} = \frac{\dot{E}_{\mathrm{e}}}{\dot{E}_{\mathrm{i}}} \times 100 = \frac{1153.38}{1487.11} \times 100 = 77.56\,\% \tag{A19.3}$$

The flue gases from preheater tower are normally used to preheat raw feed when the kiln system is operated in a compound mode. However, in the simulation model of the kiln system, it was assumed that the raw mill was off and therefore, flue gases were passed through the cooler. Exergy of the fuel and product as well as exergy destruction was calculated based on the heat exchanger model:

$$\dot{e}_{\mathrm{D,GASCOOL}} = \dot{e}_{\mathrm{S\text{-}4}} - \dot{e}_{\mathrm{PHGASOUT}} \tag{A19.4}$$

$$\dot{e}_{\mathrm{D,\ GASCOOL}} = 692.72 - 608.06 = 84.66\ \mathrm{kJ\cdot kg_{cl}^{-1}} \tag{A19.5}$$

$$\varepsilon_{\mathrm{GASCOOL}} = \frac{\dot{e}_{\mathrm{P,GASCOOL}}}{\dot{e}_{\mathrm{F,GASCOOL}}} = \frac{608.06}{692.72} \times 100 = 87.78\,\% \tag{A19.6}$$

Combustion of coal fuel in a rotary kiln takes place in the kiln burner here modelled as BURN. Thus, the combustor model was used for definition of exergy of fuel and product as well as exergy destruction:

$$\dot{e}_{\mathrm{D,BURN}} = \dot{e}_{\mathrm{F,BURN}} - \dot{e}_{\mathrm{P,BURN}} \tag{A19.7}$$

$$\dot{e}_{\mathrm{D,BURN}} = \left[\left(\dot{e}^{\mathrm{CH}}_{\mathrm{FUEL}} + \dot{e}^{\mathrm{CH}}_{\mathrm{OXIDANT}}\right) - \left(\dot{e}^{\mathrm{CH}}_{\mathrm{GASES}} + \dot{e}^{\mathrm{CH}}_{\mathrm{ASHPROD}}\right)\right] - \left[\left(\dot{e}^{\mathrm{PH}}_{\mathrm{GASES}} + \dot{e}^{\mathrm{PH}}_{\mathrm{ASHPROD}}\right) - \left(\dot{e}^{\mathrm{PH}}_{\mathrm{FUEL}} + \dot{e}^{\mathrm{PH}}_{\mathrm{OXIDANT}}\right)\right] \tag{A19.8}$$

$$\dot{e}_{\mathrm{D,\ BURN}} = [(3259.59 + 0) - (351.19 + 17.44)] - [(2584.11 + 69.13) - (0 + 385.70)] \tag{A19.9}$$

$\dot{e}_{D,\,BURN} = 623.42\ kJ \cdot kg_{cl}^{-1}$ (A19.10)

$$\varepsilon_{BURN} = \frac{\dot{e}_{P,BURN}}{\dot{e}_{F,BURN}} \times 100 = \frac{2267.54}{2890.96} \times 100 = 78.44\% \quad \text{(A19.11)}$$

Clinker burning in a rotary kiln takes place in the burning zone of the kiln where heat exchange between combustion gases from the kiln burner and the compound from calcination of preheated raw feed takes place to form clinker. Thus, the cross flow heat exchanger was assumed for definition of exergy of fuel and product as well as calculation of exergy destruction:

$$\dot{e}_{D,\,BURNING} = \left(\dot{e}_{F,\,BURNING} - \dot{e}_{P,\,BURNING}\right) \quad \text{(A19.12)}$$

$$\dot{e}_{D,\,BURNING} = \left(\dot{e}_{F,\,BURNING} - \dot{e}_{P,\,BURNING}\right) = \left(\dot{e}_{GASES} - \dot{e}_{ASHPRODUCT} - \dot{e}_{KLN1GAS}\right) - \left(\dot{e}_{KLN1SOLD} - \dot{e}_{KLN2SOLD}\right) \quad \text{(A19.13)}$$

$\dot{e}_{D,\,BURNING}$ = (2,935.30 + 86.57 – 1613.17) – (2070.56 – 1810.03) (A19.14)

$\dot{e}_{D,\,BURNING} = 1{,}148.17\ kJ \cdot kg_{cl}^{-1}$ (A19.15)

$$\varepsilon_{BURNING} = \frac{\dot{e}_{P,BURNING}}{\dot{e}_{F,BURNING}} \times 100 = \frac{260.53}{1408.7} \times 100 = 18.49\ \% \quad \text{(A19.16)}$$

Belite formation (C_2S) takes place at the reactor belite and hence, exergy of fuel and product as well as exergy destruction were given by:

$$\dot{e}_{D,BELITE} = \dot{e}_{F,BELITE} - \dot{e}_{P,BELITE} \quad \text{(A19.17)}$$

$$\dot{e}_{D,BELITE} = \left(\dot{e}_{KLN1GAS} - \dot{e}_{KLN2GAS}\right) - \left(\dot{e}_{KLN3SOLD} - \dot{e}_{KLN2SOLD}\right) \quad \text{(A19.18)}$$

$\dot{e}_{D,\,BELITE}$ = (1,613.17 –1,315.07) – (1895.38 – 1810.03) (A19.19)

$\dot{e}_{D,\,BELITE} = (298.1 - 85.35) = 212.75\ kJ \cdot kg_{cl}^{-1}$ (A19.20)

$$\varepsilon_{BELITE} = \frac{\dot{e}_{P,BELITE}}{\dot{e}_{F,BELITE}} \times 100 = \frac{85.35}{298.1} \times 100 = 28.63\ \% \quad \text{(A19.21)}$$

Calcination takes place in the reactor CALCINAT. Cross flow heat exchanger was assumed for definition of exergy of fuel and product:

$$\dot{e}_{D,\,CALCINAT} = \left(\dot{e}_{F,\,CALCINAT} - \dot{e}_{P,\,CALCINAT}\right) \quad \text{(A19.22)}$$

$$\dot{e}_{D,\,CALCINAT} = \left(\dot{e}_{F,CALCINAT} - \dot{e}_{P,CALCINAT}\right) = \left(\dot{e}_{PH4SOLID} + \dot{e}_{KLN2GAS}\right) - \left[\dot{e}_{PRODUCT4} - \left(\dot{e}_{KLN3SOLD} + \dot{e}_{PH5GAS}\right)\right] \quad \text{(A19.23)}$$

$\dot{e}_{D,\,CALCINAT}$ = (1523.10 + 1,315.07) – [5,069.58 – (1895.38 + 3,149.78)] (A19.24)

$\dot{e}_{D,\,CALCINAT} = 2{,}838.17 - 24.42 = 2{,}813.75\ kJ \cdot kg_{cl}^{-1}$ (A19.25)

$$\varepsilon_{\text{CALCINAT}} = \frac{\dot{e}_{\text{P,CALCINAT}}}{\dot{e}_{\text{F,CLCINAT}}} \times 100 = \frac{24.42}{2838.17} \times 100 = 0.86\ \% \quad \text{(A19.26)}$$

$$\dot{e}_{\text{P,MIXPH2}} = \dot{e}^{\text{PH}}_{\text{PH2FEED}} = 1247.73\,\text{kJ} \cdot \text{kg}_{\text{cl}}^{-1} \quad \text{(A19.27)}$$

$$\dot{e}_{\text{F,MIXPH2}} = \left[\left(\dot{e}^{\text{TOT}}_{\text{PH1NSOLID}} + \dot{e}^{\text{TOT}}_{\text{PHS1NSOLID}}\right) + \dot{e}^{\text{TOT}}_{\text{PH3GAS}}\right] - \left(\dot{e}^{\text{TOT}}_{\text{PH2FEEL}} - \dot{e}^{\text{PH}}_{\text{PH2FEEL}}\right) \quad \text{(A19.28)}$$

$\dot{e}_{\text{P, MIXPH2}}$ =[(240.99 + 241.05)+1394.08] – (1869.15– 1247.73) = 1254.7 kJ·$\text{kg}_{\text{cl}}^{-1}$ (A19.29)

$\dot{e}_{\text{D, MIXPH2}} = \dot{e}_{\text{F, MIXPH2}} - \dot{e}_{\text{P, MIXPH2}}$ = 1254.7 – 1247.73 = 6.97 kJ·$\text{kg}_{\text{cl}}^{-1}$ (A19.30)

$$\varepsilon_{\text{MIXPH2}} = \frac{\dot{e}_{\text{P,MIXPH2}}}{\dot{e}_{\text{F,MIXPH2}}} \times 100 = \frac{1247.73}{1254.7} \times 100 = 99.44\,\% \quad \text{(A19.31)}$$

$$\dot{e}_{\text{P,MIXPH3}} = \dot{e}^{\text{PH}}_{\text{PH3FEED}} = 1770.94\,\text{kJ} \cdot \text{kg}_{\text{cl}}^{-1} \quad \text{(A19.32)}$$

$$\dot{e}_{\text{F,MIXPH3}} = \left(\dot{e}^{\text{TOT}}_{\text{PH4GAS}} + \dot{e}^{\text{TOT}}_{\text{PHS1NSOLID}}\right) - \left(\dot{e}^{\text{TOT}}_{\text{PH3FEED}} - \dot{e}^{\text{PH}}_{\text{PH3FEED}}\right) \quad \text{(A19.33)}$$

$\dot{e}_{F,\ MIXPH3}$ = (2,471.70 + 858.44) – (2,490.59–1770.94) = 2,610.49 kJ·$\text{kg}_{\text{cl}}^{-1}$ (A19.34)

$\dot{e}_{\text{D, MIXPH3}} = \dot{e}_{\text{F, MIXPH3}} - \dot{e}_{\text{P, MIXPH3}}$ = 2,610.49 – 1770.94 = 839.55 kJ·$\text{kg}_{\text{cl}}^{-1}$ (A19.35)

$$\varepsilon_{\text{MIXPH3}} = \frac{\dot{e}_{\text{P,MIXPH3}}}{\dot{e}_{\text{F,MIXPH3}}} \times 100 = \frac{1770.94}{2610.49} \times 100 = 67.84\,\% \quad \text{(A19.36)}$$

$$\dot{e}_{\text{D,B-FAN}} = \dot{e}_{\text{F,B-FAN}} - \dot{e}_{\text{P,B-FAN}} = \dot{W}_{\text{B–FAN}} - \left(\dot{e}_{\text{S-4}} - \dot{e}_{\text{EXGAS}}\right) \quad \text{(A19.37)}$$

$$\dot{e}_{\text{D, B-FAN}} = \dot{W}_{\text{B–FAN}} - \left(\dot{e}_{\text{S-4}} - \dot{e}_{\text{EXGAS}}\right) \quad \text{(A19.38)}$$

$\dot{e}_{\text{D, B-FAN}}$ = 13.37– (692.72 – 682.82) = 3.47 kJ·$\text{kg}_{\text{cl}}^{-1}$ (A19.39)

$$\varepsilon_{\text{B–FAN}} = \frac{\dot{e}_{\text{P,B–FAN}}}{\dot{e}_{\text{F,B–FAN}}} = \frac{9.9}{13.37} \times 100 = 74.05\% \quad \text{(A19.40)}$$

$$\dot{e}_{\text{D, ID-FAN}} = \dot{e}_{\text{F, ID-FAN}} - \dot{e}_{\text{P, ID-FAN}} \quad \text{(A19.41)}$$

$$\dot{e}_{\text{D, ID-FAN}} = \dot{W}_{\text{ID–FAN}} - \left(\dot{e}_{\text{PHGASOUT}} - \dot{e}_{\text{S-1}}\right) \quad \text{(A19.42)}$$

$\dot{e}_{\text{D, ID-FAN}}$ = 67.88 – (608.06 – 554.15) = 13.97 kJ·$\text{kg}_{\text{cl}}^{-1}$ (A19.43)

$$\varepsilon_{\text{ID–FAN}} = \frac{\dot{e}_{\text{P,ID–FAN}}}{\dot{e}_{\text{F,ID–FAN}}} = \frac{53.91}{67.88} \times 100 = 79.42\% \quad \text{(A19.44)}$$

$$\dot{e}_{\text{D, P-AIR FAN}} = \dot{e}_{\text{F, P-AIR FAN}} - \dot{e}_{\text{P–AIR FAN}} \quad \text{(A19.45)}$$

$$\dot{e}_{\text{D, P-AIR FAN}} = \dot{W}_{\text{P-AIR FAN}} - \left(\dot{e}_{\text{S-3}} - \dot{e}_{\text{AIR}}\right) \quad \text{(A19.46)}$$

$$\dot{e}_{\text{D, P-AIRFAN}} = 7.60 - (4.34 - 0) = 3.26 \text{ kJ·kg}_{\text{cl}}^{-1} \quad \text{(A19.47)}$$

$$\varepsilon_{\text{P-AIRFAN}} = \frac{\dot{e}_{\text{P,P-AIRFAN}}}{\dot{e}_{\text{F,P-AIRFAN}}} = \frac{4.34}{7.60} \times 100 = 57.11\% \quad \text{(A19.48)}$$

$$\dot{e}_{\text{D, C-AIR FAN}} = \dot{e}_{\text{F, C-AIR FAN}} - \dot{e}_{\text{P, C-AIR FAN}} \quad \text{(A19.49)}$$

$$\dot{e}_{\text{D, C-AIR FAN}} = \dot{W}_{\text{C-AIR FAN}} - \left(\dot{e}_{\text{S-2}} - \dot{e}_{\text{COLD AIR}}\right) \quad \text{(A19.50)}$$

$$\dot{e}_{\text{D, C-AIRFAN}} = 7.60 - (4.3 - 0) = 3.3 \text{ kJ·kg}_{\text{cl}}^{-1} \quad \text{(A19.51)}$$

$$\varepsilon_{\text{C-AIRFAN}} = \frac{\dot{e}_{\text{P,C-AIRFAN}}}{\dot{e}_{\text{F,C-AIRFAN}}} = \frac{4.3}{7.6} \times 100 = 56.58\% \quad \text{(A19.52)}$$